Prediction and validation of pool fire development in enclosures by means of CFD Models for risk assessment of nuclear power plants (Poolfire) – Final Report

Van Hees, Patrick; Wahlqvist, Jonathan; Hostikka, Simo; Sikanen, Topi; Husted, Bjarne; Magnusson, Tommy; Jörud, Fredrik

2014

Prediction and validation of pool fire development in enclosures by means of CFD Models for risk assessment of nuclear power plants (Poolfire) –

Final Report

Patrick van Hees
Jonathan Wahlqvist
Simo Hostikka[1,5]
Topi Sikanen[1]
Bjarne Husted[2]
Tommy Magnusson[3]
Fredrik Jörud[4]

Department of Fire Safety Engineering
Lund University, Sweden

Brandteknik
Lunds tekniska högskola
Lunds universitet

Report 3183, Lund 2014

1. **VTT Technical Research Centre of Finland**
2. **Haugesund College**
3. **Ringhals AB**
4. **ESS AB, European Spallation Source AB**
5. **Aalto University School of Engineering**

This report has been funded by NKS with co-financing of SSF, VYR, Ringhals AB and Brandforsk

Prediction and validation of pool fire development in enclosures by means of CFD Models for risk assessment of nuclear power plants (Poolfire) – Final Report

Patrick van Hees
Jonathan Wahlqvist
Simo Hostikka[1,5]
Topi Sikanen[1]
Bjarne Husted[2]
Tommy Magnusson[3]
Fredrik Jörud[4]

1. VTT Technical Research Centre of Finland
2. Haugesund College
3. Ringhals AB
4. ESS AB, European Spallation Source AB
5. Aalto University School of Engineering

Lund 2014

Prediction and validation of pool fire development in enclosures by means of CFD (Poolfire) - Final Report

Patrick van Hees, Jonathan Wahlqvist
Simo Hostikka[1,5], Topi Sikanen[1]
Bjarne Husted[1]
Tommy Magnusson[3]
Fredrik Jörud[4]

1. VTT Technical Research Centre of Finland
2. Haugesund College Norway
3. Ringhals AB Sweden
4. ESS AB, European Spallation Source Sweden
5. Aalto University School of Engineering Finland

Report 3183
ISSN: 1402-3504
ISRN: LUTVDG/TVBB--3183--SE

Number of pages: 96
Illustrations: Patrick van Hees, Jonathan Wahlqvist, Simo Hostikka, Bjarne Husted

Keywords
Fire, nuclear power plants, pool fires, modelling

Sökord
Brand, kärnkraftverk, pölbränder, modellering

Abstract

Fires in nuclear power plants can be an important hazard for the overall safety of the facility. One of the typical fire sources is a pool fire. It is therefore important to have good knowledge on the fire behaviour of pool fire and be able to predict the heat release rate by prediction of the mass loss rate. This final report describes the state of the art within the area of pool fire modelling and the need for further development of pool fire models. As a result of the research in this project two new models are presented: one pyrolysis model and one engineering model. In the project the models were validated and pool fire experiments were included. Also a number of real case studies were incorporated to show the need for the development of pool fire models.

Brandteknik
Lunds tekniska högskola
Lunds universitet
Box 118
221 00 Lund
brand@brand.lth.se
http://www.brand.lth.se
Telefon: 046-2227360
Telefax: 046-2224612

Department of Fire Safety Engineering
Lund University
P.O. Box 118
SE-221 00 Lund, Sweden
brand@brand.lth.se
http://www.brand.lth.se/english
Telephone:+46462227360
Fax: +46462224612

Preface

This report is the final report of the POOLFIRE project financed by NKS, which is gratefully thanked. NKS conveys its gratitude to all organisations and persons who by means of financial support or contributions in kind have made the work presented in this report possible. The names and organisation are listed below.

First, the authors would like to thank all who provided them with literature and information on the subject pool fires and performed tests such Depeng Kong, Denis Hellebuyck and David Johansen.

Secondly this project is a co-financed project where the following other financing bodies are thanked for their contribution:

SSF (Strategic Research Foundation, Sweden)

VYR (State Nuclear Waste Management Fund, Finland)

Ringhals AB (Sweden)

Brandforsk (Swedish Board of fire research (PRISME project))

Finally the authors would like to thank all the partners in the OECD PRISME project for the discussions and cooperation in this project and especially IRSN (Institut de Radioprotections et de sûreté de nucléaire) in France for providing us with information, figures and data.

Lund, December 2014.

Patrick van Hees

Jonathan Wahlqvist

Simo Hostikka

Topi Sikanen

Bjarne Husted

Tommy Magnusson

Fredrik Jörud

Disclaimer

Contents

1. INTRODUCTION....1

1.1. BACKGROUND....1

1.2. SCOPE....2

2. OVERVIEW OF THE POOLFIRE PROJECT....3

2.1. WORK PACKAGE 1 CURRENT STATE OF THE ART....3

2.2. WORK PACKAGE 2 DEVELOPMENT OF ADVANCED MODEL....3

2.3. WORK PACKAGE 3 VALIDATION OF THE MODEL....3

2.4. WORK PACKAGE 4 IMPLEMENTATION OF THE MODEL IN A REAL CASE SCENARIO FOR RISK IDENTIFICATION....3

2.5. WORK PACKAGE 5 DISSEMINATION OF RESULTS....4

2.6. WORK PACKAGE 6 MANAGEMENT....4

3. CURRENT STATE OF THE ART....5

3.1. LITERATURE REVIEW....5

3.2. MODEL....6

3.3. VALIDATION OF THE CURRENT MODEL....7

3.3.1. MODELS FOR PRESCRIBED BURNING AND PRESCRIBED VENTILATION....7

3.3.2. RESULTS WITH PRESCRIBED BURNING/PRESCRIBED VENTILATION....10

3.3.3. RESULTS WITH PRESCRIBED BURNING/VENTILATION MODULE FDS AND CFX....11

4. EXTENDED VALIDATION OF VENTILATION MODEL IN FDS....17

4.1. FIRE EXPERIMENTS....17

4.1.1. DESCRIPTION OF THE EXPERIMENTAL FACILITY....17

4.2. OVERVIEW OF THE PERFORMED TEST SERIES....18

4.3. MODELING WITH FDS....19

4.3.1. MASS LOSS RATES....19

4.3.2. MODELING OF THE HVAC SYSTEM....19

4.3.3. INLET- AND EXHAUST FANS....21

4.3.4. ROOM LEAKAGE....22

4.3.5. INITIAL CONDITIONS....22

4.4. RESULTS....23

4.5. RESULTS SOURCE TESTS....23

4.5.1. SOURCE D1....23

4.5.2. SOURCE D3....24

4.5.3. SOURCE D6A 25
4.6. RESULTS DOOR TESTS 26
4.6.1. DOOR 2 (D2) 26
4.6.2. DOOR 5 (D5) 28
4.6.3. DOOR 6 (D6) 29
4.7. RESULTS LEAK TESTS 31
4.7.1. LEAK 1 31
4.8. SUMMARY OF RESULTS 33
4.8.1. INITIAL CONDITIONS 33
4.8.2. FIRE CONDITIONS 33
4.9. CONCLUSIONS 35
4.10. FUTURE WORK 35

5. DEVELOPMENT OF A NEW MODEL 37

5.1. MODEL DESCRIPTION 37
5.2. PRELIMINARY COMPARISONS OF OLD AND NEW LIQUID EVAPORATION MODELS 37
5.2.1. MODELS FOR OPEN ATMOSPHERE PRISME TESTS (PRISME SOURCE) 37
5.3. SENSITIVITY STUDIES OF THE NEW LIQUID EVAPORATION MODEL 40
5.3.1. SENSITIVITY OF THE EVAPORATION MODEL TO THE MASS TRANSFER COEFFICIENT 40
5.3.2. A WORD OF CAUTION ON THE IN-DEPTH RADIATION ABSORPTION MODELS 41
5.3.3. DEFINITIONS 42
5.3.4. GRID CONVERGENCE STUDIES 42
5.4. MODEL DESCRIPTION – ENGINEERING MODEL 47

6. EXPERIMENTAL SET-UPS FOR VALIDATION 51

6.1. EXPERIMENTAL SET-UP 1 (STORD/HAUGESUND UNIVERSITY COLLEGE). 51
6.1.1. DESCRIPTION 51
6.1.2. PARTICLE IMAGE VELOCIMETRY (PIV) MEASUREMENTS OF FIRES WITH PRESENCE OF PIPES 52
6.2. EXPERIMENTAL SET-UP 2. 56
6.3. EXPERIMENTAL SET-UP 3 59
6.4. EXPERIMENTAL SET-UP 4. 62

7. VALIDATION OF THE MODELS 63

7.1. VALIDATION OF NEW LIQUID EVAPORATION MODEL 63
7.1.1. FUEL PROPERTIES FOR VALIDATION SIMULATIONS 63

7.1.2. LARGE POOL FIRES IN OPEN ATMOSPHERE 63
7.1.3. COMPARISON OF FDS PREDICTIONS WITH EMPIRICAL CORRELATIONS 64
7.1.4. MODELS FOR OPEN ATMOSPHERE PRISME TESTS (PRISME SOURCE) 66
7.1.5. RESULTS FOR OPEN ATMOSPHERE PRISME TESTS (PRISME SOURCE) 67
7.1.6. COMPARTMENT FIRES WITH PREDICTED BURNING/PRESCRIBED VENTILATION (PRISME_SOURCE AND PRISME_DOOR) 69
7.2. VALIDATION OF THE ENGINEERING MODEL 70

8. REAL CASE APPLICATIONS 73

8.1. FINDINGS FROM THE HEYSHAM NUCLEAR POWER STATION (65) 73
8.2. FIRE IN SWEDISH POWER PLANT IN ÖREBRO (66) 73
8.2.1. INTRODUCTION 73
8.2.2. GENERAL 73
8.2.3. CAUSE OF ACCIDENT 74
8.2.4. CHAIN OF ACTION 74
8.2.5. EXPERIENCES 74
8.3. REAL SCALE EXPERIMENTS AND SIMULATION WITH ENGINEERING MODELS ..75
8.3.1. EXPERIMENTAL SET-UP 75
8.3.2. TEST RESULTS 78
8.3.3. VALIDATION WITH ENGINEERING MODEL 81

9. DISSEMINATION 83

9.1. SCIENTIFIC PUBLICATIONS 83
9.2. WORKSHOP. 84

10. CONCLUSIONS 85

REFERENCES
ANNEXES

1. Introduction

1.1. Background

Safe shutdown of a reactor after an incident is a key factor in the overall safety design of a nuclear power plant. When the incident is a fire, the fire can not only be the cause for the shutdown but can also jeopardize the safe shut down by destroying critical components needed for the shutdown process. In order to prevent this redundant systems are built up which can guarantee safety shut down if the major system fails. In fire terms one is primarily interested in the functional performance of the components such as cables, electronic circuits, etc. With respect to fire, events can be classified in 3 major groups depending on the position of the subsystems. The three cases are given illustrative in Figure 1. In the first event (left), the redundant systems A and B are in the same enclosure within a fire compartment and a fire can have a much greater impact on one or both subsystem if it happens and the risk is consequently high for failure of the redundancy. Probability for failure might e.g. be 1 on 100 years. In the second event the systems A and B are in the same fire compartment but not in the same enclosure and the risk of failure will depend on the fire spread between enclosures. Probability will be 1 on 1000 years. Finally the subcomponents A and B can be in 2 different fire compartments and risk for failure will be due to failure of fire compartments, something very seldom to happen.

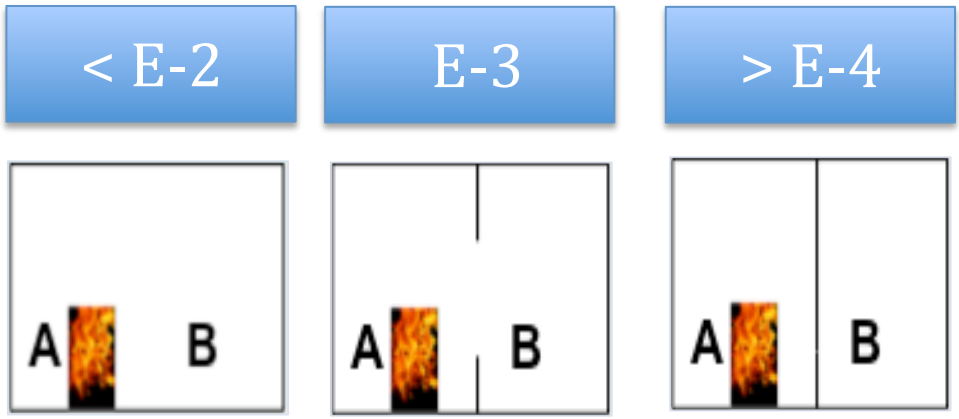

Figure 1 Example of event classification for fire incidents with probability for failure

One way to determine the overall risk in a PSA analysis is by using probabilistic methods using statistics. Another possibility is to investigate the likelihood for critical conditions by using calculation methods, which predicts fire growth, fire and smoke spread and critical temperature of the components. This is a so-called deterministic approach, which can be a complement to the probabilistic methods in PSA analysis. Today more and more CFD (Computational Fluid Dynamics) methods are used instead of empirical and zone models. The use of the method puts however high requirements on the correctness of the prediction methods and therefore validation experiments are necessary. Another key issue here is the correct prediction of the fire growth within an enclosure. This fire growth depends on the properties and geometry of the enclosure, ventilation conditions and the type and load of the fire fuel.

In an actual international OECD project called PRISME a large amount of experimental data is gathered with respect to enclosure fires where mechanical ventilation is involved. The project has been using a number of fuel loads defined by the different international partners (regulators and industry). One of the actual fuel loads is a defined pool fire using the same liquid. A liquid waste fire is namely one of the major fire incidents reported. Experiments in one or more enclosures under different ventilation conditions and by using different connections between enclosures (doors, wall openings, ducts, etc.) have been conducted. The project will be extended by another 3 years and will include also experiments with other set-ups (e.g. two enclosure above each other with a horizontal opening), another liquid fuel, cables as fire load, and extinguishment systems (sprinklers). This international project constitutes of an important and unique database set of experiments. The international project focuses mainly on the fire tests while use of the fire test results and validation of CFD models is a national or regional responsibility and subject to local funding.

Up to now Sweden and Finland have participated on national basis but it has been seen clearly that synergy is possible between the research groups involved in the project (Lund university and VTT). Activities have been related to validation of experiments with the most commonly used CFD tool called FDS and by conducting sensitivity analyses for this tool. In the future the important aspect of coupling fire growth with the enclosure conditions as mentioned above is an important aspect if a deterministic model approach would be successful for risk assessment of nuclear power plants.

1.2. Scope

The scope of the project is to provide improved tools for deterministic evaluation of the risk for loss of functional performance in redundant systems critical for shut down of the reactor within PSA analyses. The improved tool will contain an advanced pool fire model, which takes into account all aspects of the enclosure (geometry, properties, ventilation) and fuel (amount, type, surface area, thermal boundaries).

2. Overview of the Poolfire project

This chapter gives a short overview of the overall 3-year project. The project major core of activity is the development and validation of a pyrolysis model for pool fires in enclosures and will contain the following work packages.

2.1. Work package 1 Current state of the art.

Evaluation of the actual state of the art of pool fire models within CFD codes especially FDS, and the validation data available within the OECD project PRISME. The result of this work package will be an overview of the need for further development and the requirements for additional data both as input data for the models and for validation purposes.

Responsible organisations: VTT and Lund University

2.2. Work package 2 Development of advanced model

This work will contain the development of an advanced model for pool fires, which takes into account important aspects form the enclosure and pool fire. The enclosure geometry (volume, openings, height, etc.) will define e.g. the hot smoke layer temperature, which on its turn defines the thermal radiation levels towards the burning liquid. Ventilation inside the enclosure is also an important factor since the ventilation affects the burning rate (ventilation controlled or not) and the burning rate affect on its turn the ventilation (overpressures, back flow, etc). Finally the type of fuel and how it is located in the enclosure is of importance. Fuel leakages mainly run of on surface and hence the thermal boundaries are important, as they will affect the heat losses of the burning liquid and needed to be incorporated in the model. Advanced pyrolysis models for liquid pools need special input data. It will be investigated how these can be obtained form literature or small-scale test data.

Responsible organisations: VTT and Lund University

2.3. Work package 3 Validation of the model

Test from the international OECD project PRISME will be used for validation of the model. Both previously run experiment in the first project will be used but also data from the second project to be started in 2011. Both experiments in single and multi rooms will be used and validation will not only be limited to the pool fire growth but also to parameters such as temperature of the gas layer, gas concentrations, door flows, surface temperatures and temperatures of components. As part of the validation also a parameter investigation will be performed.

Responsible organisations: Lund University, VTT and Haugesund University College.

2.4. Work package 4 Implementation of the model in a real case scenario for risk identification.

In this work package the obtained knowledge will be applied on a real case study in a nuclear power plant within a deterministic evaluation of the risk for loss of functional performance of critical components.

Responsible organisations: Lund University and Vattenfall Ringhals.

2.5. Work package 5 Dissemination of results

Results from the project will be reported in scientific journals and at conferences. A small workshop for interested parties will be organised at the end of project.

Responsible organisations: All partners

2.6. Work package 6 Management

Management of the project includes aspects such as communication with partners, meeting organisation, economical follow up and progress follow up.

Responsible organisation: Lund University

3. Current State of the art

3.1. Literature review

The pool fire scenario has been widely used by researchers to study the vaporization process at the fuel surface since the pyrolysis process of fuel is one of the most important stages of combustion, along with the ignition and the flaming processes. Prescribed constant conditions for burning rate or fuel mass loss rate, so called open simulations or a posteriori, have been used in various numerical fire studies using CFD codes showing good agreement with experimental results. But the burning rate or fuel mass loss rate is often not easy to obtain without experiments. Therefore it is desired to be able to predict these parameters beforehand, a priori.

A practical way to determine the burning rate of large pool fires was described by Babrauskas (1). He showed that the fuel mass loss rate or the burning rate in an open-atmosphere system could be estimated with a simple correlation that only requires the knowledge of certain fuel properties. It is generally based on a simple heat balance of the poolfire taking into account mainly the effect of radiation. Other investigations of hazardous conditions associated with compartment fires have included empirical methods such as that given by the work of Peatross and Beyler (2) as well as theoretical approach proposed by Quintiere and Rangwala (3) and Utiskul (4). The empirical correlation, obtained from a steady-state combustion regime by Peatross and Beyler (2), provides fuel mass loss rate against oxygen concentration measured at the flame base for large-scale fire compartments. One of the main drawbacks of this empirical relationship lies in that it was obtained in conditions for which external heat fluxes were negligible. This limits its relevance to situations where high gas and wall temperatures, affecting incoming heat fluxes, are present. In more recent theoretical work by Melis et al (5), which made use of a well-stirred reactor approach, a good agreement between the measured fuel mass loss rate with the linear correlation of Peatross and Beyler was obtained.

Utiskul (4) presented a theoretical model that is based on the burning rate approach in an open-atmosphere and includes fuel response to vitiated air along with burning enhancement due to hot gases and confinement. In this study, the predicted mass loss rate was properly validated with small-scale heptane pool fire experiments. However, because flame radiant heat feedback to the pool fire was ignored, this theory was found to be insufficient for large-scale fires, which later was shown by Nasr et al. (7). Only a few studies have addressed the problem of the determination of the heat fluxes back to the fuel surface in order to determine the fuel mass loss rate. One of these studies was performed by Tewarson et al. (8), which focused on the determination of convective and radiant fluxes by using a steady-state heat balance equation at the fuel surface with a radiation correction for the Spalding number. Further work on how to estimate the flame heat feedback to the fuel surface was also done by Orloff and de Ris (9), who illustrated the application of Froude modelling principles to the development of a homogeneous fire radiation model. The convective heat transfer from the flame to the fuel surface was determined according to the stagnant film layer theory, which gives its variation with the mass transfer at the pyrolyzing surface. Later Klassen et al. (10) developed an equation of radiative transfer to account for the effects of fluctuations on the heat feedback. An experimental study was also performed to obtain measurements of radiative heat feedback in a 30 cm diameter, heavily sooted, toluene pool fire (10). This work was

further developed by Hamins et al. (11, 12) who formulated a global model to predict the mass burning flux for pool fires. Total radiation to the pool surface was given according to Siegel and Howell (13), and the convective heat transfer was determined using the stagnant film layer model.

Beaulieu and Dembsey (14) later carried out an analytical study to quantify the effect of enhanced ambient oxygen concentration on flame heat flux. An advanced flammability measurements apparatus was used to measure the flame heat flux back to the burning surface for 20.9% and 40% ambient oxygen concentrations. In this work, the flame was considered as a surface emitter, so that a view factor was used to express the flame radiant heat flux. They also measured the flame emissivity, temperature, and height to calculate the convective and radiant heat fluxes. Although the calculated values were in good agreement with the experimental measurements, there was no relationship reported between the heat fluxes from the flame or the effect of the oxygen concentration.

Concerning the complete coupling between the liquid/solid and gas phases, few computational fluid dynamics (CFD) works (15, 16) have been carried out, in which the burning rates are satisfactory reproduced in the wide range from small to large pool sizes. The main reason is due to the difficulties in the prediction of the radiative and convective heat fluxes emitted by a turbulent flame and received by the pool surface. For this reason, any predictive fire simulations in a large compartment have yet to be reported. A simpler modeling approach, based on an energy balance at the fuel surface and on the stagnant film layer theory, was derived by Nasr et al. (7) and first applied in a CFD code to predict the fuel mass loss rate of a hydrogenated tetrapropylene (TPH) pool fire in a confined and mechanically ventilated compartment as a part of the PRISME program (6). This model was validated against experimental measurements and showed good agreement for the prediction of the transient heat release rate of a fire compartment (17, 18). However, air vitiation effect on the fuel mass loss rate was not investigated in this study.

This literature review displays the need of further work in the area of predicting burning rate or fuel mass loss rate instead of simply prescribing it, especially in the case of significant external heat fluxes, where the current published work is incomplete.

3.2. Model

In FDS, fires can be modelled in two ways: as a prescribed fuel inlet boundary condition or utilizing the built in pyrolysis model. In this section, a description of the FDS liquid pyrolysis model is given and the two investigated evaporation models are presented.

When the liquid pyrolysis model is invoked FDS solves a one dimensional heat conduction equation for the liquid fuel

$$\rho_f c_f \frac{\partial T_f}{\partial t} = \frac{\partial}{\partial x} \lambda_f \frac{\partial}{\partial x} T_f + \dot{q}''' . \qquad (1)$$

Here ρ_f, c_f, λ_f *and* T_f are respectively the fuel density, specific heat, thermal conductivity and temperature. The radiative transport can be described as volumetric heat-source term $\dot{q}'''$ in Equation 1.

The FDS condensed phase model uses a "two-flux" model, where the radiative intensity is assumed to be constant in "forward" and "backward" hemispheres. The forward radiative heat flux into the fuel is

$$\frac{d\dot{q}_r^+}{dx} = \kappa_S\left(\sigma T_f^{\,4} - \dot{q}_r^+\right). \tag{2}$$

A corresponding formula can be written for the backward flux $\dot{q}_r^-$. The heat source term in Equation 1 is the difference between the forward and backward fluxes

$$\dot{q}''' = \frac{d\dot{q}^+}{dx} - \frac{d\dot{q}^-}{dx}. \tag{3}$$

Boundary condition at the fuel surface is given by

$$\dot{q}_r^+\Big|_{x=0} = \dot{q}''_{r,in} + (1-\varepsilon)\dot{q}_r^-\Big|_{x=0}, \tag{4}$$

where **ε** is the fuel emissivity.

In the present (FDS version 5) model, the rate of liquid fuel evaporation is a function of the liquid temperature T_S and the concentration of the fuel vapour above the pool surface. The volume fraction of fuel vapour above the pool surface is found from the Clausius - Claupeyron relation

$$X_f = \exp\left(-\frac{h_v W_f}{R}\left(\frac{1}{T_S} - \frac{1}{T_b}\right)\right). \tag{5}$$

Here h_v is the heat of vaporization, W_f is the molecular weight, T_s is the surface temperature of the pool and T_b is the boiling temperature of the fuel. In the old evaporation model the mas flux on the fuel surface is adjusted so that the fuel vapour equilibrium above the pool is maintained.

3.3. Validation of the current model

3.3.1. Models for prescribed burning and prescribed ventilation

The PRISME DOOR and PRISME SOURCE tests consider pool fires in ventilated compartments. The ventilation rates and pool sizes are varies between the tests. Different air supply locations are also considered. The PRISME SOURCE series considers a single room and the PRISME DOOR series considers two rooms with a door connecting them.

Room dimensions and material properties used are taken from the PRISME documentation (19-23). 10 cm discretization interval is used in all cases. In addition to the ventilation system, a leak with an area 0.009 m^2 is described for the whole compartment. Without the small leak, the simulations often stopped with numerical instabilities.

The PRISME SOURCE test series considers a single room connected to other rooms through ventilation. The computational model used in the simulations consists of only the fire room, with ventilation modelled as inflow and outflow boundaries with prescribed flow rates. The flow rates on the inflow and outflow

boundaries follow the measured inflow and outflow rates closely. The pool fire is likewise modelled as a fuel inlet boundary with a prescribed mass flux of fuel (burning rate). The mass flux is again obtained from mass loss rate measurements. Figure 2 shows the computational model used for the SOURCE series of tests. The room dimensions are 5 ×6 ×4 meters. The pan is 0.4 meters high. Walls are 30 cm thick and made of concrete. In the ceiling there is a 5 cm layer of rock wool on top of the concrete. The concrete is backed by void.

Notice that the air supply had two possible positions: 'high' or 'low'. In Figure 2 the air supply is in the 'low' position. The parameters varied were the ventilation and burning rates (pool size) and the air supply position. Table 1 gives a summary of the simulation cases.

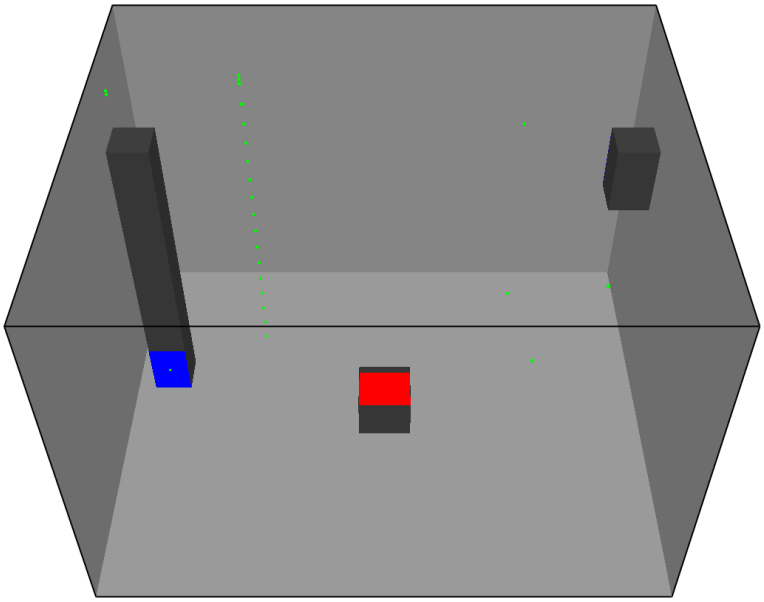

Figure 2 Model of the PRISME SOURCE series test PRS-SI-D6a. Air supply vent is in the 'low' position.

Table 1 Description of PRISME SOURCE test series

Test name	*S* m^2	*D* *m*	*Tr* $1/h$	dv_{air}/dt m^3/h	*Air supply position*
PRS-SI-D1	0.4	0.71	4.666667	560	High
PRS-SI-D2	0.4	0.71	8.416667	1010	High
PRS-SI-D3	0.4	0.71	1.5	180	High
PRS-SI-D4	0.4	0.71	4.708333	565	High
PRS-SI-D5	0.2	0.50	4.625	555	High
PRS-SI-D5a	0.2	0.50	1.583333	190	High
PRS-SI-D6	0.4	0.71	4.666667	560	Low
PRS-SI-D6a	0.4	0.71	1.666667	200	Low

The PRISME DOOR series considers two rooms, the fire room and the target room, connected by a door as shown in Figure 3. The purpose of this test series is to study the propagation of smoke and hot gases from the fire room to the target room. The

room dimensions are the same as in the SOURCE test series. The dimensions of the computational domain are 10.2×6 × 4. There is a 20 cm thick wall separating the two 5 meter wide rooms. The door is 70 cm wide and 215 cm high.

Table 2 gives a summary of the simulated PRISME DOOR tests. The varied parameters are burning rate and ventilation rate. This time there are two air supply vents and two air exhaust vents: one of each in each room. All the vents are in the 'high' position for all the simulations. In addition two gas phase measurements, additional cable targets have been added to both rooms. Temperatures on the surface and inside these cables and the flow rates and temperatures in the doorway are the focus of this test series. The cable targets are located on the walls opposite the door in both rooms and on top of the door in the target room.

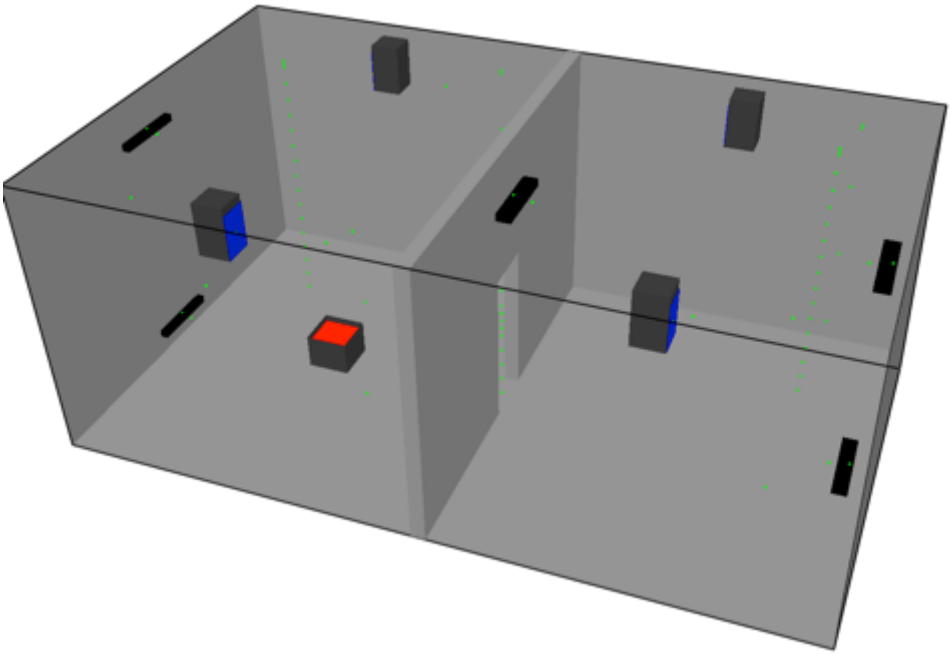

Figure 3 Model of the PRISME DOOR test PRS-D1. Both air supply vents in the 'high' position.

Table 2 Description of PRISME DOOR test series

Test name	*S* *m2*	*D* *m*	*Tr* *1/h*	dv_{air}/dt m^3/h	*Air supply position*
PRS-D1	0.4	0.71	0	0	High
PRS-D2	0.4	0.71	1.5	180	High
PRS-D3	0.4	0.71	4.666667	560	High
PRS-D4	0.4	0.71	8.333333	1000	High
PRS-D5	1	0.5	8.333333	1000	High
PRS-D6	1	0.5	8.333333	1000	High

3.3.2. Results with prescribed burning/prescribed ventilation

The uncertainty of the simulation predictions is determined using the methodology described in FDS Validation guide (25). Figure 4 shows scatter plots of predicted vs. simulated quantities in the compartment fire tests. The values in the plot correspond to maximum values of given quantity over the entire fire test or simulation. The red dashed lines indicate the confidence limits of the simulated quantities and solid line indicates the bias. The uncertainty in the experimental results was not known at the moment of this writing, and therefore the relative standard deviations are probably too large.

The gas species quantities considered are the CO_2 concentration and the reduction of O_2 concentration. The bias factor is very close to one and the relative standard deviation is 10 %. Uncertainties in predicted gas concentrations seem to be slightly larger at smaller concentrations.

The gas phase temperatures show a significantly larger amount of scatter. In the PRISME DOOR simulations, a significant number of peak gas temperatures is underestimated even by hundreds of degrees The PRISME SOURCE shows much better agreement with the observations, although there are few considerable over predictions.

Many of the predicted wall heat fluxes are clearly too high, and the bias factor is 1.36. There is also considerable variation in the values which is reflected in the large relative standard deviation. The accuracy of the wall temperature predictions is much better, which is somewhat surprising, considering that the wall heat flux predictions were too large in average.

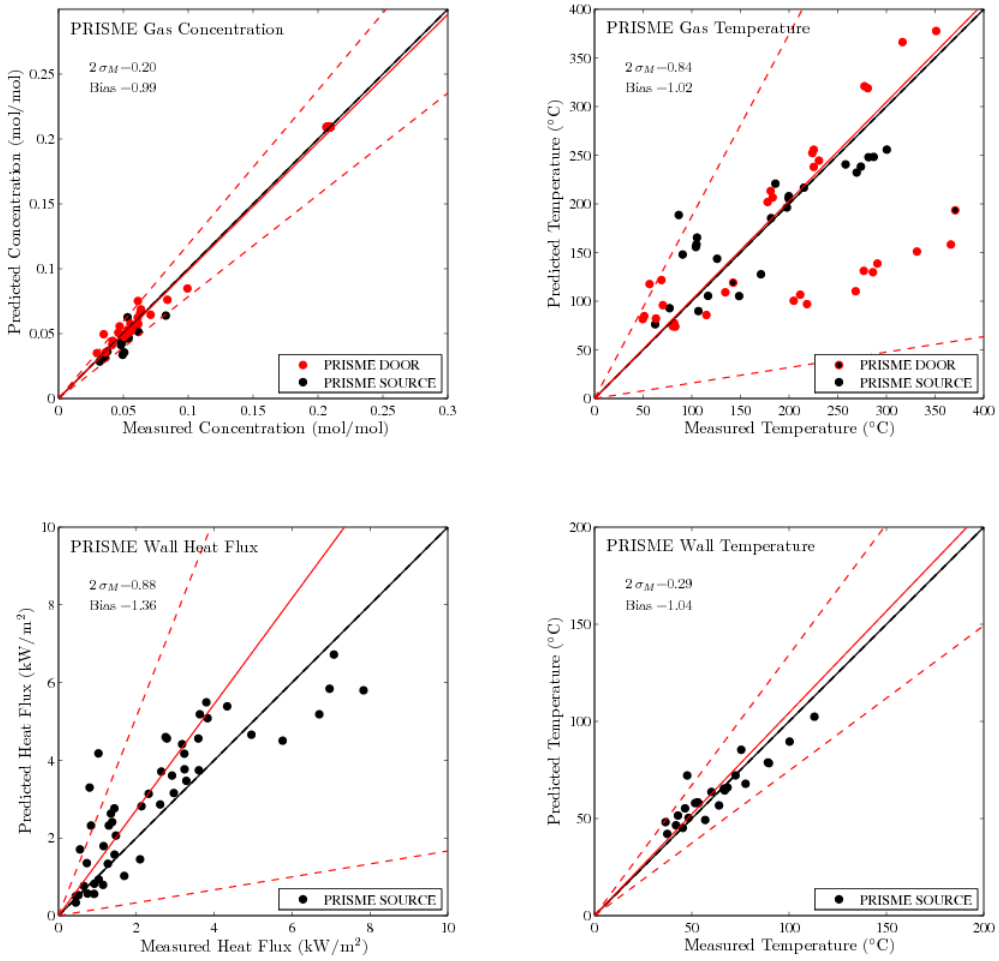

Figure 4 Measured vs. predicted quantities in the PRISME SOURCE and PRISME DOOR test series.

3.3.3. Results with prescribed burning/ventilation module FDS and CFX.

In the previous paragraphs simulation results were shown of a number of the PRISME tests where both the burning and ventilation were prescribed. In this project focus is put on developing a pyrolysis model for the pool fire but since part of the validation will done on the PRISME project results it is also important to see if the newly developed ventilation model (25) in FDS can be used to predict the ventilation changes during a test. Therefore validation of this model was done. Simulations with data from the PRISME SOURCE test used in Benchmark 1 (26) were performed and reported below. Both FDS (24) and CFX () were used.

The leak area from the fire room to surroundings was calculated using data from PRISME SOURCE – Ventilation Tests. Leakage between the fire room and surroundings was assumed to be a quadratic function of pressure difference. The calculated total leakage area from the fire room was in the order of 4 cm^2. The sensitivity of this parameter was tested by doing two more calculations with FDS, one with zero leakage, and one with 10 cm^2 leakage. As seen in Figure 5, the impact is quite large. When changing the total leakage with 4-6 cm^2, the first pressure peak in the experiment changes in the order of 50 Pa.

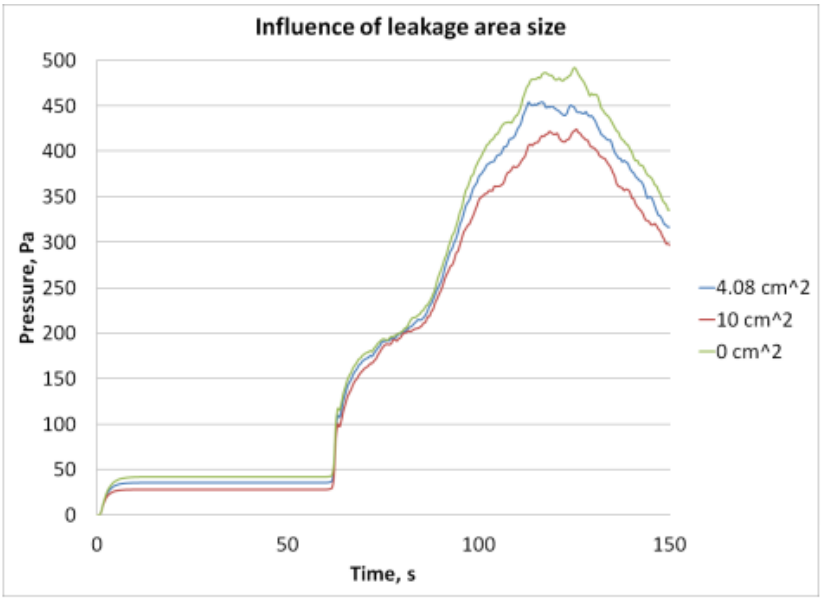

Figure 5 Influence of changing the room leak area in FDS.

Since the full ventilation system (Figure 7) was modelled with FDS, it was necessary to compare the experimental data in every node of interest with the data produced with FDS, prior to the fire being ignited. If this proved to give a good prediction, the likelihood of getting good results when compared to the full experiment would be far larger. As seen in Table 3, the results agree very well with the experimental data. Only one node shows a relative pressure difference larger than 10%, though the pressure difference is only about 40 Pa.

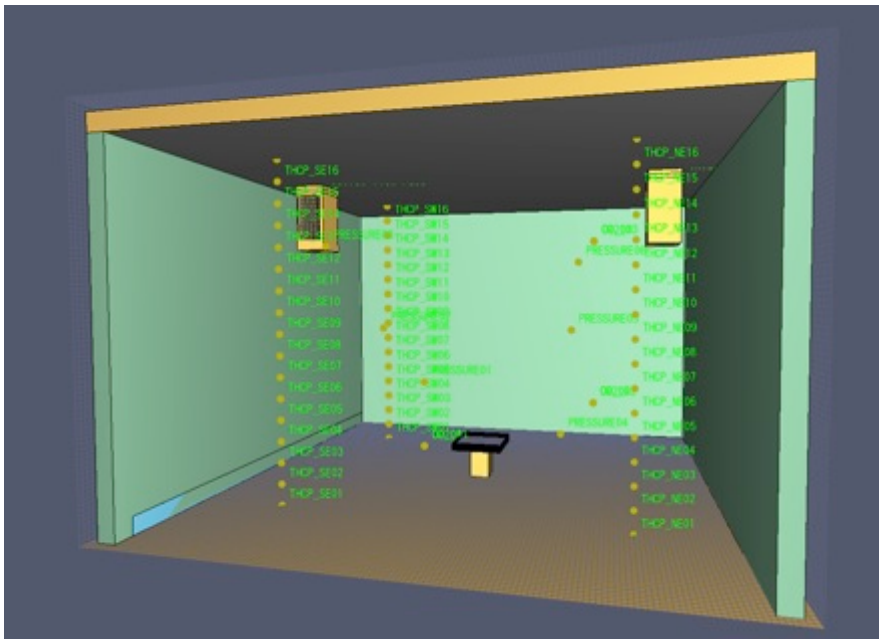

Figure 6 Geometry for the simulations with ventilation module.

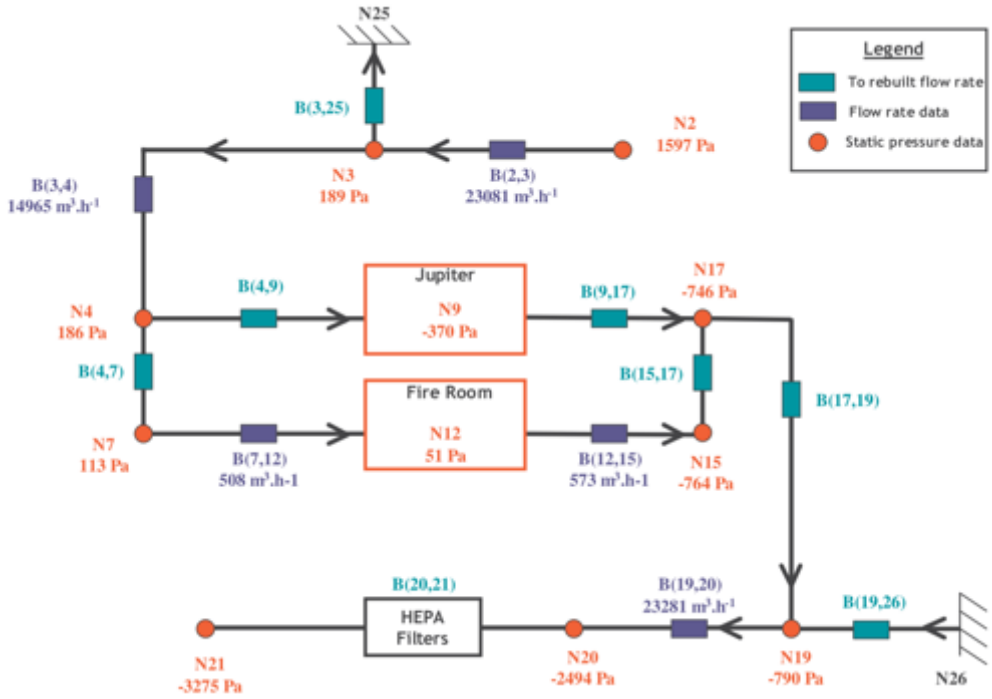

Figure 7 Layout of the ventilation network (picture IRSN, courtesy to IRSN) and a comparison between FDS data and experimental data

Table 3 Comparison of FDS5 results and measured pressure in each ventilation node.

	N2	N3	N4	N7	Fire room	N15	N17	N19	N20	N21
FDS, Pa	1575.73	191.71	188.81	162.77	35.5	-706.71	-726.09	-769.46	-2446.5	-3228.18
Experiment, Pa	1597	189	186	113	37.9	-764	-746	-790	-2494	-3275
Difference, %	1.33	1.43	1.51	44.04	6.33	7.50	2.67	2.60	1.90	1.43

An overview of the temperatures calculated with both CFX and FDS compared to the experimental data can be seen in Figure 8. FDS manages to give a good prediction of the temperatures (within 10-15 %) on a relatively coarse grid (10 cm cubes), providing a good basis for evaluating the ventilation system behaviour. Unfortunately the same cannot be said about CFX. CFX over-predicts the temperature by far (30-50 %), however, it cannot be ruled out that errors made by the software operator influences this deviation. Also, the way CFX handles combustion, for example internally calculating heat of combustion, prevented use of the experimental value obtained. This will likely impact the temperatures in the fire room. Also, heat transfer to the surrounding walls has been taken into account, but it was unclear if it was properly set up even though initial tests were performed.

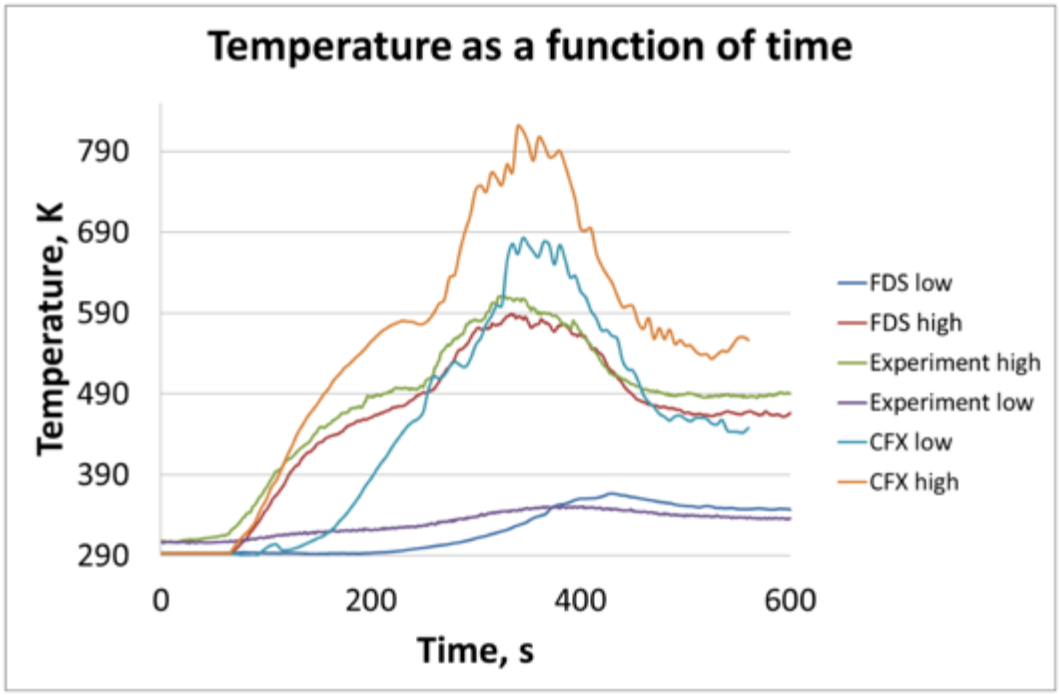

Figure 8 Temperature (highest and lowest measure point) as a function of time for the first 600 seconds.

Since full capabilities concerning ventilation system modelling is not present in CFX (simplifications were made at the in- and outlet branch, specifying appropriate boundary conditions to get realistic pressures in the fire room), only results from calculations made with FDS are presented when comparing pressure in fire room and mass flow in the ventilation branches. As seen in Figure 9, the calculated pressure in the fire room is very close to the experimental data. All pressure peaks are fairly well predicted, and this is using only data available prior to the fire being ignited (except for HRR).

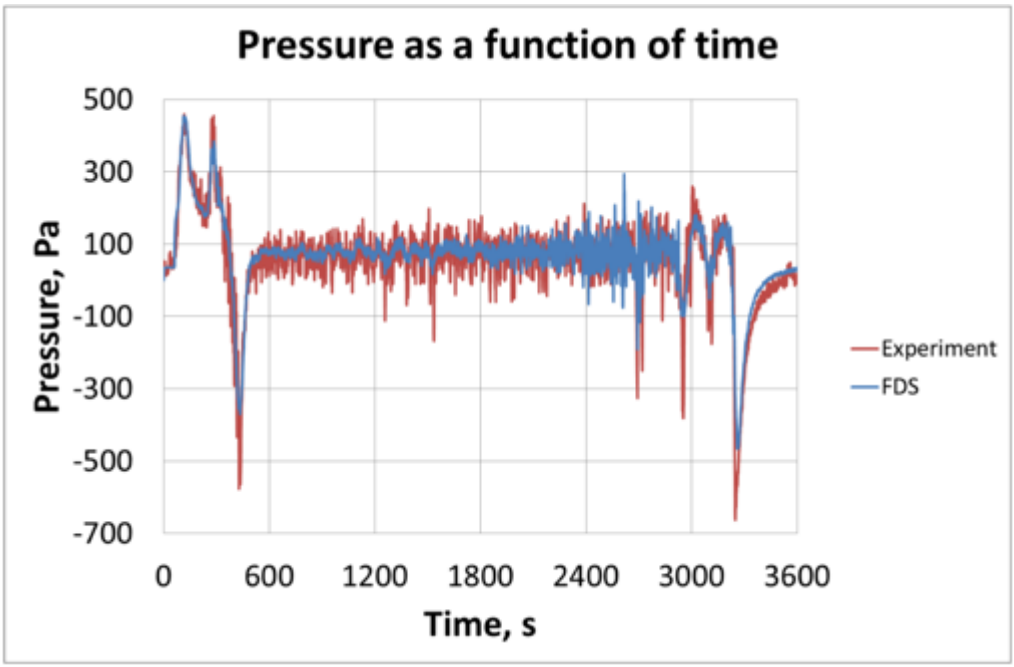

Figure 9 Pressure in the fire room as a function of time, the blue line is the pressure predicted with FDS.

Looking at the inlet and outlet branches (Figure 10) it is shown that FDS manages to predict the backflow in the inlet branch correctly. However, due to differences in the reported data from the experiment (actual measured mass flow not the same as reported in figure 3), the mass flow at the in- and outlet before the fire was ignited does not correspond to the FDS values. This in turn affects the "steady-state" mass flow in the later part of the experiment (after 600 seconds) making the FDS prediction somewhat incorrect. But it can be seen that the difference is constant, indicating that with the right starting values, FDS would give a better prediction.

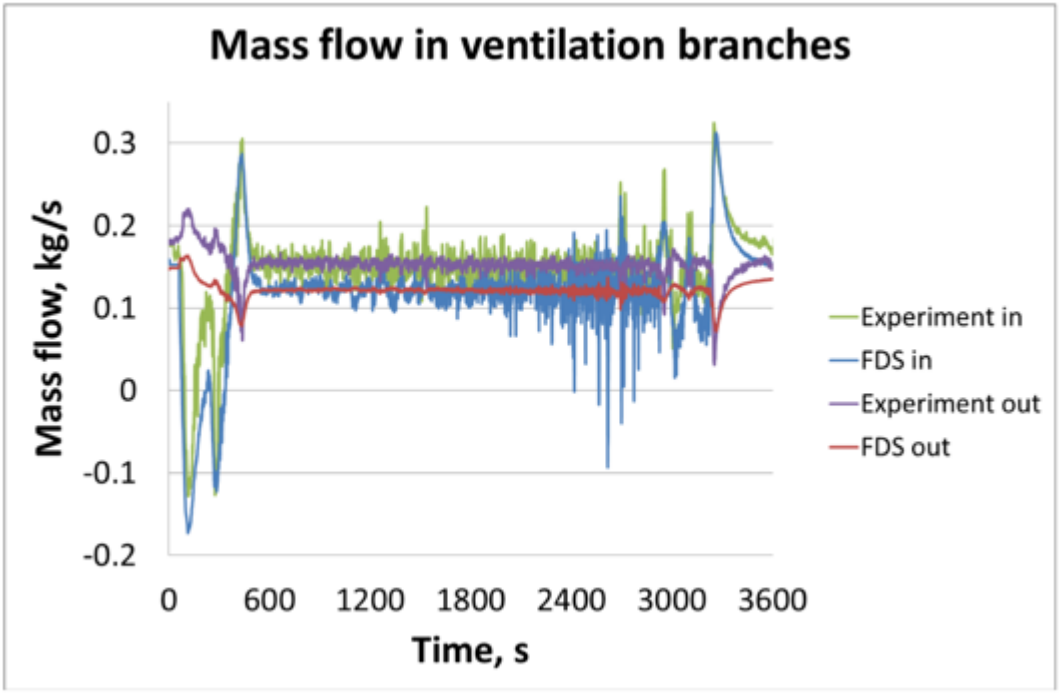

Figure 10 Mass flow in the ventilation branches as a function of time during the experiment.

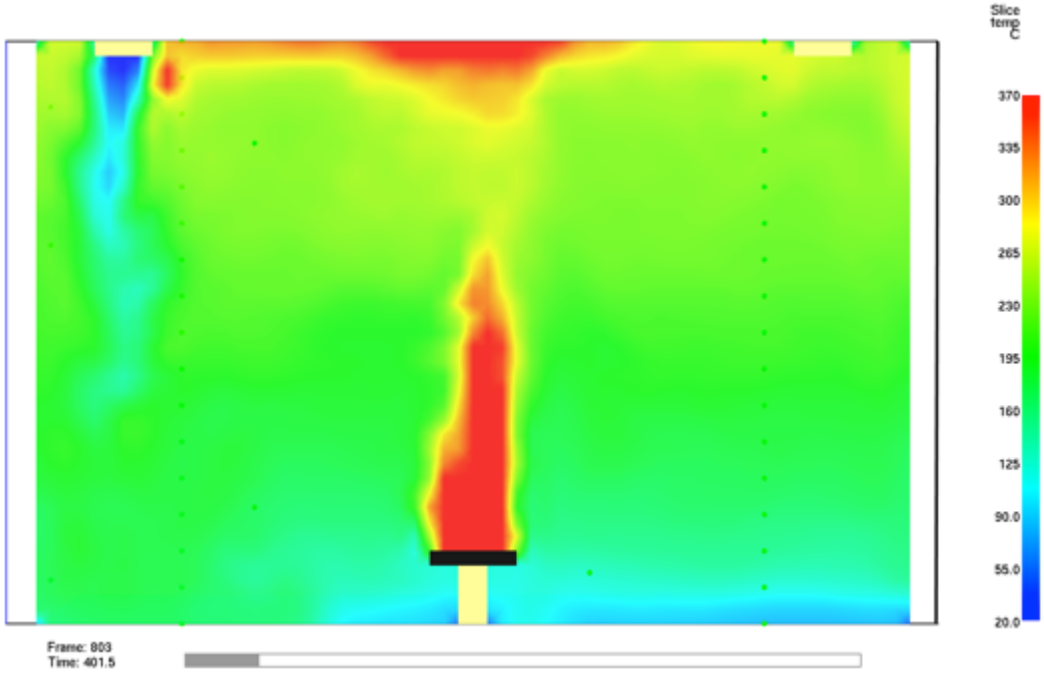

Figure 11 Snapshot of a temperature slice during the simulations done with FDS5. The incoming cold air is clearly visible at the top left corner.

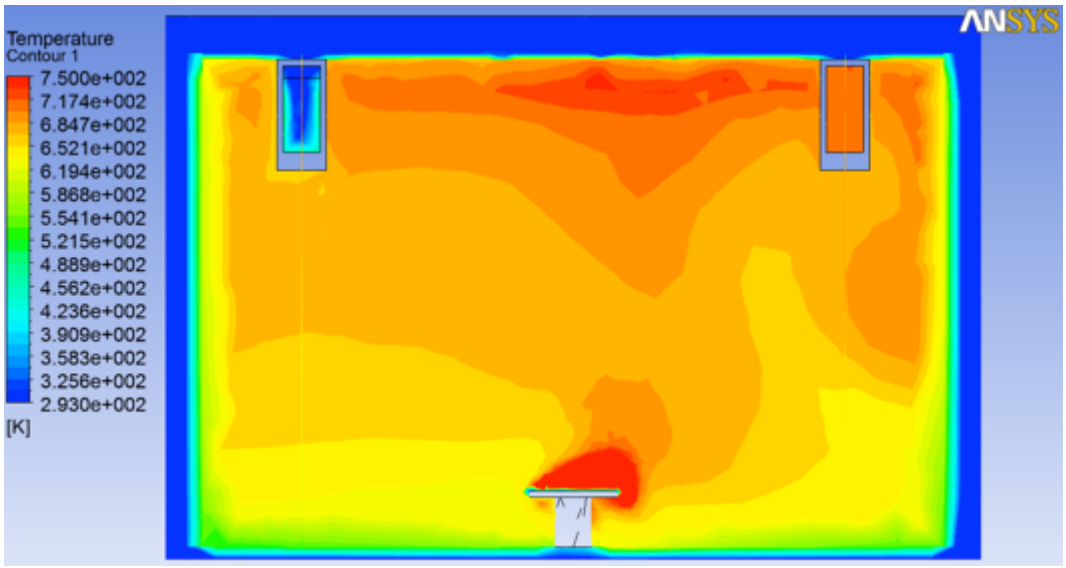

Figure 12 Snapshot of a temperature slice during the simulations done with CFX. The incoming cold air is clearly visible at the top left corner. It can also be seen that the temperature gradient from ceiling to floor is not as steep as shown with FDS5. The maximum temperature is also overestimated to a quite large degree.

From these simulation results it can be seen that the ventilation module is working well when exact data from the complete ventilation system is available. For this project FDS will only be used when it is decided to use the ventilation module.

4. Extended validation of ventilation model in FDS

This work is a part of a larger effort (29-35) to quantify comparisons between several computational results and measurements performed during a pool fire scenario in a well-confined compartment with forced ventilation. The experimental scenarios were conducted at the French "Institut de Radioprotection et de Sûreté Nucléaire" (IRSN) between 2007 and 2011. Most of the PRISME 1 project will remain confidential until 2015 for non-participating countries, which unfortunately mean that some information will be withheld in this paper. However, enough specifications will presented to allow the reader to understand the objective and setup for each test series.

4.1. Fire Experiments

4.1.1. Description of the experimental facility

The DIVA rig (see Figure 13) is located in the IRSN laboratories within a facility known as JUPITER (30). It offers a large-scale multi-room set-up comprising four rooms (labeled from 1 to 4) and a corridor in 0.3 m thick concrete walls equipped with a mechanical ventilation system. The facility can be used both with a single room-setup as well as combinations of connected rooms and a connecting corridor. Inlet and exhaust ducts are normally situated in the upper part of each room, near the ceiling, unless changed for specific tests. The complete ventilation system is very complex installation with extensive use of valves, bends and changes in duct dimensions to be able to control the flow and air resistance to each branch and room. All tests that have been analyzed in this work were performed in the DIVA

facility.0

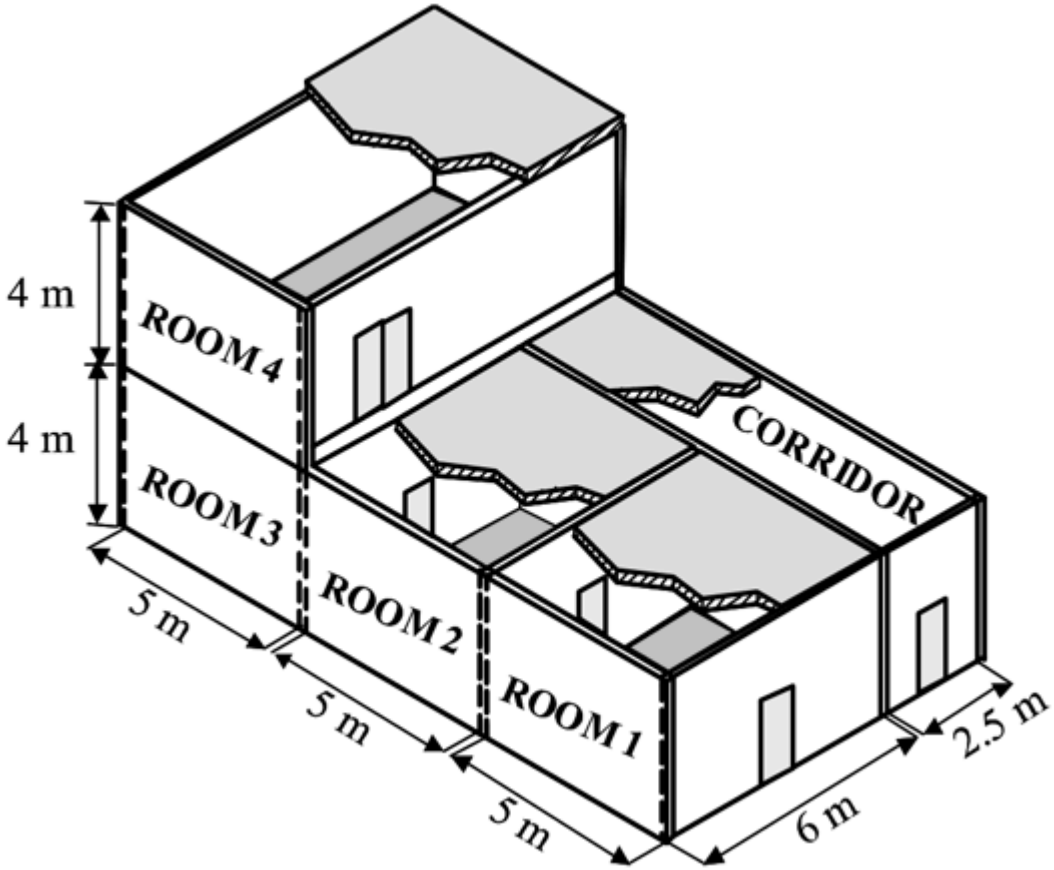

Figure 13 Schematic of the DIVA facility. Figure courtesy of IRSN.

4.2. Overview of the performed test series

In total 4 different test series focusing on large-scale, well-confined, mechanically ventilated fire scenarios were performed within PRISME 1. An overview of the project was published for public access (30) but a short summary of the tests is presented for quick reference:

- **PRISME Source**; tests containing open calorimeter tests and pool fires in a ventilated enclosure. Open calorimeter tests were not considered in this work since the ventilation system behavior was the main focus. Since some tests were similar with only minor changes (height placement of inlet branch) only 4 tests in total were compared to simulations performed with FDS 6.
- **PRISME Door**; tests with a pool fire in one mechanically ventilated room connected to one or more than one mechanically ventilated room. Some tests in this series included evaluation of the functional performance of cables when exposed to hot and sooty gasses. Simulations including the cable response were not performed since it was not required to predict the ventilation system behavior.
- **PRISME Leak**; tests with a pool fire in one room connected to other rooms by means of several types of leakages. Two tests from this series were chosen since they were the most suitable for the application. The excluded tests included more complex leak flow mechanisms that would only aggravate the intended application of predicting the ventilation system behavior. More

detailed work done on the experimental and theoretical aspect of parts of this tests series has been published for public access (33).

- **PRISME Integral**; tests containing test with real objects such as cables and cabinets but also with sprinkler systems. None of the tests in this series were chosen due to the complex phenomena that occurred in these experimental setups. For example, the activation of the sprinkler system would create large pressure peaks that would affect the ventilations system behavior, making the tests unsuitable for initial validation of a model. More detailed work done on the experimental and theoretical aspect of parts of this tests series has been published for public access (34).

4.3. Modeling with FDS

Previous versions of Fire Dynamics Simulator (FDS) (38) only had the ability to specify either fixed flow boundary conditions (velocity or mass flux) or a simple pressure boundary condition. While these inputs could adequately represent very simple HVAC features, they could not model an entire multi-room system. There was no coupling of the mass, momentum, and energy solutions amongst the multiple inlets and outlets comprising the HVAC network (39). To address this limitation, an HVAC network solver was added to FDS (40). The solver computes the flows through a duct network described as a mapping of duct segments and nodes where a node is either the joining of two or more ducts (a tee for example) or where a duct segment connects to the FDS computational domain. The current HVAC solver does not allow for mass storage in the duct network (i.e. what goes in during a time step, goes out during a time step) (41). HVAC components such as fans and binary dampers (fully open or fully closed) can be included in the HVAC network and are coupled to the FDS control function capability. There is also an option to select from three fan models (39). A series of verification exercises has demonstrated that the network model correctly models HVAC flows and that it's coupling with FDS maintains mass conservation (40). A simple and a complex validation exercise show that the combined solvers can accurately predict HVAC flows for a duct network in a complex geometry with fire effects (40), but there is still need for validating the model with more complex and detailed experimental scenarios. The tests performed in the DIVA facility was a perfect candidate for this task, since it is a multi-room setup with an elaborate mechanical HVAC system and a very tightly sealed compartment.

All simulations were done using FDS 6 (SVN 11220) since the latest officially released version (FDS5, SVN 7031) did not have the full functionality for simulating the HVAC network.

4.3.1. Mass loss rates

The mass loss rate calculated from the experimental data (42,43) has been used as input for all simulations without smoothing. No smoothing was used since filtering too much fluctuation could end up removing certain phenomena that are dependent on short pressure peaks, such as back flow in the inlet/inlets.

4.3.2. Modeling of the HVAC system

Since the ventilation system used in the DIVA facility was rather complex, a simplified approach had to be taken when modeling the HVAC system. Instead of

trying to model every pipe, bend, valve and other components, the flow resistance coefficient between nodes were calculated using initial pressure data from each test. The flow resistance, or loss coefficients, between each node were calculated using Equation 6(44):

$$K = \frac{2 \cdot \Delta p_{nodes}}{\rho_{air} \cdot u_{duct}^2} \qquad \textbf{Equation 6}$$

Where K is the loss coefficient, Δp_{nodes} is the pressure difference between two nodes, ρ_{air} is the density [kg/m^3] of air at before ignition and u_{duct} is the velocity in each specific duct section (calculated by dividing volume flow by duct section area). Figure 14 displays how the experimental data before ignition was reported (right) and how the simplified HVAC network in the DIVA facility was setup (left).

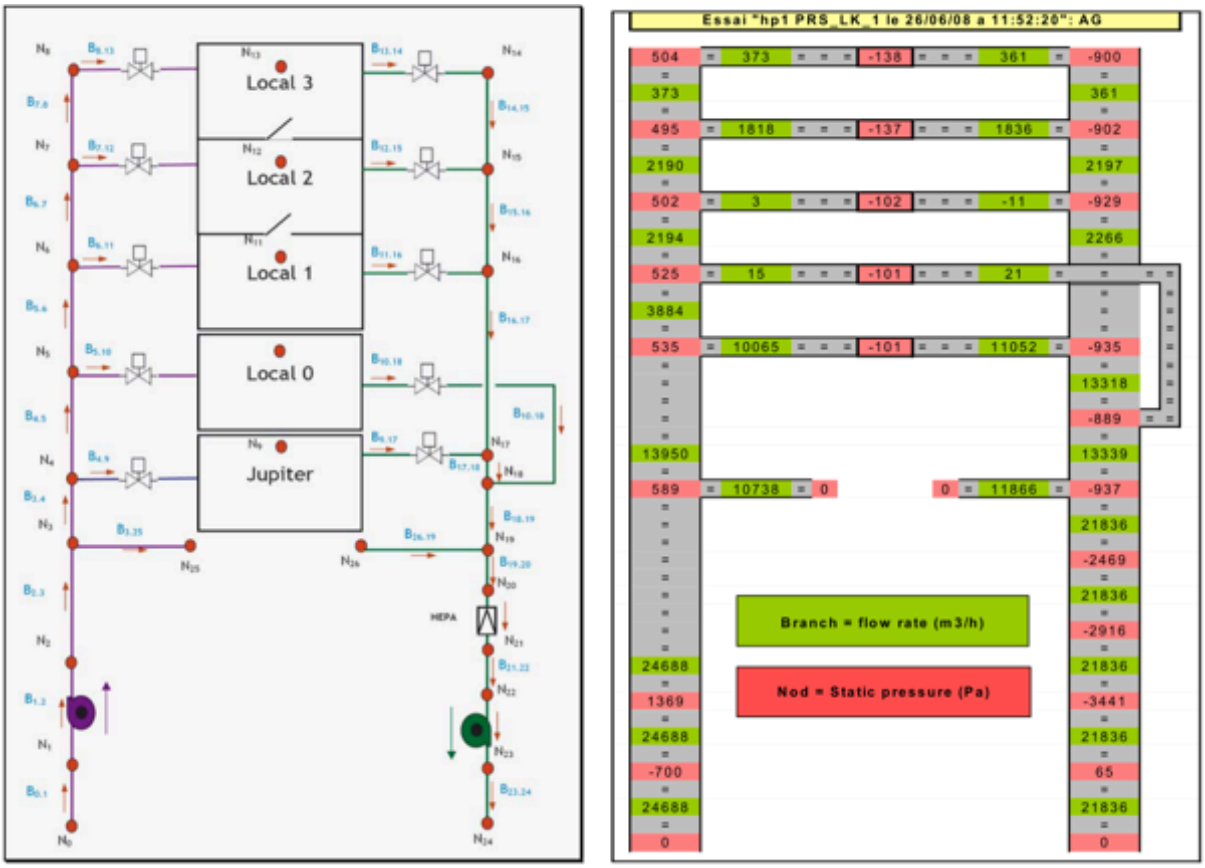

Figure 14 Initial ventilation data before ignition for PRISME Leak 1. Figure courtesy of IRSN.

4.3.3. Inlet- and exhaust fans

The fans were operating at a fixed speed throughout each individual test (and simulation). The fans that were used were a good match to the basic quadratic fan model built into FDS (29) for the working area of the fans during all tests. The quadratic fan model is shown in Equation 7:

$$\dot{V}_{fan} = \dot{V}_{max} \cdot sign(\Delta p_{max} - \Delta p) \cdot \sqrt{\frac{|\Delta p - \Delta p_{max}|}{\Delta p_{max}}} \qquad \textbf{Equation 7}$$

where $\dot{V}_{fan}$ is the resulting volume flow of the fan [m^3/s], $\dot{V}_{max}$ is the free flow value of the fan [m^3/s], Δp_{max} is the stall pressure of the fan [Pa] and Δp is the current downstream pressure difference [Pa]. An example of a resulting fan curve can be seen in Figure 15.

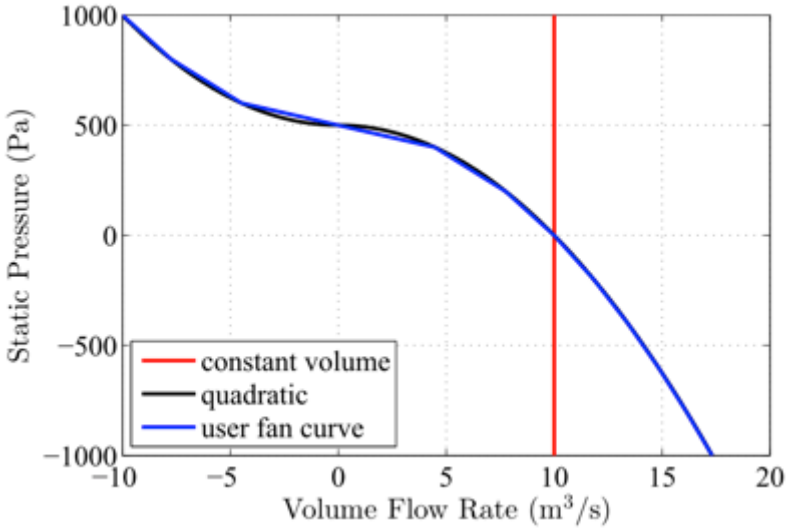

Figure 15 Example of a resulting fan curve when using the quadratic fan model built into FDS (39).

Since each test had changes in the ventilation network (changed valve values and thereby loss coefficients and changed rotations per minute (RPM) of the fan) and consequently different volume flow, the fan curve had to be adapted for each test by changing the fan curve using the fan affinity laws shown in Equation 8 and Equation 9 (45):

$$\dot{V}_{max,2} = \dot{V}_{max,1} \cdot \frac{RPM_2}{RPM_1} \qquad \textbf{Equation 8}$$

$$\Delta p_{max,2} = \Delta p_{max,1} \cdot \sqrt{\frac{RPM_2}{RPM_1}} \qquad \textbf{Equation 9}$$

Using these relations simplified the changes to the fan curves so that the initial conditions for each test could be matched as close as possible to the experiments.

The ventilation system was started 60 seconds prior to ignition of the fire, making sure that the flow pattern had stabilized.

4.3.4. Room leakage

Tests to measure the leak rate of rooms in the DIVA facility were conducted and quantified for each test series. The reported leak rate was given in volume flow/hour for a given pressure, which had to be modified for appropriate use in FDS. The leakage model in FDS shown in Equation 10 (38):

$$\dot{V}_{leak} = A_L \cdot sign(\Delta p) \cdot \sqrt{2\frac{|\Delta p|}{\rho_\infty}} \qquad \textbf{Equation 10}$$

Where $\dot{V}_{leak}$ is the volume flow through the leak [m^3/s], A_L is the size of the leakage area [m^2], Δp is the pressure difference between the adjacent compartments [Pa] and ρ_∞ is the ambient density [kg/m^3]. The discharge coefficient normally seen in this type of formula is assumed to be 1 (38). By rearranging Equation 10 the leakage area could be calculated from the experimental data:

$$A_L = \frac{\dot{V}_{leak}}{sign(\Delta p) \cdot \sqrt{2\frac{|\Delta p|}{\rho_\infty}}} \qquad \textbf{Equation 11}$$

The calculated total leakage area of the DIVA facility was in the order of 2-8 cm^2 depending on the configuration (amount of rooms). This was considered to be a tightly sealed structure compared to leakage class tight specified in the in the SFPE handbook, Table 4-12.1 (46), which would give a total leak area of about 135 cm^2.

4.3.5. Initial conditions

To be able to predict the ventilation behavior in fire conditions it would be crucial to also be able to model the non-fire situation. Table 4 summarizes the difference in node pressure between the experimental data and simulations at the inlets and exhausts for all tests. The pressures at these nodes were the most critical ones since they govern the flow behavior to a large extent. As seen in Table 4 the results were in good agreement with the experimental data.

	Difference between experiment and simulation [%]										
Node	SI-D1	SI-D2	SI-D3	SI-D6a	D2	D3	D4	D5	D6	LK1	LK3
N6 (R1 in.)	-	-	-	-	-0.84	0.29	-2.37	-1.22	-1.13	-	-
N7 (R2 in.)	-4.87	0.50	0.14	-0.37	-0.83	0.30	-2.52	-1.21	-0.88	0.15	0.05
N8 (R3 in.)	-	-	-	-	-	-	-	-	-0.87	-3.46	0.05
N14 (R3 ex.)	-	-	-	-	-	-	-	-	-3.42	0.20	-0.04
N15 (R2 ex.)	0.15	-2.57	-0.03	-0.25	0.17	0.29	-1.37	-0.90	-3.41	0.20	-0.05
N16 (R1 ex.)	-	-	-	-	0.23	0.32	-1.39	-0.88	-4.45	-	-

Table 4 Comparison of the pressure at critical nodes in the HVAC system prior to ignition.

4.4. Results

The next sections present the comparison between experimental data and simulations done using FDS 6 for some selected simulated scenarios. Since the objective of this initial work was to characterize and simulate the ventilation system and its behavior, only results concerning pressure and flows at inlets and exhausts are presented.

4.5. Results Source tests

4.5.1. Source D1

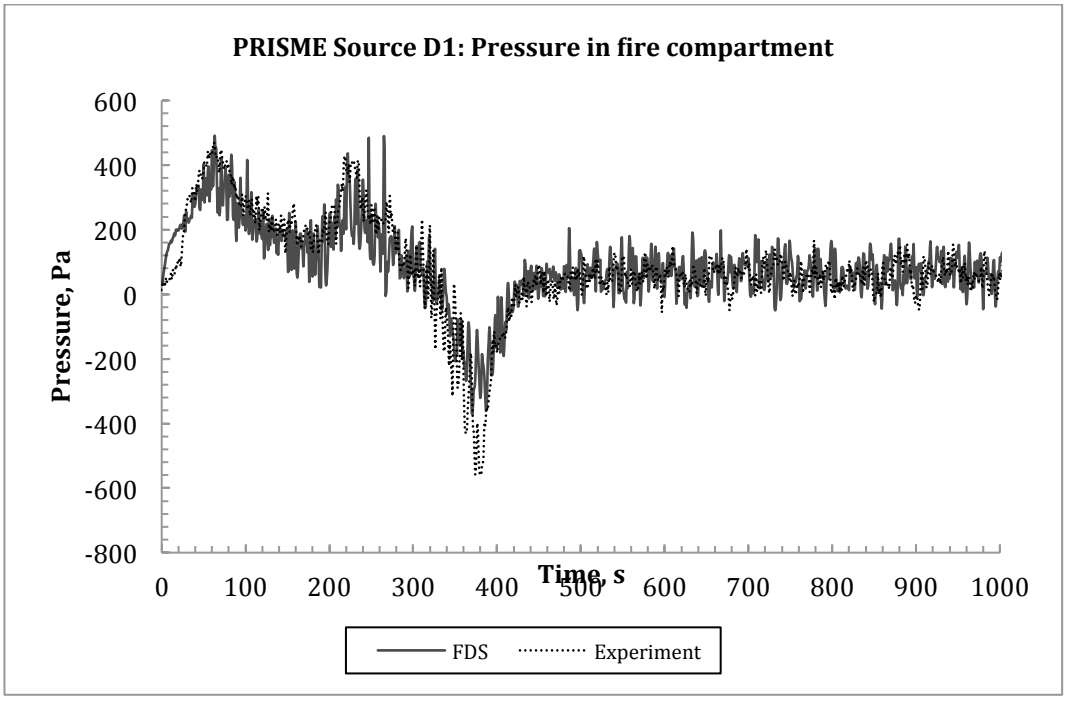

Figure 16 The predicted pressure inside the fire compartment compared to the experimental data from test Source D1 (SI_D1).

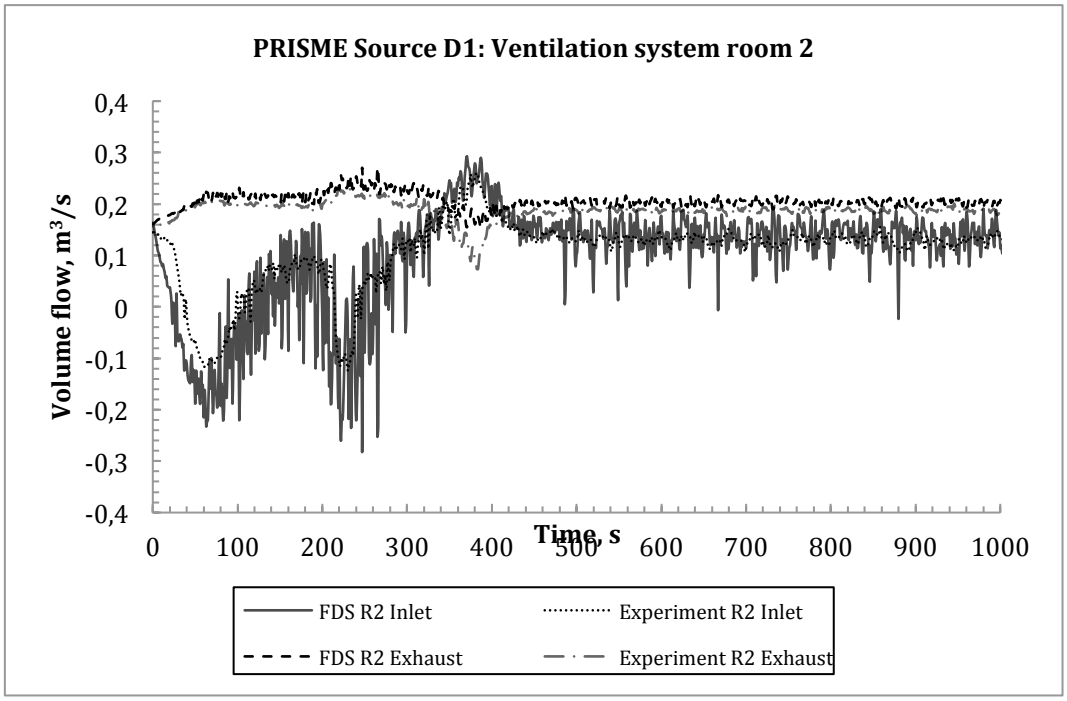

Figure 17 The predicted flow rates at inlet and exhaust in the fire compartment compared to the experimental data from test Source D1 (SI_D1).

4.5.2. Source D3

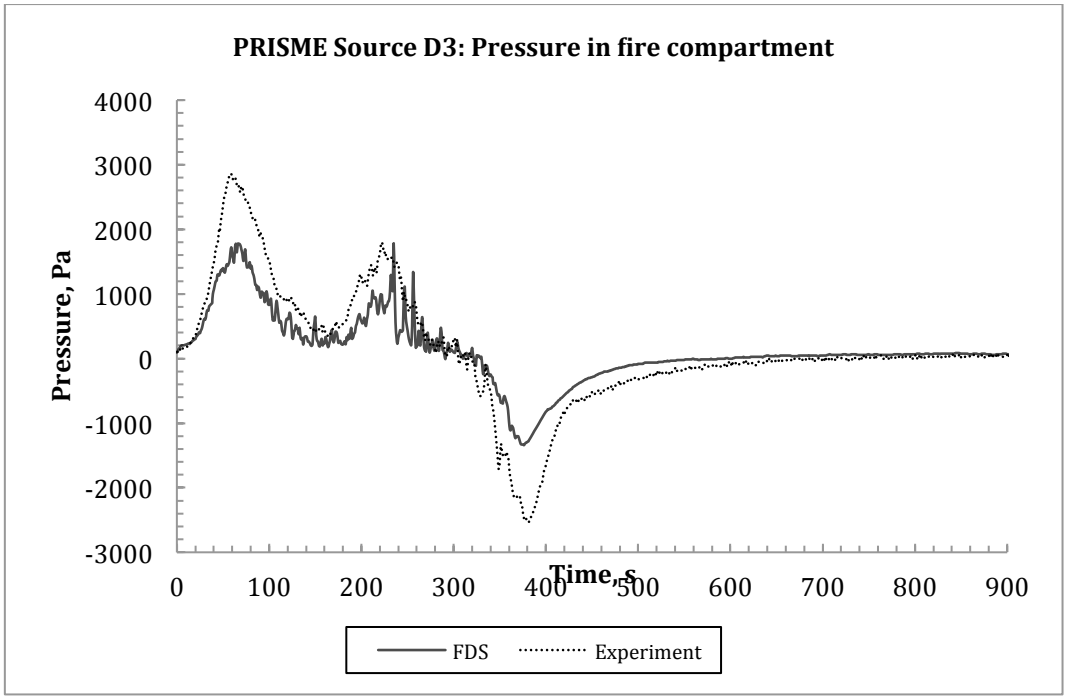

Figure 18 The predicted pressure inside the fire compartment compared to the experimental data from test Source D3 (SI_D3).

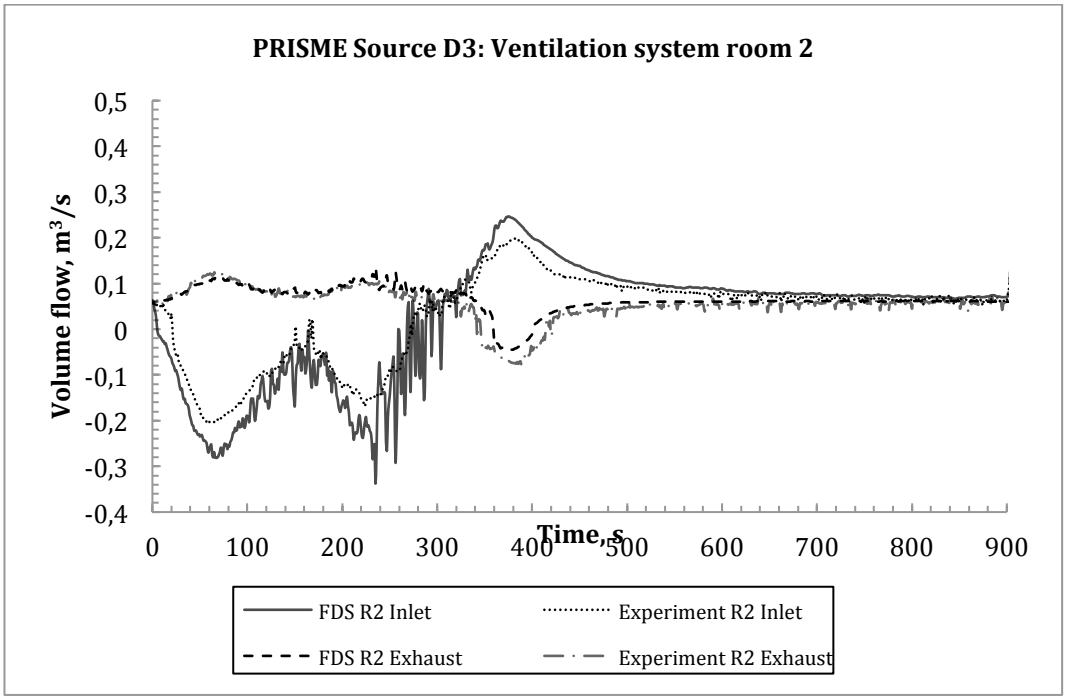

Figure 19 The predicted flow rates at inlet and exhaust in the fire compartment compared to the experimental data from test Source D3 (SI_D3).

4.5.3. Source D6a

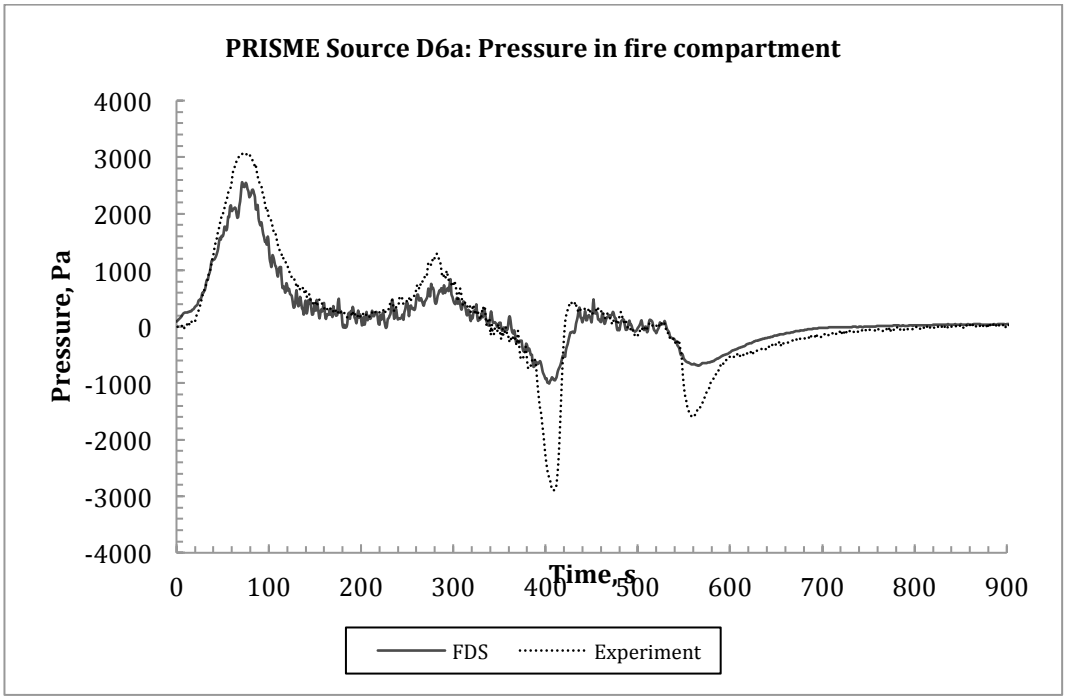

Figure 20 The predicted pressure inside the fire compartment compared to the experimental data from test Source D6a (SI_D6a).

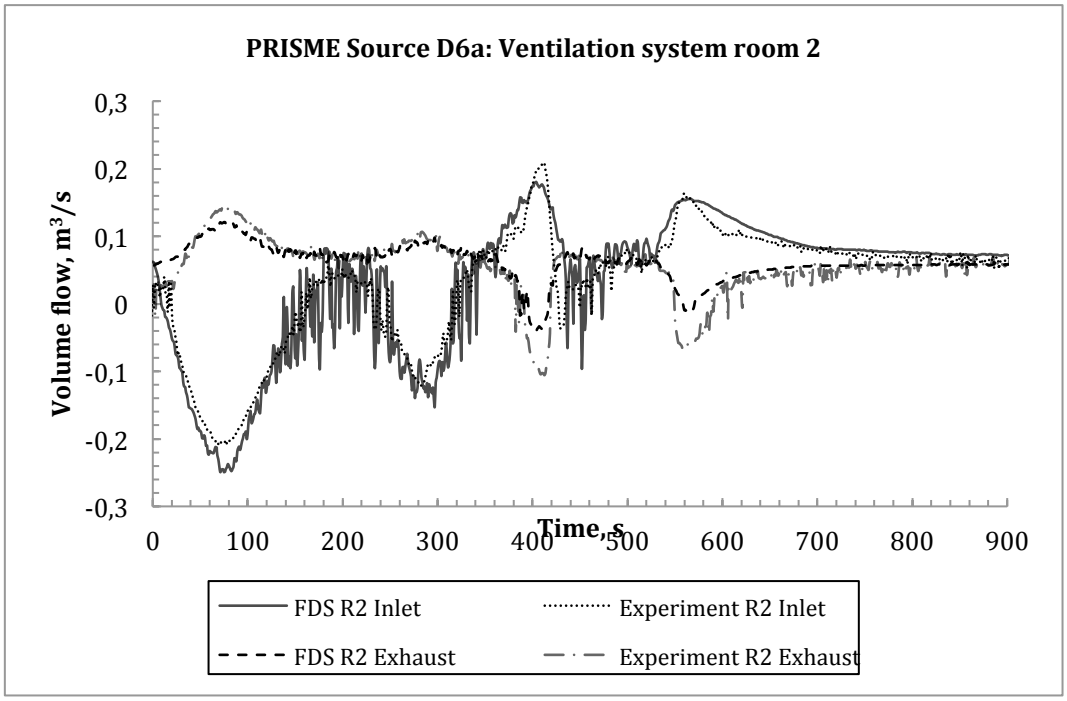

Figure 21 The predicted flow rates at inlet and exhaust in the fire compartment compared to the experimental data from test Source D6a (SI_D6a).

4.6. Results Door tests

4.6.1. Door 2 (D2)

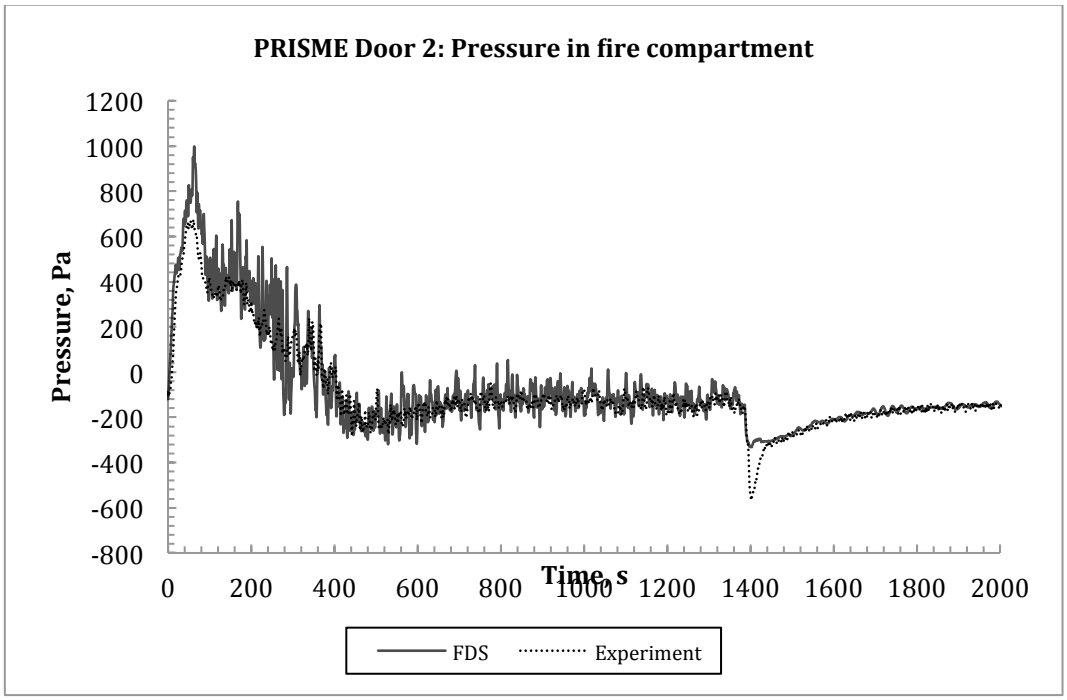

Figure 22 The predicted pressure inside the fire compartment compared to the experimental data from test Door 2 (D2).

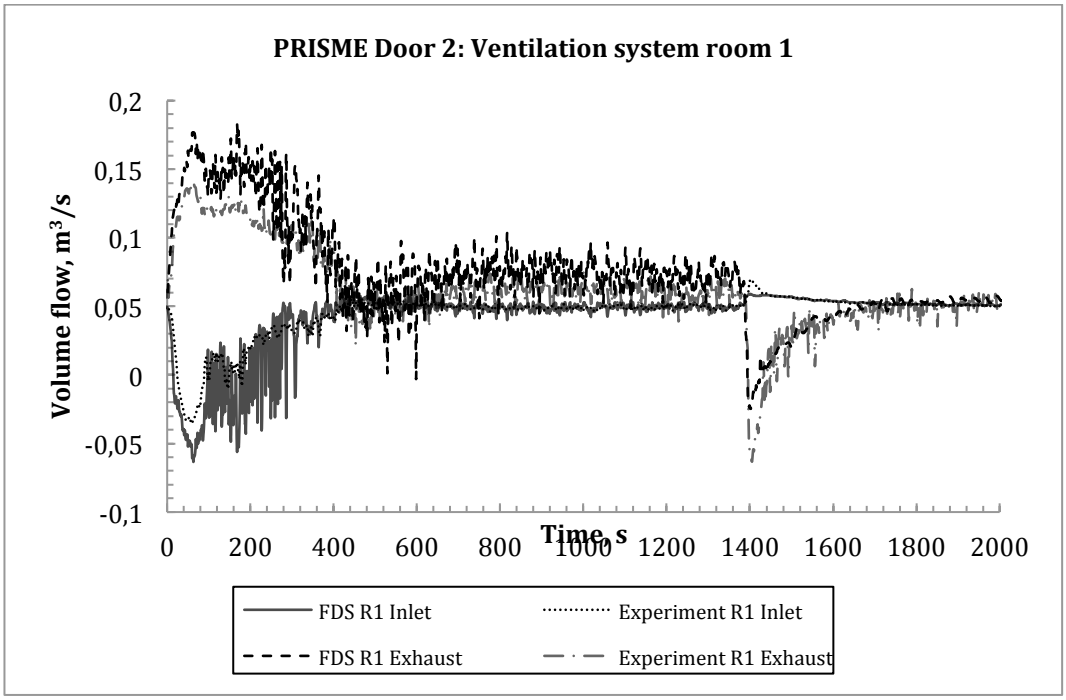

Figure 23 The predicted flow rates at inlet and exhaust in the fire compartment compared to the experimental data from test Door 2 (D2).

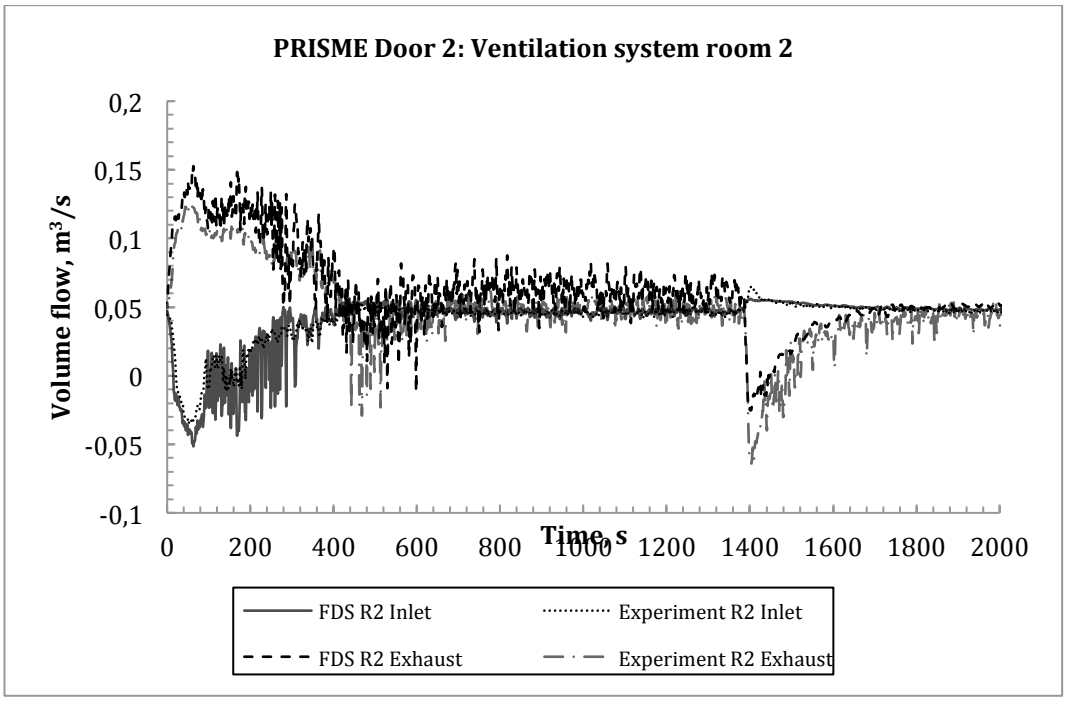

Figure 24 The predicted flow rates at inlet and exhaust in the fire compartment compared to the experimental data from test Door 2 (D2).

4.6.2. Door 5 (D5)

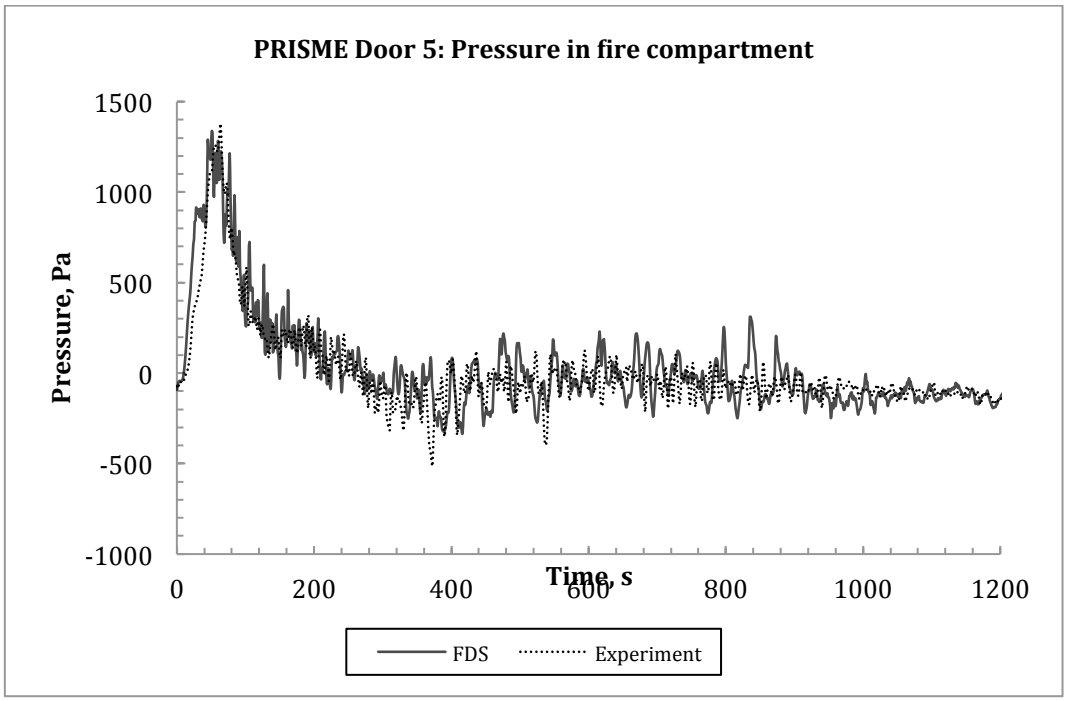

Figure 25 The predicted pressure inside the fire compartment compared to the experimental data from test Door 5 (D5).

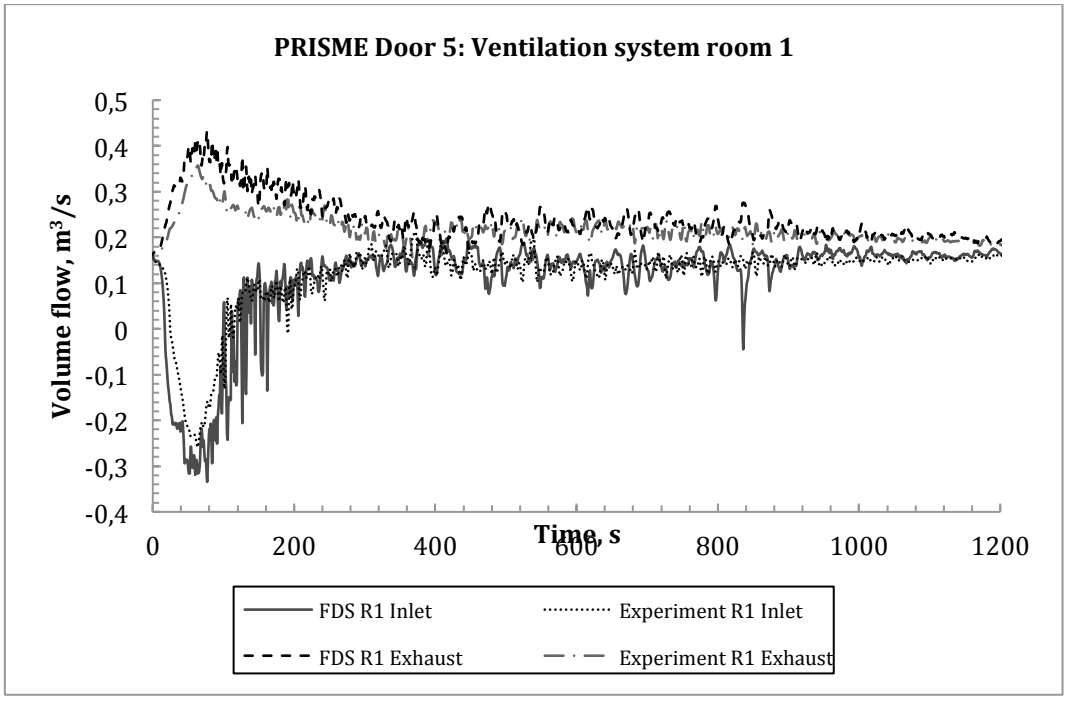

Figure 26 The predicted flow rates at inlet and exhaust in the fire compartment compared to the experimental data from test Door 5 (D5).

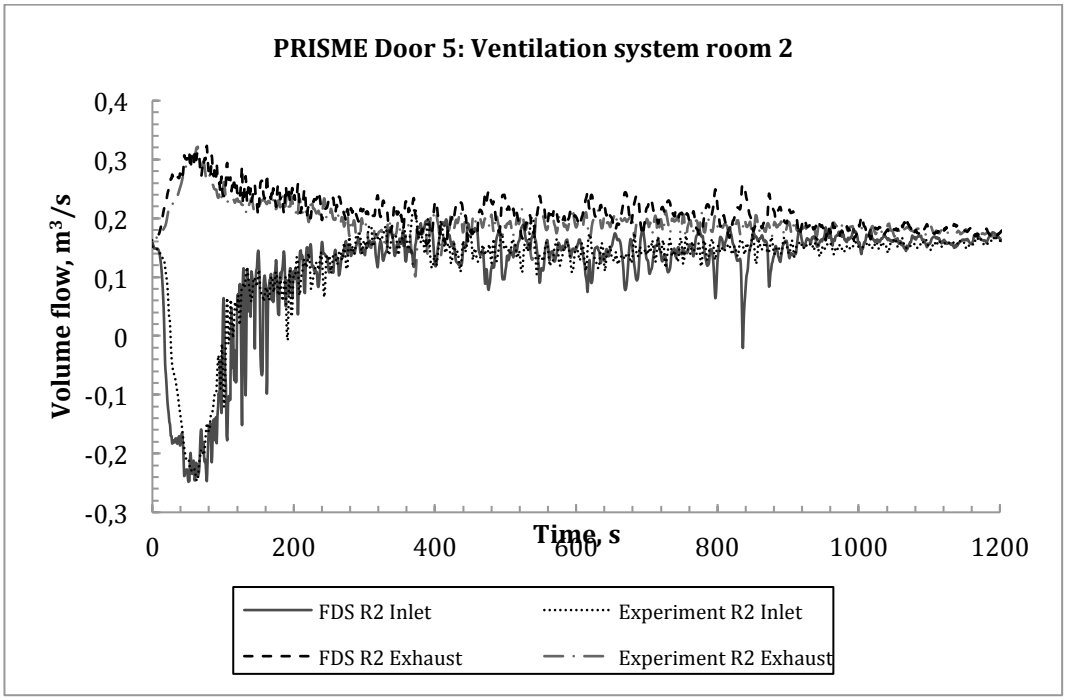

Figure 27 The predicted flow rates at inlet and exhaust in the fire compartment compared to the experimental data from test Door 5 (D5).

4.6.3. Door 6 (D6)

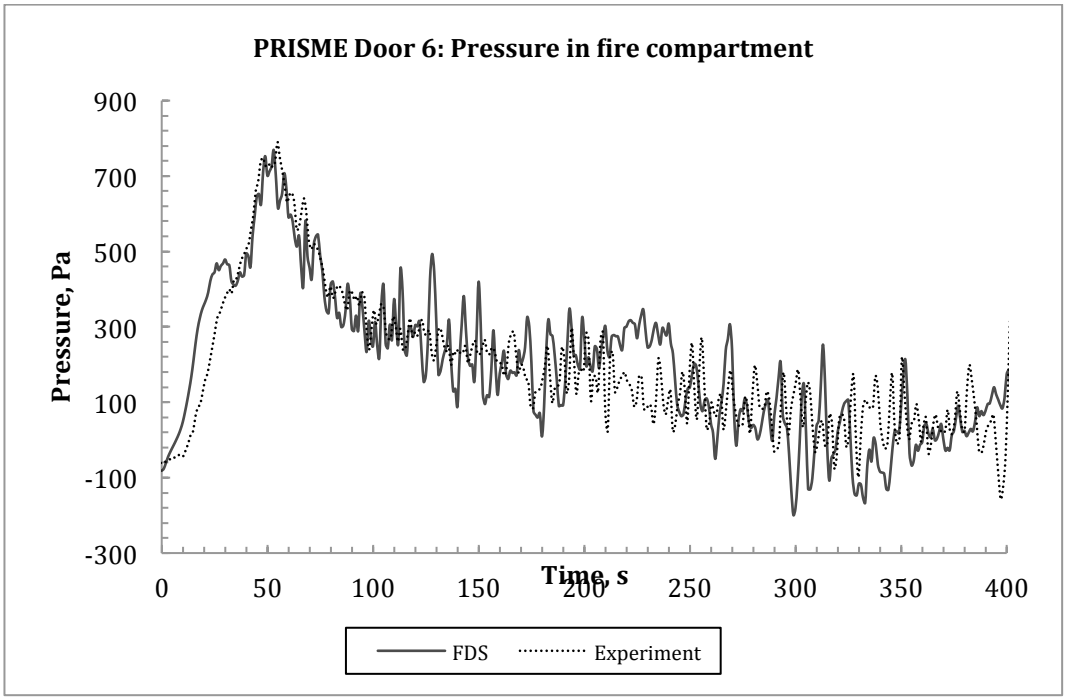

Figure 28 The predicted pressure inside the fire compartment compared to the experimental data from test Door 6(D6).

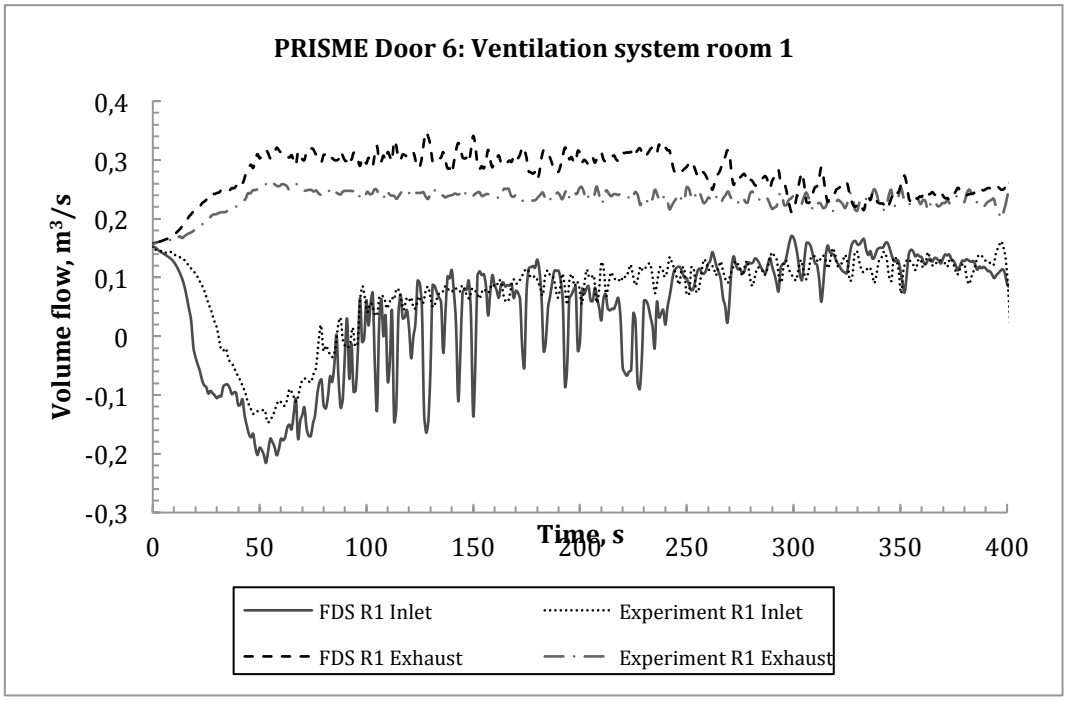

Figure 29 The predicted flow rates at inlet and exhaust in the fire compartment compared to the experimental data from test Door 6 (D6).

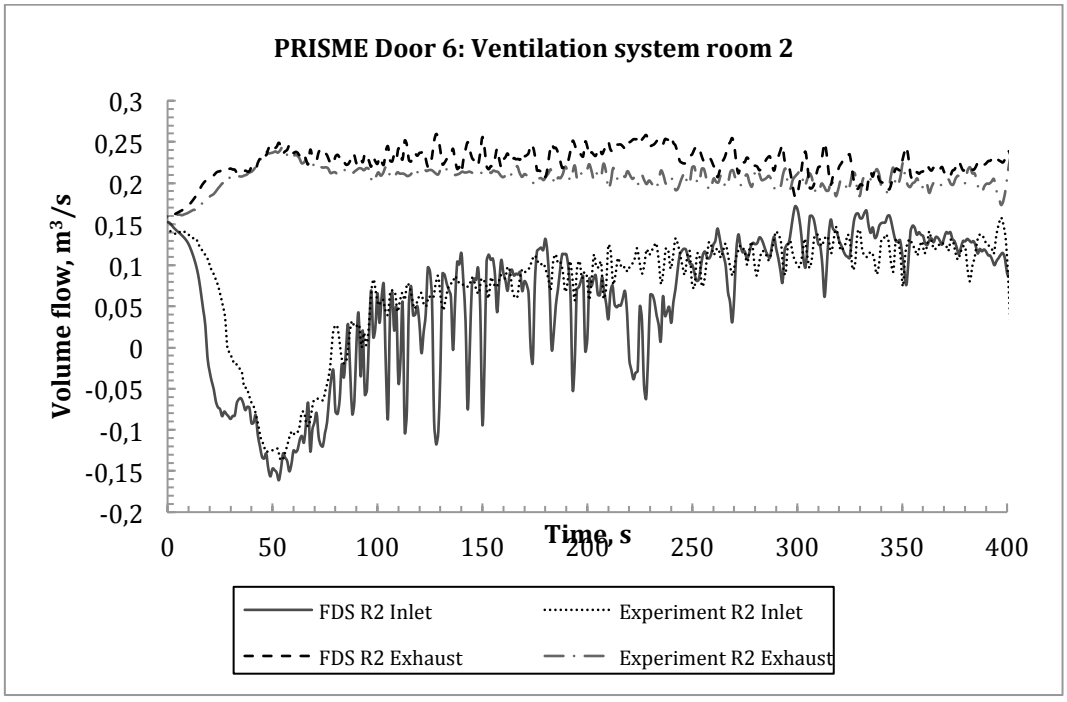

Figure 30 The predicted flow rates at inlet and exhaust in the fire compartment compared to the experimental data from test Door 6 (D6).

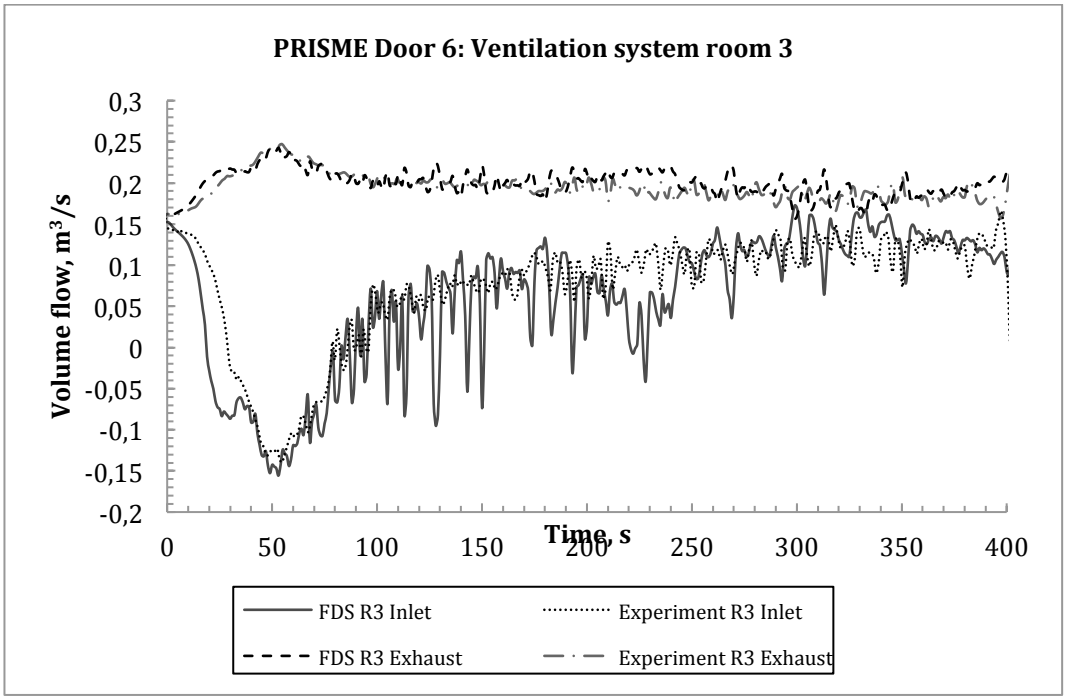

Figure 31 The predicted flow rates at inlet and exhaust in the fire compartment compared to the experimental data from test Door 6 (D6).

4.7. Results Leak tests

4.7.1. Leak 1

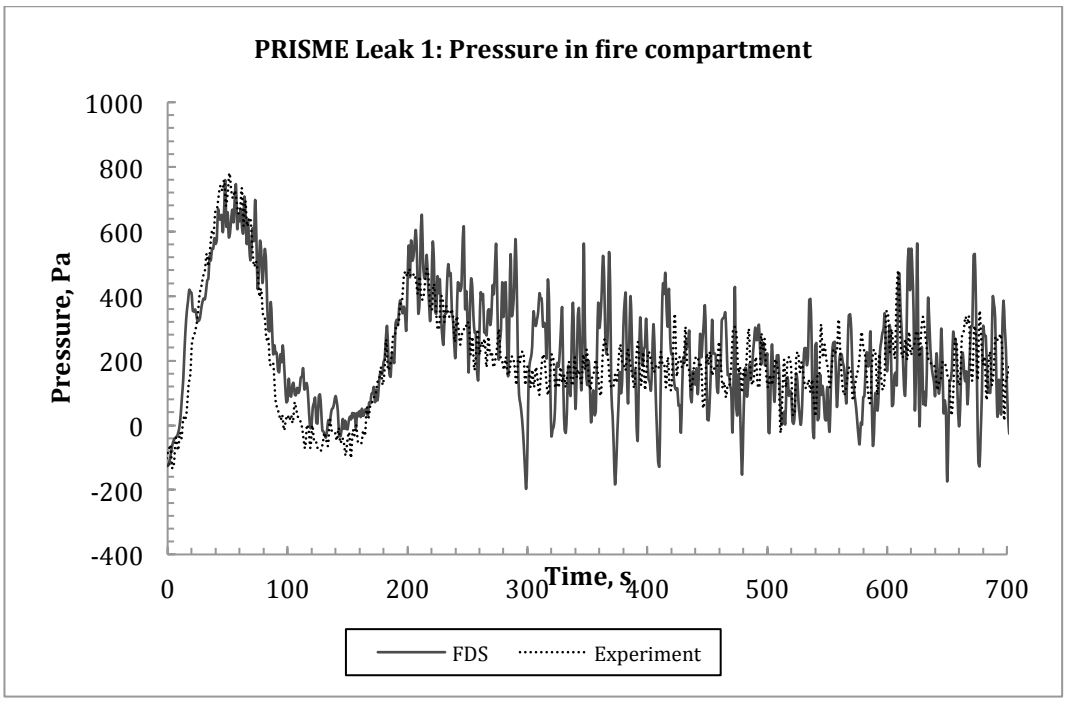

Figure 32 The predicted pressure inside the fire compartment compared to the experimental data from test Leak 1 (LK1).

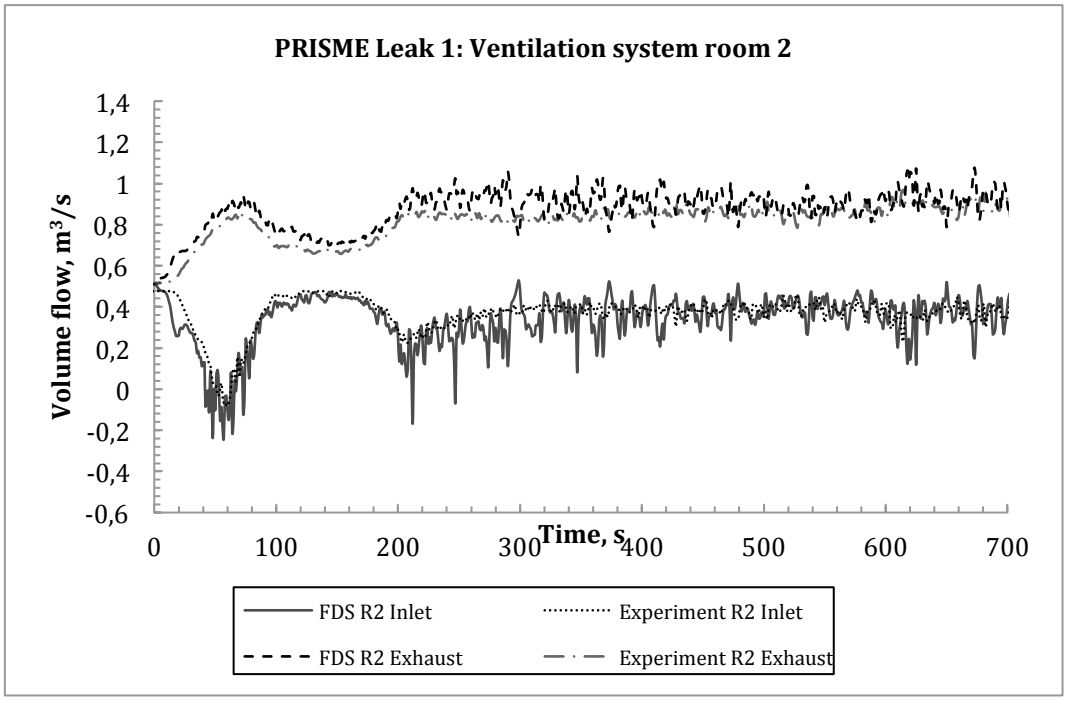

Figure 33 The predicted flow rates at inlet and exhaust in the fire compartment compared to the experimental data from test Leak 1 (LK1).

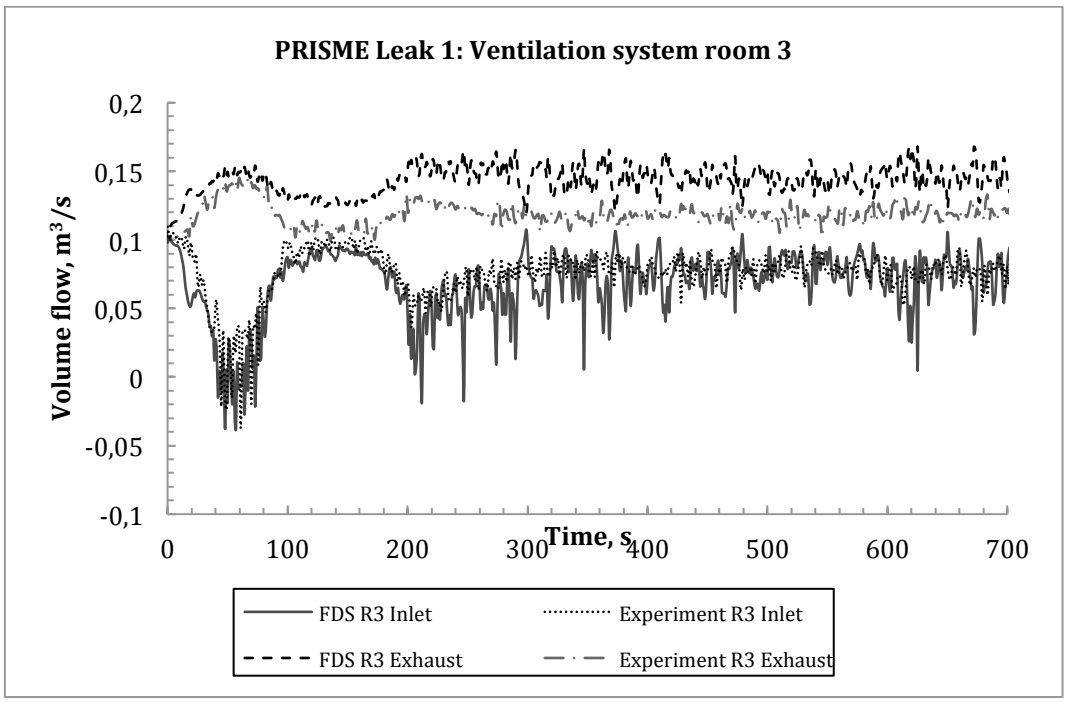

Figure 34 The predicted flow rates at inlet and exhaust in the fire compartment compared to the experimental data from test Leak 1 (LK1).

4.8. Summary of results

4.8.1. Initial conditions

Pressure data at inlets and exhausts prior to ignition are in good agreement with the experimental data. All results are within 5% difference margin and most cases even less. This was an important step for giving confidence in the model to continue with the fire scenarios and try to model more advanced HVAC system behavior.

4.8.2. Fire conditions

Overall FDS manages to correctly predict the pressure peaks induced by the fire in most tests with acceptable accuracy.

In Source D3 and Source D6 it can clearly be seen that there is a strong mismatch between experimental results and simulation. The magnitude of the pressure peaks are not well captured at all, underestimating the first pressure peak by almost 1000 Pa. Looking at the ventilation results for the same case it is evident that the inlet starts to reverse under less pressure than in the experiment. The inlet acts as a pressure relief, making the predicted pressure peak much lower. The most probable cause is some discrepancy in the experimental data used for calculating the loss coefficients in the inlet branch. The fact that the temperatures inside the fire compartment are in good agreement with the experimental data supports this hypothesis. Changing values for certain loss coefficients would probably result in a better match with experiments, but these two cases serves as good examples of how sensitive the input data can be. This should be kept in mind if doing smoke spread calculations in ventilation systems for engineering purposes.

In other cases there are only minor differences between the experimental data and the simulations. For example, in test Door 6 (D6) it can be seen that the initial pressure peak is not correctly predicted and this can clearly be seen in the inlets to all three rooms. The mass loss rate (which was prescribed from experimental data) in FDS corresponds well with the small pressure peak during the initial pressure rise (Figure 21), while the pressure measured during the experiment does not (Figure 28). A probable cause for this mismatch is either a direct error in the measurement of the experimental mass loss rate or a difference in the mass loss rate and heat release rate, as in un-combusted fuel evaporating. The same initial pressure peak can also be seen in test Door 5 (D5) although not as prominent.

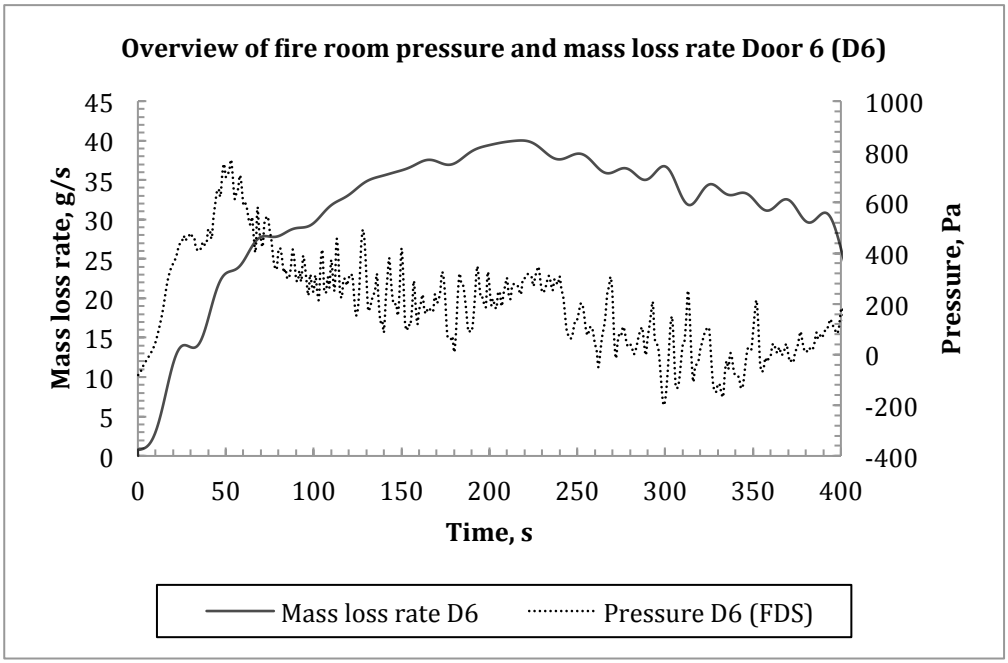

Figure 35 Overview of fire room pressure and mass loss rate during (MLR) test Door 6 (D6).

It can be seen that the sudden decrease of the MLR (at 25 s) directly influences the pressure and in turn the ventilation system behavior (Figure 29-Figure 31), but the same response is not seen in the experimental data (Figure 28). The same observation has been made for test Door 5 (D5).

Generally FDS produces more frequent and more ample pressure fluctuations for all cases. This is probably due to the difference between the given mass loss rate and actual heat release rate in FDS. As seen in Figure 36 the heat release rate fluctuates to a greater extent compared to the prescribed mass loss rate, especially after the initial phase once oxygen levels are lowered. These oscillations correspond to the fluctuations that can be seen in the pressure graphs and are probably partly a product of the large eddy simulation (LES) approach used in FDS, and partly caused by the lowered oxygen levels in the fire compartment(s) combined with the suppression model of FDS (26).

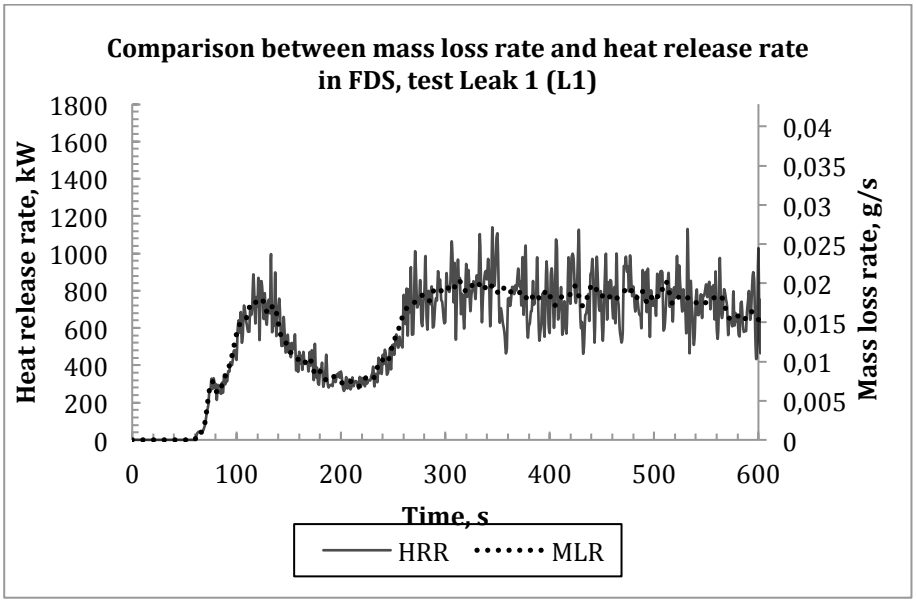

Figure 36 Comparison between mass loss rate and heat release rate in FDS, test Leak 1 (LK1).

4.9. Conclusions

The possibility of simulating a tightly sealed fire room connected to a mechanical ventilation network using FDS has been demonstrated with success. Using only data collected before the fire was ignited (with the exception of mass loss rate from the pool fire), FDS manages to correctly predict the pressure inside the fire room and consequently the effects on the ventilation system, for example backflow in the inlet branch in the early stages of the fire. Although it must be noted that the input parameters are quite sensitive, this could be seen especially in two tests. When the loss coefficients of the inlet and exhaust branches were not correctly characterized, FDS failed to predict the magnitude of the pressure peak and subsequently the magnitude of the response of the ventilation system.

4.10. Future Work

Prescribed constant conditions for burning rate or fuel mass loss rate, so called a posteriori, have been used in the first step of this study, as well as in various numerical fire studies. Using prescribed burning rate CFD codes often show good agreement with experimental results but the burning rate or fuel mass loss rate in an enclosed space with mechanical ventilation is often not easy prescribed without experiments of the exact same configuration. Future work will focus on predicting the mass loss rate of enclosed fires using data collected in a free burning environment or data derived from correlations (for example Babrauskas (47)) by taking the environment feedback and environment interaction into account. This will hopefully increase the understanding of phenomena such as oscillating burning behavior, where the ventilation and fire source interacts coupled to each other.

This model is intended to be a simplified "engineering model" in the sense that the actual liquid phase will not be taken into account, only the incoming radiation to the

surface and the surrounding oxygen fraction will be considered. The model is further described in 5.4.

In order to quantify the leakage in the rooms the air leakage rate could be measured by a door fan test according to DS/EN 13829.

5. Development of a new model

5.1. Model description

In the new evaporation model, the effect of the unresolved concentration boundary layer near the pool surface is taken in to account. In this model the mass flux is given by

$$\dot{m}'' = h_m \rho_{f,g} log\left(\frac{X_G - 1}{X_f - 1}\right). \quad (12)$$

Here $h_m = Sh\mu_g/Sc\Delta x$ is the mass transfer coefficient and $\rho_{l,g}$ and X_G are the density of the fuel vapour and the volume fraction of fuel vapour in the grid cell adjacent to the pool surface. The Schmidt number Sc is 1 and the Sherwood number is given by

$$Sh = 0.037 Sc^{\frac{1}{3}} Re^{\frac{4}{5}}. \quad (13)$$

The Reynolds number $Re = \rho_g v_g/\Delta x \mu_g$ is calculated based on conditions in the cell adjacent to the surface.

5.2. Preliminary comparisons of old and new liquid evaporation models

5.2.1. Models for open atmosphere PRISME tests (PRISME SOURCE)

The test data considered here is from the PRISME project. The tests were conducted in free atmosphere under the SATURNE hood (20). The fuel in all the tests considered here was hydrogenated tetrapropylene (TPH). The tests involve a single pan of TPH under the SATURNE hood. The pan is 100 mm deep and the fuel depth is 50 mm in all except one test where it was 80mm. The surface area of the pan was varied. The physical properties of the fuel are listed in Table 5. The pan is modelled as a layer of TPH followed by a steel plate, followed by insulation. The pan is defined by following FDS lines. An overview of the tests is given in Table 6.

```
&SURF ID='POOL'
    STRETCH_FACTOR=1
    CELL_SIZE_FACTOR=0.25
    COLOR='RED'
    MATL_ID(1,1)='TPH'
    MATL_ID(2,1)='STEEL'
    BACKING = 'INSULATED'
    THICKNESS= 0.05 0.005 /
```

Table 5 Properties of the fuel (TPH)(23)

Property	Value	Units
EMISSIVITY	1	-
HEAT OF REACTION	1098.94	kJ/kg
CONDUCTIVITY	0.18	W/mK
SPECIFIC HEAT	2.4	kJ/kgK
BOILING TEMPERATURE	188	°C
DENSITY	758	kg/m^3
ABSORPTION COEFFICIENT	1000	1/m

Table 6 Test scenarios under investigation

Test name	*Pool Surface Area*	*Fuel Depth*
Units	**m^2**	**mm**
PRS-SI-S1	0.2	50
PRS-SI-S3	0.4	50
PRS-SI-S5	0.1	50
PRS-SI-S7	0.1	80

The purpose of these simulations was to predict the burning rates of the pools. The computational model of the experiments includes only the pan and not the hood. All boundaries, except the bottom boundary are defined open for flow. The bottom boundary is inert. The computational model includes the 50 mm lip of the fuel pan. Two different grid resolutions are used for both the new and the old evaporation model: 25 mm grid cells and 50 mm grid cells. The full set of experiments is run with all parameter combinations. The simulation matrix is given in Table 7.

Table 7 Simulation matrix.

#	Test name	Evaporation model	ΔX
1	PRS-SI-S1	Old	5 cm
2	PRS-SI-S3	Old	5 cm
3	PRS-SI-S5	Old	5 cm
4	PRS-SI-S7	Old	5 cm

5	PRS-SI-S1	New	5 cm
6	PRS-SI-S3	New	5 cm
7	PRS-SI-S5	New	5 cm
8	PRS-SI-S7	New	5 cm
9	PRS-SI-S1	Old	2.5 cm
10	PRS-SI-S3	Old	2.5 cm
11	PRS-SI-S5	Old	2.5 cm
12	PRS-SI-S7	Old	2.5 cm
13	PRS-SI-S1	New	2.5 cm
14	PRS-SI-S3	New	2.5 cm
15	PRS-SI-S5	New	2.5 cm
16	PRS-SI-S7	New	2.5 cm

5.2.2. Results for open atmosphere PRISME tests (PRISME SOURCE)

Figure 37 shows the comparisons of measured and predicted burning rates in the open atmosphere simulations. In all cases, the burning rate is overestimated. Both the new and the old evaporation models exhibit considerable grid dependency. The effect is slightly diminished for the smaller pools. However in these cases the problem could be that the pool fires are not adequately resolved by the grid.

The overall shape of the burning rate curve with slight rise in burning rate towards the end seems hard to reproduce. Some of this dynamic is visible in all the simulations but it is not as pronounced as in the experimental data.

Initially, the new evaporation model, represented by the red lines in Figure 4, suffered from large overshoots. Sharp spikes were observed in the burning rate, which often lead to numerical instabilities. These spikes were caused by the temperature in the surface cell rising very close to the boiling point of the fuel. This in turn would lead to an equilibrium vapour fraction close to unity. Occasionally this would cause the logarithm in Equation (6 to diverge leading to very large mass transfer rates. This problem was solved by limiting the fuel mass fraction at the surface to a value of 0.9999.

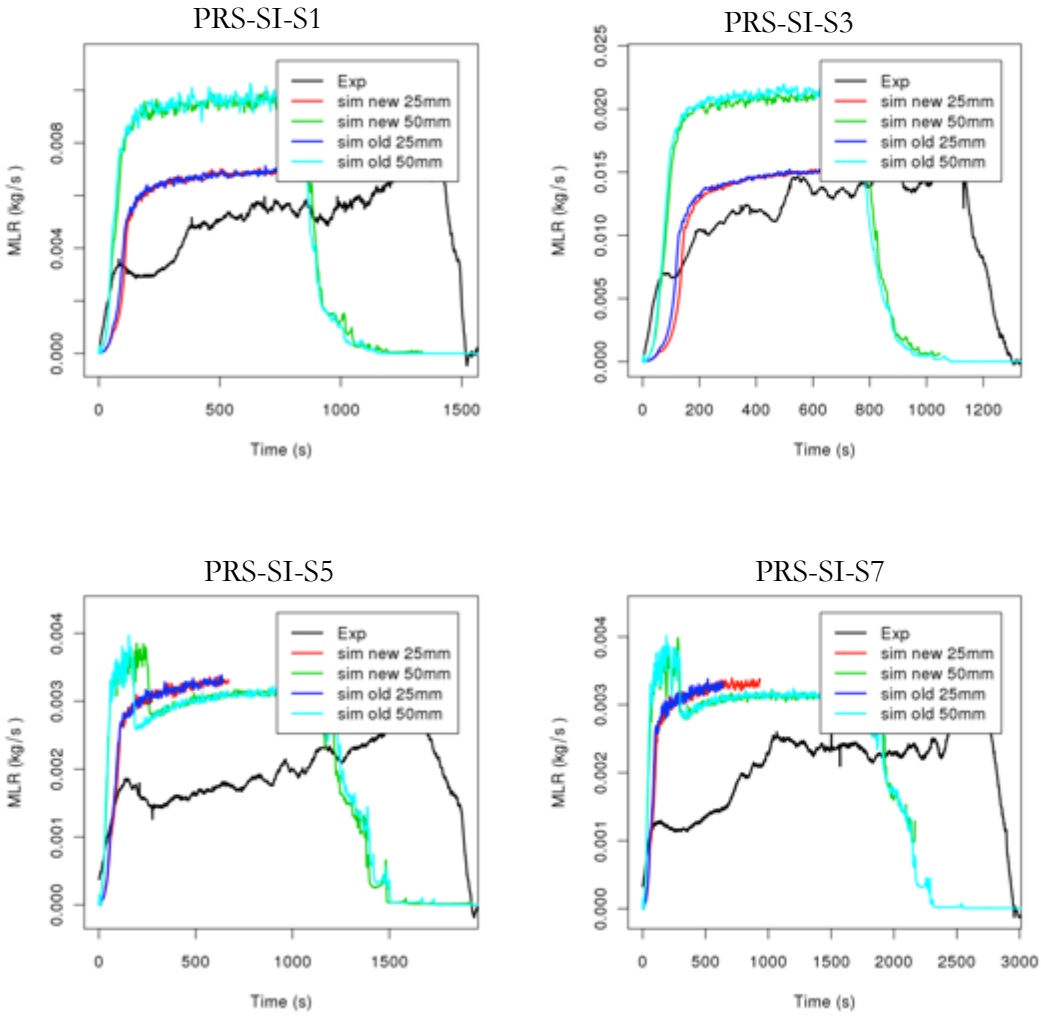

Figure 37 Comparison of pool evaporation models and different grid resolutions.

5.3. Sensitivity studies of the new liquid evaporation model

5.3.1. Sensitivity of the evaporation model to the mass transfer coefficient

The mass transfer calculation in Equation 12 contains a single adjustable parameter: the mass transfer coefficient. Various correlations exist for calculating the overall mass transfer coefficient for various geometries. None of these methods is really valid for use as a boundary condition for a CFD code, since what really is needed is a local mass transfer coefficient. Furthermore, the flow situation in a CFD simulation may be a lot more complex than the correlation allows. Figure 38 shows the burning rate for a 0.3 m x 0.3 m heptane pool fire, as a function of the mass transfer coefficient. The mass transfer coefficient was held constant for the duration of the simulation. The burning rates are not very sensitive to the mass transfer coefficient when the mass transfer coefficient is larger than 10^{-3}. Above that value, an order of magnitude change in the mass transfer coefficient will cause change of only a few percent in the burning rate.

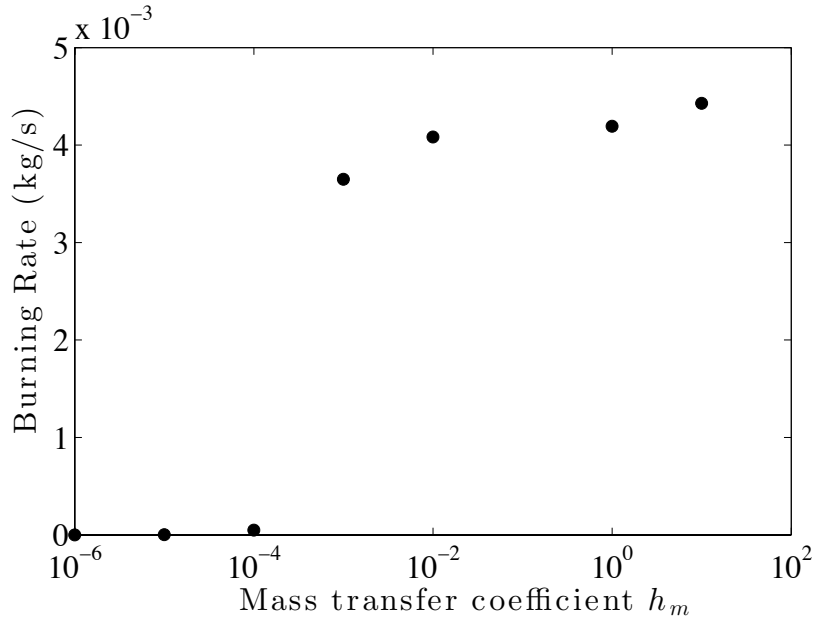

Figure 38 Sensitivity of pool fire burning rate predictions to the mass transfer coefficient.

5.3.2. A word of caution on the in-depth radiation absorption models

The liquid fuel absorption coefficients used in this report are based on curve fits to the experimental data. The details of the fitting procedure are described in the FDS Technical Reference Guide (25). This fitting procedure should ensure that the heat source term distribution within the fuel pools is roughly correct. However the use of in-depth radiation absorption together with the FDS default model of liquid as a semi-transparent solid can lead to some unphysical temperature profiles. Figure 39 shows an instantaneous vertical temperature profile within the fuel when using the radiation transport model. There is a hotspot below the surface, where the temperature has risen significantly over the fuel boiling point, which seems unphysical. In reality, profiles like the one in Figure 39 would probably be smoothed out by convection.

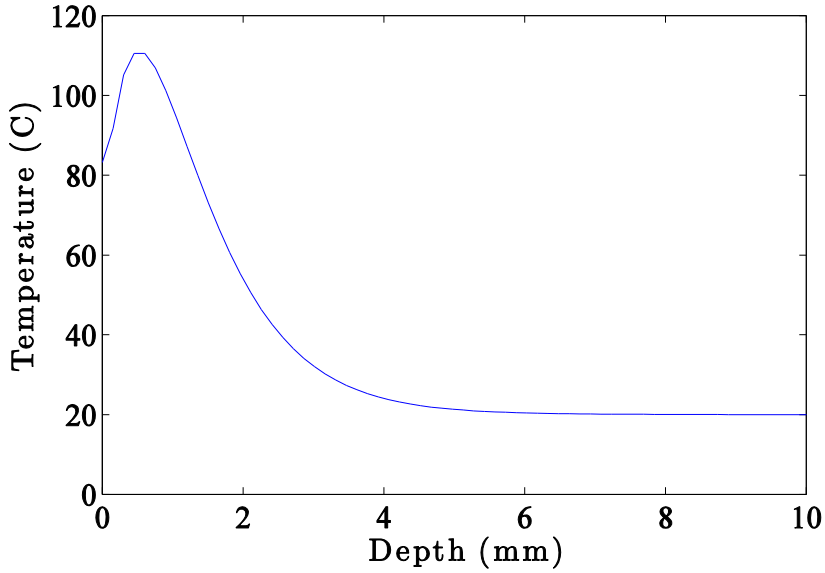

Figure 39 Instantaneous temperature profile within a pool of heptane with the radiation heat transfer within the liquid.

5.3.3. Definitions

To assess the heat feedback to the fuel surface, a set of simulations with the pool fires described as fuel inlet boundary conditions were conducted. The fuel injection rate was obtained from either correlations or from experimental data. Similarly the expected heat flux to the fuel surface was obtained from experimental measurements where available. When measurements were not available, the expected radiative feedback was approximated from the given mass-burning rate using the following formula:

$$\dot{q}''_{in} = \frac{\dot{m}''}{h_{v,sen}}. \tag{14}$$

Here $\dot{m}''$ is the fuel injection rate per unit area and $h_{v,sen}$ is the sensible enthalpy of vaporization of the fuel, defined as

$$h_{v,sen} = h_v + \int_{T_0}^{T_b} c_p dT. \tag{15}$$

In the above equation, h_v is the enthalpy of vaporization and c_p is the specific heat of the fuel. T_0 and T_b refer to the initial temperature of the fuel and the boiling temperature, respectively.

The grid resolution for each case is quantified using the Resolution Index RI. The RI is defined as

$$RI = \frac{D^*}{\Delta x}, \tag{16}$$

where Δx is the grid resolution and

$$D^* = \left(\frac{\dot{Q}}{\rho_\infty c_p T_\infty \sqrt{g}}\right)^{\frac{2}{5}}, \text{ and } \dot{Q} = \dot{m}'' A h_c. \tag{17}$$

Here ρ_∞, T_∞ ,c_p and *g* are the ambient density and temperature, specific heat of air and the gravitational acceleration respectively. In the equation for heat release rate $\dot{Q}$, h_c is the heat of combustion of the fuel gas and *A* is the surface area of the fuel pan.

5.3.4. Grid convergence studies

First, a model of experiments by A. Hamins on radiative feedback to the surface of heptane pool fires is considered. Rectangular burners with side length 0.3m model the circular 0.3 m diameter pool fires in FDS. The burners in turn are modeled as fuel inlet boundary condition with a mass flux of 0.026 kg/s of heptane. The expected radiative heat flux to the fuel surface is 16.6667 kW/m^2. Simulations are run on uniform grids with 125mm, 25 mm and 50 mm discretization intervals. The heat feedback to the surface decreases as the grid resolution increases. With the smallest grid size, the relative error in predicted heat feedback to the surface is 5%.

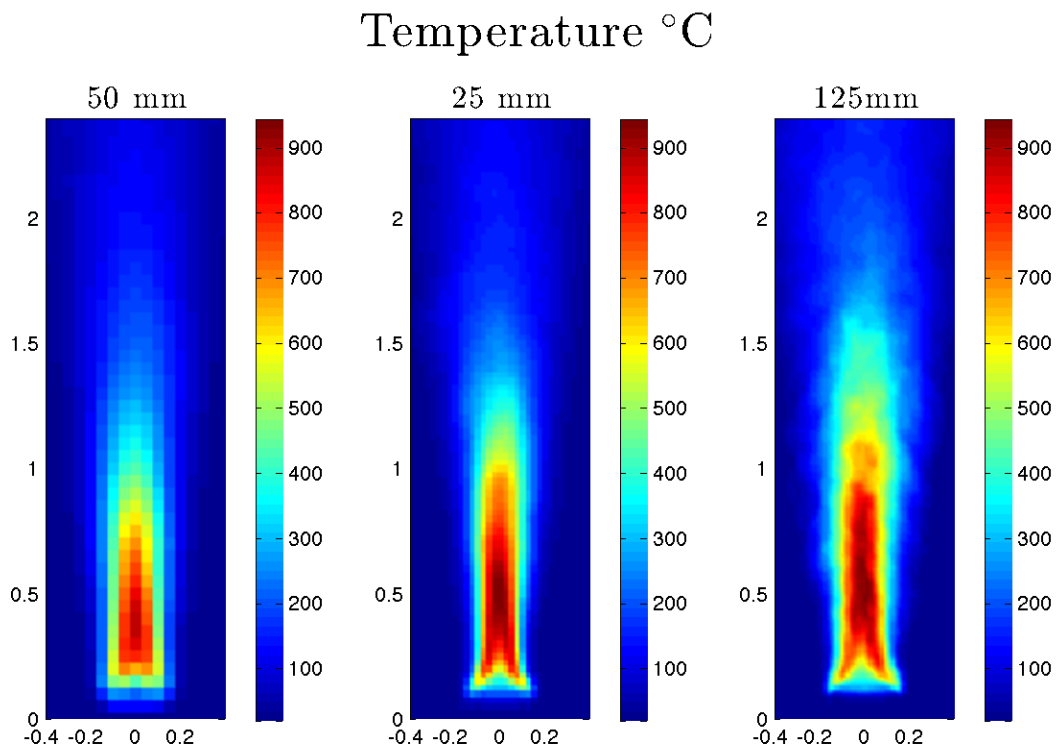

Figure 40. Temperature slices for three different grid resolutions.

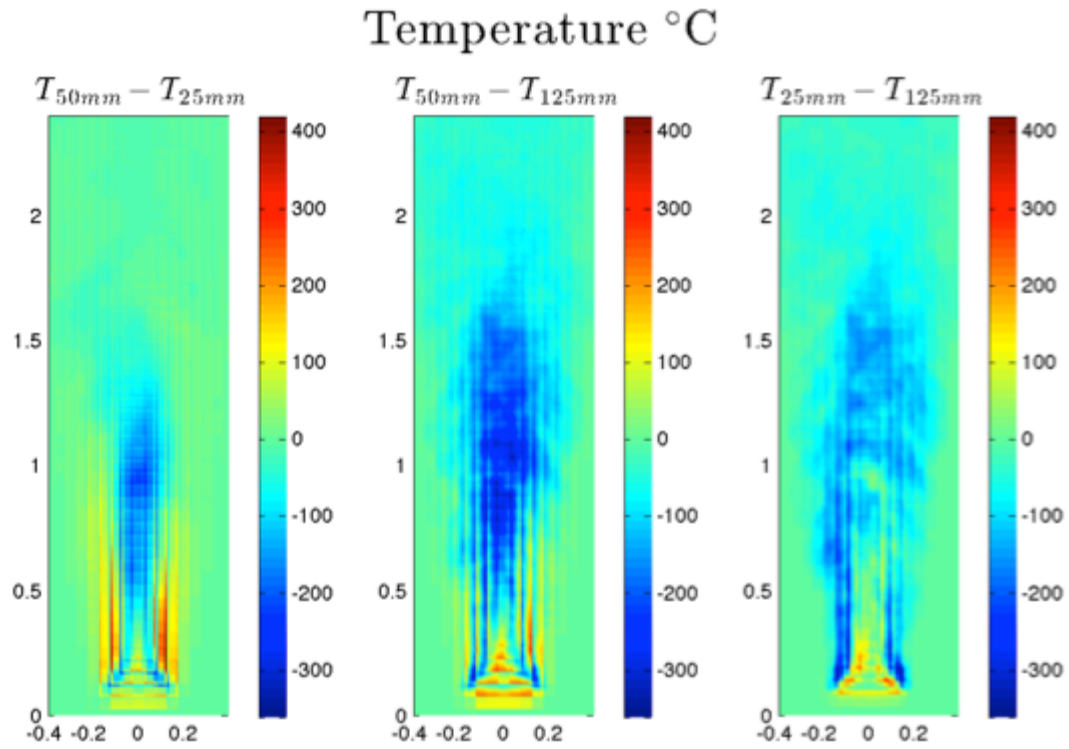

Figure 41. Differences between temperature slices at three different resolutions

Figure 40 shows slices of temperature at three different grid resolutions and Figure 41 shows the differences in the temperatures between these slices. The difference is obtained by interpolating the slice data on a uniform grid with 1cm discretization interval, using nearest neighbor interpolation. The difference is then calculated as

$$\Delta f_{\Delta x_1,\Delta x_2}(x,z) = f_{\Delta x_1}(x,z) - f_{\Delta x_2}(x,z), \quad (18)$$

where $f_{\Delta x_1}$ and $f_{\Delta x_2}$ are the value of the quantity in question on two different grid resolutions. In Figure 41 the value on the finer grid is always deducted from the value on the coarser grid. Thus positive values of the difference mean that the coarser grid predicted a larger temperature at this point. Accordingly, negative values correspond to cases where the simulation on finer grid resulted in higher predictions

There is a clear trend, that as the grid gets finer the temperatures near the surface decrease slightly and the flame seems to be getting thinner and longer overall. The reason for is most likely related to the radiation source term in the radiative transport equations.

In LES simulations the grid resolution is usually too low to accurately predict the position and temperature of the flame sheet. For this reason the radiation source term in FDS is related to the gas phase reaction rate. Where gas phase reaction is occurring, a constant fraction χ_r of the released energy is released as thermal radiation. Therefore it is useful too look at the distribution of heat release rate as a function of height.

Figure 42 Shows the Heat Release Rate Per Unit Volume (HRRPUV) on the three grids. Here it is clear that as the grid gets finer, the distribution of HRRPUV moves further away from the fuel surface. There is an exception to this rule at the very base of the flame, where the heat release rate gets larger on a finer grid. Figure 43 shows the differences between the slices on the three grid sizes. This figure confirms the findings of the previous paragraph. Also notable is that even at 1.25 cm grid size, the HRR field has not converged: There are still large differences between the solutions on the 25 mm grid and the 12.5 mm grid.

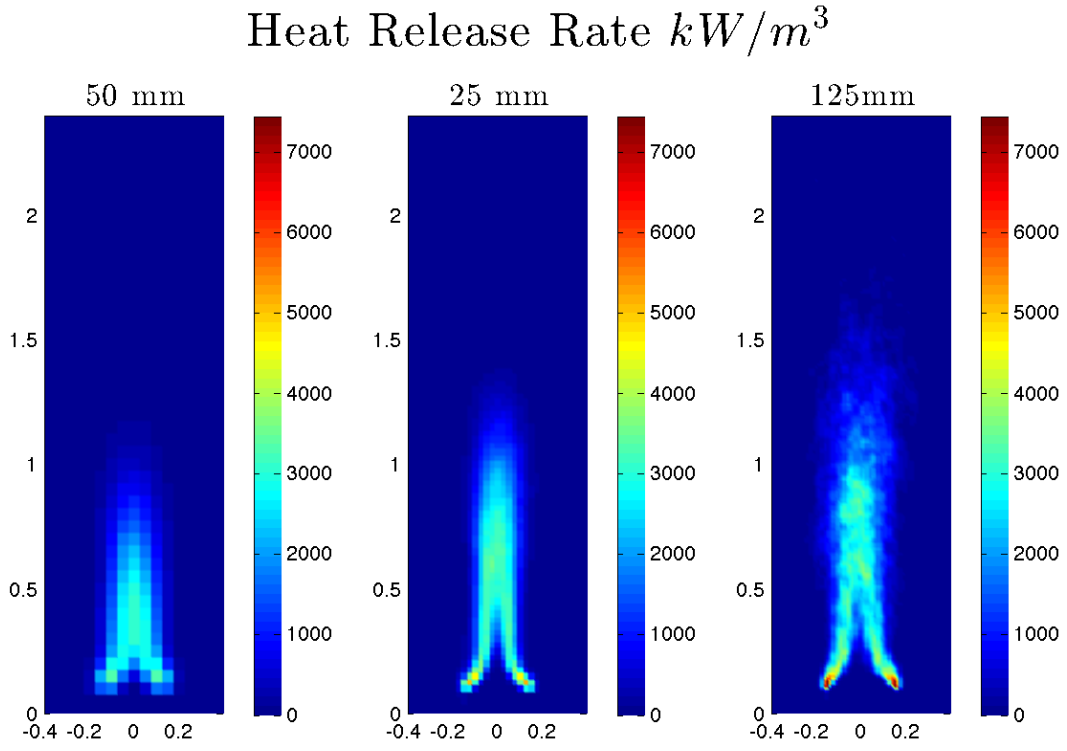

Figure 42. HRRPUV slices for three different grid resolutions

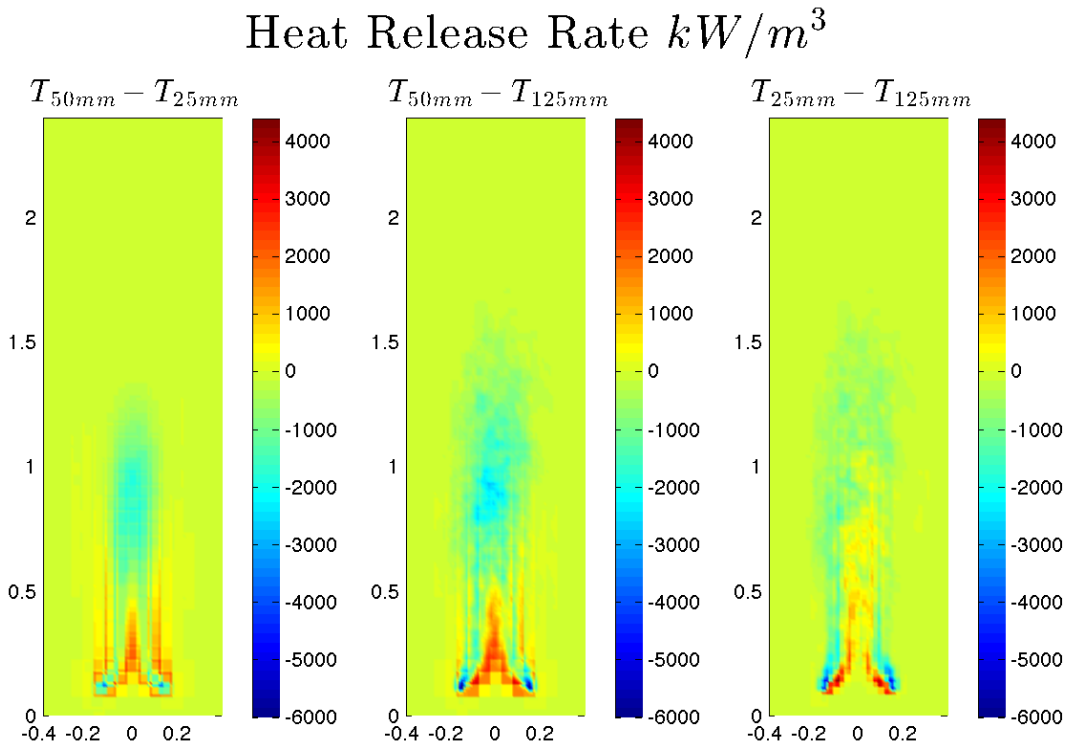

Figure 43. Differences between HRRPU slices at three different resolutions

Table 8. Dimensions of the rectangular heptane pool fires and burners

Pan Width (m)	RI	NY	NX	NZ	dx	Width	Depth	Height
1	10	11	11	41	0.15	1.6	1.6	5.96
1	20	22	22	81	0.07	1.6	1.6	5.89
1	30	32	32	117	0.05	1.6	1.6	5.85
2	10	11	11	39	0.29	3.2	3.2	11.35
2	20	22	22	77	0.15	3.2	3.2	11.20
2	30	33	33	115	0.10	3.2	3.2	11.15
3	10	12	12	39	0.40	4.8	4.8	15.60
3	20	24	24	78	0.20	4.8	4.8	15.60
3	30	35	35	114	0.14	4.8	4.8	15.63
0.5	10	11	11	39	0.07	0.8	0.8	2.84
0.5	20	23	23	81	0.03	0.8	0.8	2.82
0.5	30	34	34	119	0.02	0.8	0.8	2.80

Second, a series of simulations of rectangular heptane pool fires are considerer. For each pool size, simulations are run at three different values of the grid Resolution Index RI. The values selected for this study were 30, 20 and 10. A larger number corresponds to a finer grid. It was determined from the simulations of the 0.3m pool fires that the flames get longer as grid resolution is increased. To further study this effect two kinds of simulations were conducted. The first set of simulations models the pool as fuel inlet boundary condition. This is done to remove the possible interactions of the evaporation model with grid-size. Second set of simulations uses the FDS liquid fuel model to predict the fuel evaporation rates.

Figure 44 shows the heat release rate per unit length as function of height for different sizes of heptane burners. For all sizes, the distribution of heat release rate shifts away from the burner surface. This is consistent with the findings from the 0.3m pool fire simulations. The difference between successive grids clearly decreases as the RI value is increased. As we go to finer grids, the distribution of heat release rate seems to become bimodal.

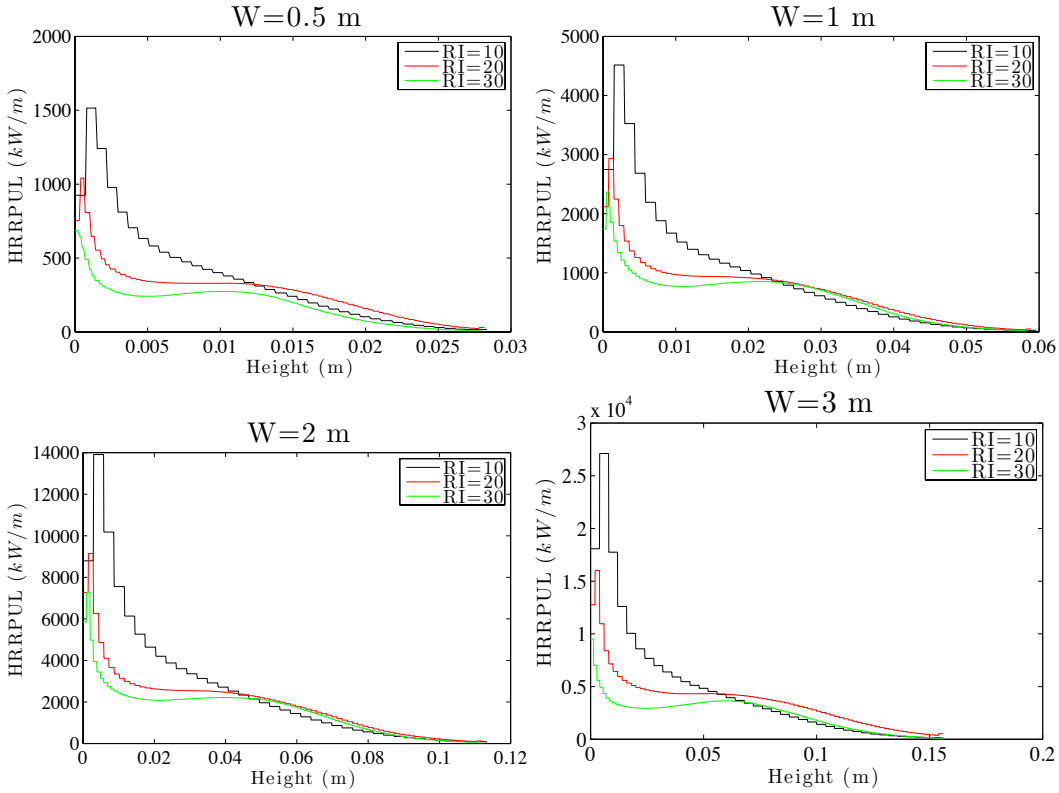

Figure 44. Heat Release Rate per Unit Length as function of height from floor. Fuel surface is at z=0.05.

5.4. Model description – Engineering model

Regarding the influence of the oxygen fraction on the burning rate, an empirical correlation has been obtained from a steady-state combustion regime by Peatross and Beyler (48). This correlation provides fuel mass loss rate against oxygen concentration measured at the flame base for large-scale fire compartments:

$$\dot{m}''_{fuel,O_2} = \dot{m}''_{\infty,21\%} \cdot (0.1 \cdot O_2[\%] - 1.1)$$

One of the main drawbacks of this empirical relationship lies in that it was obtained in conditions for which external heat fluxes were negligible. This limits its relevance to situations where high gas and wall temperatures, affecting incoming heat fluxes, are present. The effect of the external radiation can be taken into account in a simplified matter where the extra fuel mass loss rate is proportional to the external radiation and the heat of vaporization:

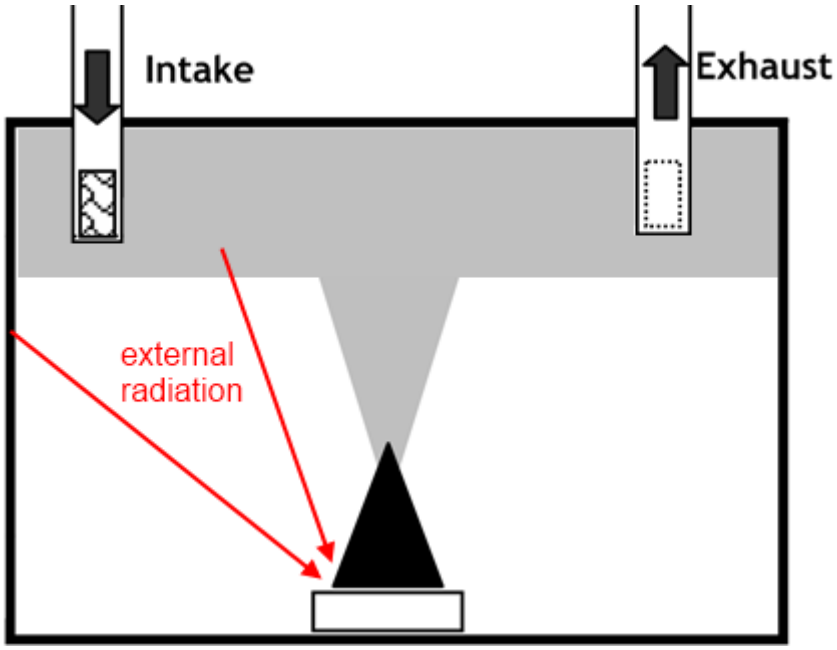

$$\dot{m}''_{external} = \frac{\dot{q}''_{rad,in\ walls} + \dot{q}''_{rad,in\ soot\ layer} - \dot{q}''_{rad,out\ fuel\ surface}}{\Delta H_{vap,fuel}}$$

When combining these to expressions the total fuel mass loss dependent on both local oxygen concentration and external radiation can be expressed as:

$$\dot{m}''_{fuel,tot} = \dot{m}''_{fuel,O_2} + \dot{m}''_{external}$$

If the initial phase of the fuel mass loss is of less importance, the term $\dot{q}''_{rad,out\ fuel\ surface}$ can be approximated using the fuel emissivity and boiling temperature to calculate the outgoing radiation. However, this will result in an over estimation of the initial fuel mass loss rate.

If the initial phase is of importance more mechanics has to be added. According to Hayasaka (49) the total heat needed for vaporization during the growth phase is expressed by the equation:

$$Q_{growth\ phase} = \dot{m}''_{growth\ phase} \cdot (c_p \cdot (T_{boil,fuel} - T_{fuel,surface}) + \Delta H_{vap,fuel}$$

When the temperature in the pre-heating layer has reached the boiling temperature of the fuel the equation reduces to:

$$Q_{steady\ state} = \dot{m}''_{growth\ phase} \cdot \Delta H_{vap,fuel}$$

Hayasaka also concludes that the total heat balance of the pool fire during all phases was approximately the same, as in $Q_{growth\ phase} = Q_{steady\ state}$. Combing the equations for the growth phase and steady state phase an expression for the fuel mass loss rate during the preheating process can be formed:

$$\dot{m}''_{growth\ phase} = \dot{m}''_{\infty,21\%} \cdot \frac{1}{\left(\frac{c_{p,fuel} \cdot (T_{boil,fuel} - T_{fuel\ surface})}{\Delta H_{vap,fuel}} + 1\right)}$$

This equation gives a reasonable fit to experiments conducted by Hayasaka (49) during the pre-heating process:

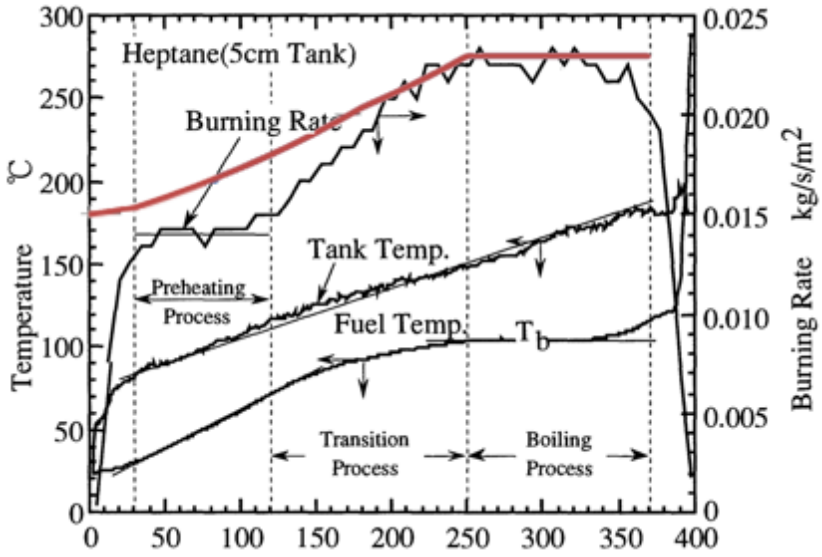

Figure 45 Comparison between experiments performed by Hayasaka (49) and the simple model to describe the initial phase of the pool fire. (reproduced from 49)

To increase the accuracy a more refined heat transfer model including heat exchange with and through the fuel vessel, especially during the very initial phase of the process since the heat loss to the vessel seems dominant during this period.

The initial work with this model focused on validating the post-ignition phase, as in the preheating process was be included.

6. Experimental set-ups for validation

This chapter describes a number of experimental set-ups, which provides a database for validation. In some cases the test results have been used for validation of the pool fire models developed in this project. I other cases it was the bases for validation of submodels in FDS which are necessary to obtain validation using a block approach validation (50)

6.1. Experimental Set-up 1 (Stord/Haugesund University College).

6.1.1. Description

One of the experimental set-ups was done at Haugesund College (51) and the set-up is given in Figure 46.

Several 0.5m x 0.5m heptane pool fire experiments with pipes obstructing above the fire were studied in the fire laboratory at HSH (Stord/Haugesund University College). Different obstruction areas in different heights above the obstruction were tested in order to verify what effects it had on the fire. An open calorimeter analysed the smoke from the fire. Additionally, temperature, radiative heat flux and mass loss rate were measured.
These experiments showed that when a pipe obstruction is located close to the pool fire it has a decreasing effect on the heat release rate and thermal radiation from the fire. In order to verify if this also was the case with increased fire diameter, outdoor pool fire experiments with increased area were performed. Due to wind conditions during these experiments the results were not valid for use in verification. However, the outdoor experiments showed that the pipe effect can be neglected for windy conditions.

This setup can be used to study additional liquids. Furthermore a number of total heat flux meters has been acquired, so the radiative heat flow from different part of the flames could be further investigated.

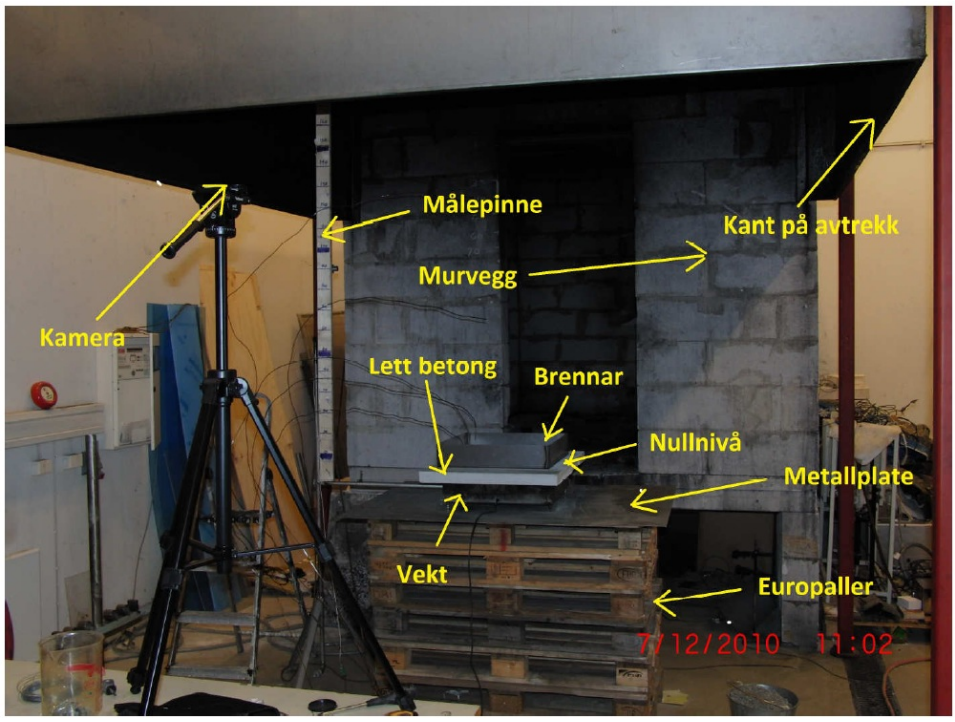

Figure 46 Set-up in Haugesund for pool fire experiments

Legend for Figure 46**:**

Kamera: Camera

Målepinne: Measuring reference for height measurements

Brennar: pool tray

Murvegg: wall from room

Kant på avtrekk: boundary of exhaust hood

Vekt: Load cell

Nullniva: Zero reference

Metallplatte: Metal sheet

Europaller: Europallets (wooden pallets)

6.1.2. Particle Image Velocimetry (PIV) Measurements of Fires with Presence of Pipes

Correct modelling of the velocity field in the flame is crucial in fire modelling and may for example give indications if the heat release rate is correctly predicted locally in the grid cells. An over prediction of the heat release rate locally will result in over prediction of temperature and velocity while the flame length is under predicted. The experimental work presented here is described in more detail in (52).

The motivation in the second series of experiments was to investigate the flow field in the flame with presence of obstacles by advanced laser measuring technique. Particle Image Velocimetry (PIV) is a sophisticated tool for measuring of instantaneous velocity vector field in the cross-section of a fluid flow. The laser is

used to illuminate the cross-section with two short pulses. A camera is synchronized with the laser and records the scattered light from particles that are seeded in the flow. Computer software is used in post-processing where velocity vectors are calculated from the movement of the seeded particles between pulses.

Table 9: Planned experimental scenarios

	Fuel	HRR	Height of Pipes
		[kW/m^2]	[m]
P1	Propane	500	0.15
P2	Propane	500	0.30
P3	Propane	500	0.45
P4	Propane	1000	0.15
P5	Propane	1000	0.30
P6	Propane	1000	0.45
P7	Propane	1500	0.15
P8	Propane	1500	0.30
P9	Propane	1500	0.45
H1	Heptane	-	0.15
H2	Heptane	-	0.30
H3	Heptane	-	0.45

Some improvements were made to the set-up in the second experimental series. The circular pipes were replaced by 60 mm x 60 mm rectangular pipes with thickness of 4 mm. The distance between the pipes was set to 40 mm. A 0.3 m x 0.3 m propane burner was planned to be used in the initial scenarios to ensure constant heat release. The planned scenarios are seen in Table 9. Furthermore, thermocouples were mounted with improvised wedges on the inside of the pipes above the fire. Numbering of the thermocouples is presented in Figure 47. The purpose of measuring the inner steel temperature was to start the recordings when steady conditions were reached. Steady state temperature may also be used as input values in simulations to eliminate errors in heat transfer calculations from the flame to the pipes.

The experiments were conducted during four days at Lund University in spring of 2012. Unfortunately, the experiments gave not enough successful PIV-data for validation. However, the work gave experience, which may be foundation of further experiments and the set-up was used for further validation of the new turbulence model in FDS (52).

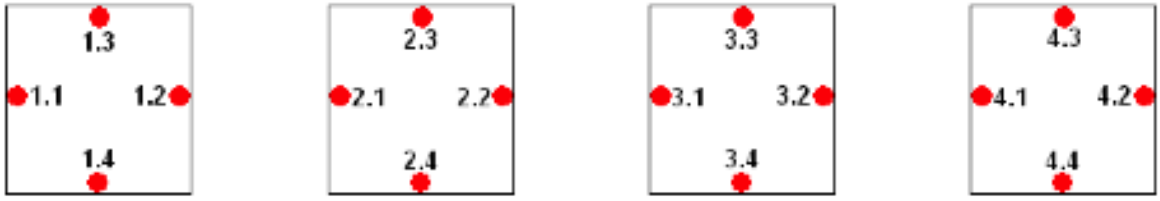

Figure 47 Numbering of thermocouples in the pipes

These kind of experiments are difficult to perform. Inhalation of seeding particles may lead to serious harms. Sufficient ventilation and breathing masks are therefore demanded. When the ventilation was set on maximum power the smallest fires got unstable. To eliminate this problem future experiments should be conducted in a vessel or a small room that no humans are occupying. Then the flame can be provided with unlimited amount of seeding particles without being a danger to people.

Calibration of the laser is the most time-consuming part of the experiments. After the laser and camera are rigged the first stage of this procedure is to focus the camera on a measuring area. A large measuring area requires a strong laser to penetrate the flame. Sooty flames are also weakening the laser signal. In early stages there were some uncertainties whether the laser could penetrate a sooty flame such as propane. Sooty flames are also emitting a large amount of thermal radiation. Since the seeding particles are traced as they are illuminated by the laser pulses, disturbing incoming light on the camera lens must be minimized. A sooty flame may therefore provide the camera with too much light. Based on these arguments methanol was chosen as fuel and the flow field was measured on a relatively small area of 40 mm x 40 m between pipe 1 and 2 in the calibration process. One way to overcome the light from the sooty flame is to use an extra shutter for the second image. However due to some technical issues with the shutter this did not work. From the experiments no conclusion could be drawn whether a propane flame is too sooty to measure a 40 mm x 40 m flow field with the Lavision equipment used.

Seeding of particles is the most challenging part of PIV measurements of flames, because no universal method exists. In these experiments the flame was seeded with particles in three different ways; by smoke sticks, smoke pellets and seeding of particles with pressurized air. All methods were somehow unsuitable and the out coming data were of rather poor quality. Seeding with smoke was unsuitable because a stable concentration of smoke particles within measurable range was not achievable in the whole measuring area on a sufficient number of the images recorded. It was also attempted to seed the particles by pressurized air in vertical direction, both

upward and downward, and also horizontal direction faced in direction along the laser beam. When the particles were seeded upwards a jet was clearly observed in the results. It was obvious that the particles were strongly influenced by the momentum release and did not move free with the local flow velocity in the flame. In downward direction, seeding particles got stuck in burner. The measuring area was not provided with enough seeding when the seeding particles were supplied horizontally. Furthermore, the flame behavior was too much influenced when pressurized air method was applied for small fires.

Further experimental work is planned. This includes using a stronger laser and improving the seeding method. If the pressurized air method is considered the air supply must be low and preferably be controllable. Several release point is recommended to disperse the seeding particles in the flame. One alternative way to achieve this is to customize the burner with wide-spreading nozzles tilted slightly toward the center of the flame along the burner's edge.

Some results where obtained from temperature measurements on the inside of the steel pipes. One example is given in Figure 48, where a propane burner with a heat release rate of 45 kW was used (experiment P1). It can be seen that the steel temperature rises to steady value of from 550°C to 600°C after about 13 minutes.

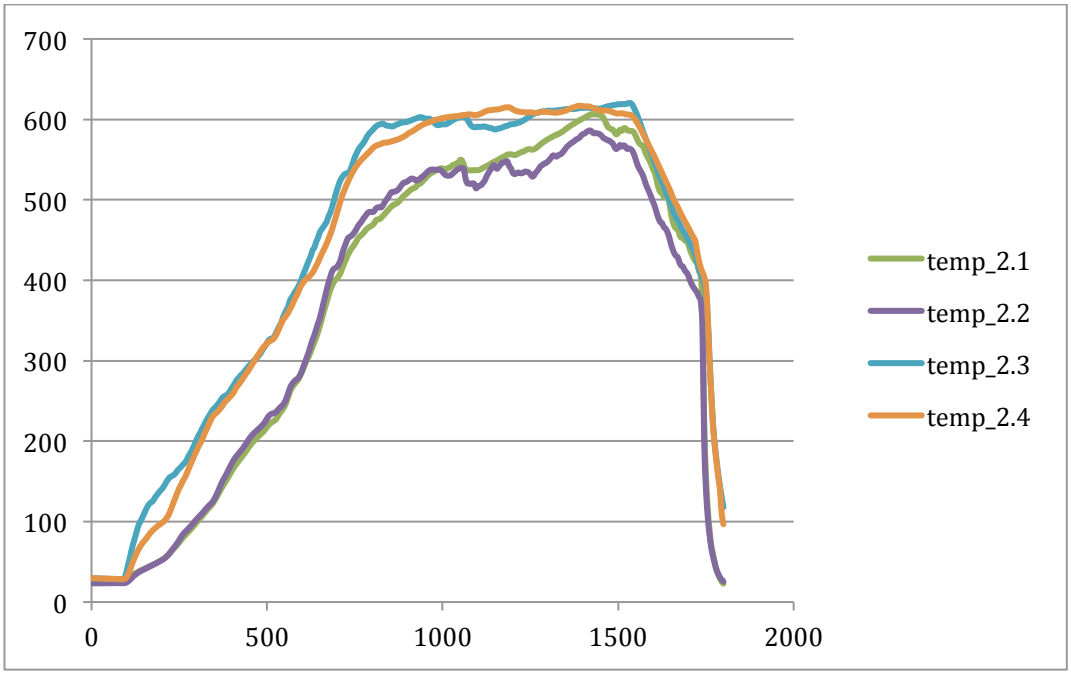

Figure 48 Measurement of temperatures inside steel bar number 2 in test P1.

6.2. Experimental set-up 2.

Another series of experiments were performed at Lund University with cooperation of guest PhD student Depeng Kong from Key State Laboratory in Hefei. The set-up is described below.

The entire experimental system consisted of squared steel trays, weight measurement system (load cell), temperature measurement system and the gas analysis system.

Three squared steel trays with the same height of 100mm but with different side lengths were used. Three side lengths are 100 mm, 200 mm and 300 mm. Two kinds of fuels were used in this study: N-heptane and methanol. The initial fuel thickness was set to be 30 mm and 42 mm.

The steel tray was positioned on a top-loading electronic balance to measure the fuel mass loss. To prevent heat transfer from the steel tray to the balance, an insulator was placed between the steel tray and electronic balance, as shown in Figure 1.

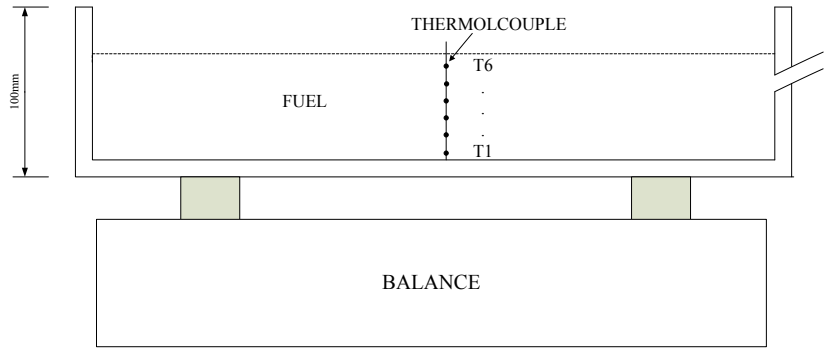

Figure 49 Schematic diagram of pool fire experimental set-up of fuel source

The effects of different initial fuel temperature on the burning rate and heat release rate were studied with vessel filled with fuel placed on a heater and pre-heated to the target temperature. The vessel was then moved on the insulator. The initial fuel temperatures were set between the ambient temperature and the fuel boiling point. For heptane, four initial temperatures were considered: 288 K, 308 K, 328 K and 348 K. For methanol, the first three initial temperatures were considered since the boiling point of methanol is 338 K. The fuel temperature distribution was measured by six 0.5 mm diameter K-type thermocouples, which were arranged in the vertical axis of the vessel. For the cases where the initial fuel thickness is 30 mm, the six thermocouples were placed at 4 mm, 8 mm, 12 mm, 16 mm, 18 mm and 24 mm above the bottom and were denominated T1-T6 from bottom to top. These six thermocouples were placed in a similar way for the cases where the initial fuel thickness is 42 mm, but the distance between two thermocouples is 6 mm. The outputs of these thermocouples were recorded by a data acquisition system. A total of 24 tests were conducted for heptane while 18 tests were conducted for methanol. The specific conditions of different tests are presented in Table 10.

Table 10: Experimental conditions of heptane pool fires

Test Number	Pool side length (mm)	Initial fuel thickness (mm)	Initial fuel temperature (K)
1	100	30	286
2	100	30	303
3	100	30	326
4	100	30	344
5	100	42	289
6	100	42	308
7	100	42	327
8	100	42	347
9	200	30	287
10	200	30	309
11	200	30	327
12	200	30	347
13	200	42	286
14	200	42	310
15	200	42	329
16	200	42	346
17	300	30	288
18	300	30	308
19	300	30	327
20	300	30	345
21	300	42	289
22	300	42	309
23	300	42	327
24	300	42	346

Table 11: Experimental conditions of methanol pool fires

Test Number	Pool side length (mm)	Initial fuel thickness (mm)	Initial fuel temperature (K)
1	100	30	290
2	100	30	308
3	100	30	327
4	100	42	289
5	100	42	307
6	100	42	328
7	200	30	289
8	200	30	306
9	200	30	327
10	200	42	286
11	200	42	307
12	200	42	326
13	300	30	289
14	300	30	310
15	300	30	327
16	300	42	288
17	300	42	307
18	300	42	327

The experimental setup was placed under the exhaust hood which gas and smoke instrumentation was installed. The concentration of different gas, such as oxygen, carbon dioxide and carbonic oxide as well as the pressure in the duct were measured and recorded by the fire gas analyzer. The whole experimental setup is arranged as shown in Figure 50.

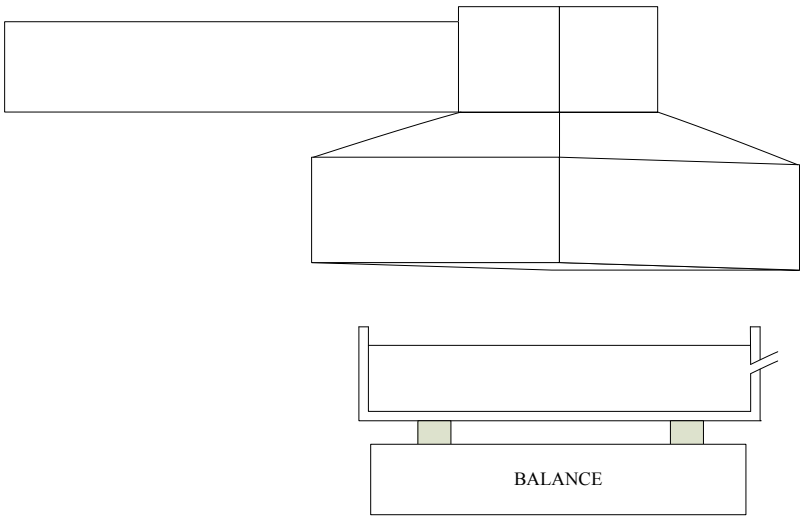

Figure 50 Schematic diagram of the whole experimental setup

The tests recorded HRR and mass loss rate of the fuel as well as temperature distribution in the fuel. Test results are available as computer files and will be later compiled in a LTH report.

6.3. Experimental set-up 3

Traditionally fuels such as methanol, ethanol, acetone, hexane, heptane, etc. are used for model validation and calculation of pool fires. In nuclear power plants the type of fuels are sometimes different and more lubricant oils are transformer oils. The third experimental set-up envisaged to provide data for transformer oils both traditional mineral oil but also different natural and synthetic esters and silicone oils. The work was performed mainly by performing small-scale tests in the cone calorimeter and was reported as a master thesis (58) and will be published in a special issue of Fire technology (59). I can be also seen as a real case application. Results from cone calorimeter tests in a round pan (see Figure 52) are given below.

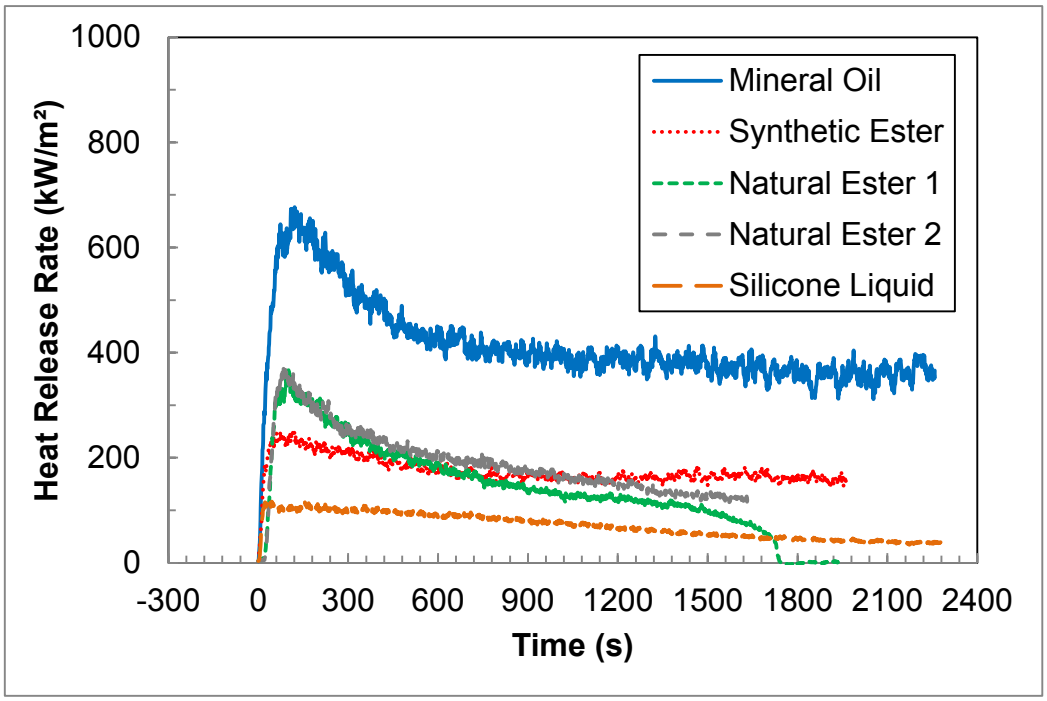

Figure 51 HRRs measured in the Cone Calorimeter with a deep round cup sample holder

The deep cup was instrumented with thermocouples (type K; Ø 0,24mm) to measure the liquid temperature at 1 cm and at 3 cm below the initial liquid surface (see Figure 52). The resulting temperature profiles are shown in Figure 54 and Figure 54, for the thermocouple at 1 cm and 3 cm below the surface, respectively.

Figure 52 Thermocouples to measure liquid temperatures in the deep round cup sample holder

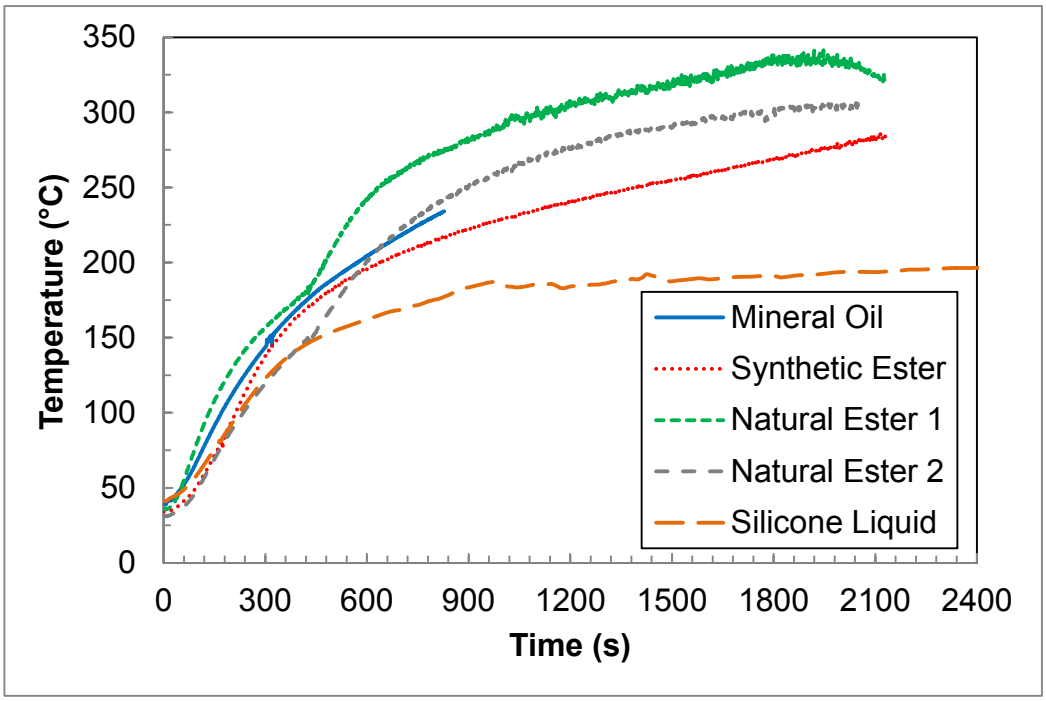

Figure 53 Liquid temperature at 1 cm below the surface in the tests with a round cup

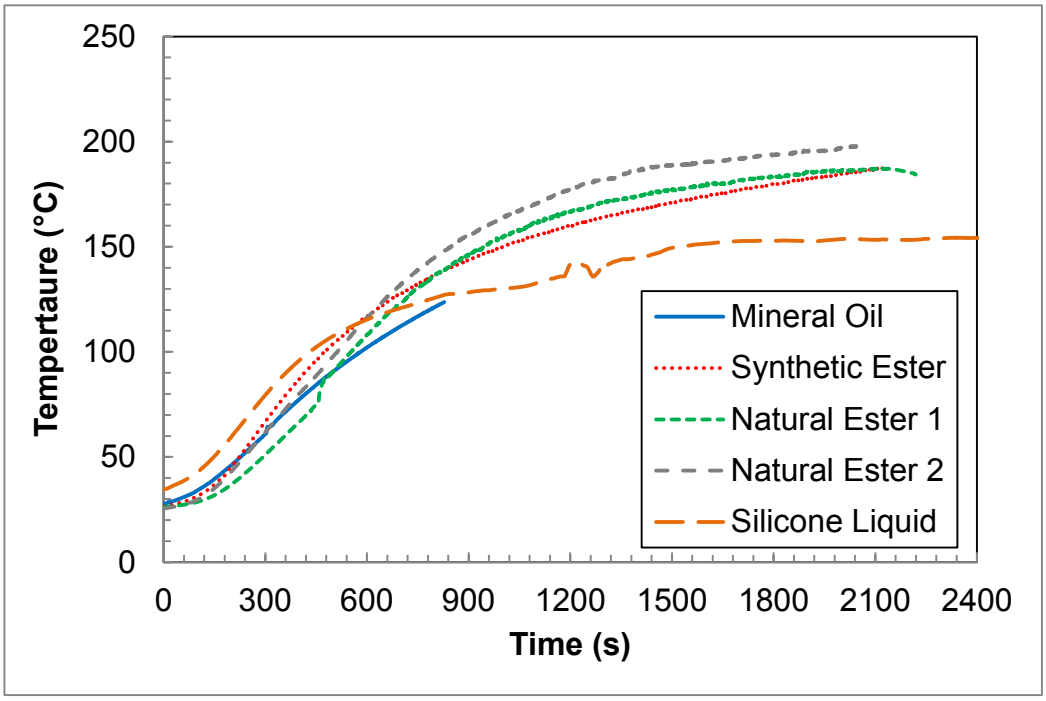

Figure 54 Liquid temperature at 3 cm below the surface in the tests with a round cup

The curves show similar behavior, except for the silicone liquid. The latter is shielded from the radiation from the flame by the crust that is formed after ignition, resulting in lower temperatures after the first 5-10 minutes. After about 15 minutes of exposure the curves taper off. This is consistent with the decreasing heat flow that eventually resulted in the extinction of the natural ester flames.

6.4. Experimental set-up 4.

The fourth experimental set-up was a set-up which originated from the discussion on real scale cases and is reported in paragraph 8.3 and in reference (67)

7. Validation of the models

7.1. Validation of new liquid evaporation model

7.1.1. Fuel properties for validation simulations

The liquid fuel model described above needs a number of fuel properties. Some of these properties are available in open literature but some need to be estimated. One parameter that needs to be estimated is the absorption coefficient of the liquid fuel. In reality, the absorption of thermal radiation in semi transparent media is highly dependent on the wavelength of the radiation and cannot be represented by a single number for all cases. The method used to estimate the absorption coefficient for the fuels used in current study is described in the Appendix I of FDS Technical Reference Guide (24).

The rest of the values used are based on NIST Webbook chemical reference (53). Table 12 lists the properties of fuels used in this study. In addition to the liquid phase thermochemistry data, the specific heats of the fuel gases are needed. The importance of the accurate specification of this property was observed during the research year 2012. It was observed that, for instance, using a too low value of specific heat for the fuel gases could lead to severe over-prediction of pool fire burning rates. Where available, polynomial fits to gas tabulated values of gas phase specific heats have been used.

Table 12 Liquid Fuel properties used in this report.

Property / Fuel	ε (-)	h_v (kJ/kg)	λ (W/m²K)	c_p (kJ/kgK)	T_b (°C)	ρ (kg/m^3)	α (1/m)
ACETONE	1	501.03	0.18	1.6529	56.3	792.5	100
BENZENE	1	393.29	0.167	1.7372	80.3	876.5	123
BUTANE	1	385.22	0.124	2.2784	0	584	100
ETHANOL	1	836.98	0.17	2.4398	78.5	789	1534.3
N-HEPTANE	1	364.9	0.14	2.2464	98.5	684	100
METHANOL	1	1098.9	0.21	2.4813	64.8	791.8	1520

7.1.2. Large pool fires in open atmosphere

To expand our selection of fuels and pool sizes. A series of large pool fires is simulated. These simulations consider large 1m x 1m rectangular pools. A 5 cm discretization interval is used for the mesh and the size of the computational domain is 1.6 m × 1.6 m × 4.8 m. The burning rates are predicted. Once more we make use of empirical correlations to validate the results. The maximum burning rates of liquid pool fires are well correlated with

$$\dot{m} = 1{\times}10^{-3}\frac{h_c}{h_{v,sen}}. \tag{19}$$

Figure 55 shows a comparison of FDS predicted burning rates versus data from SFPE Handbook Chapter 2 (54). Where data as not available it was estimated from

Equation 19. In most cases the burning rates predicted by FDS are lower than those predicted by Equation 19.

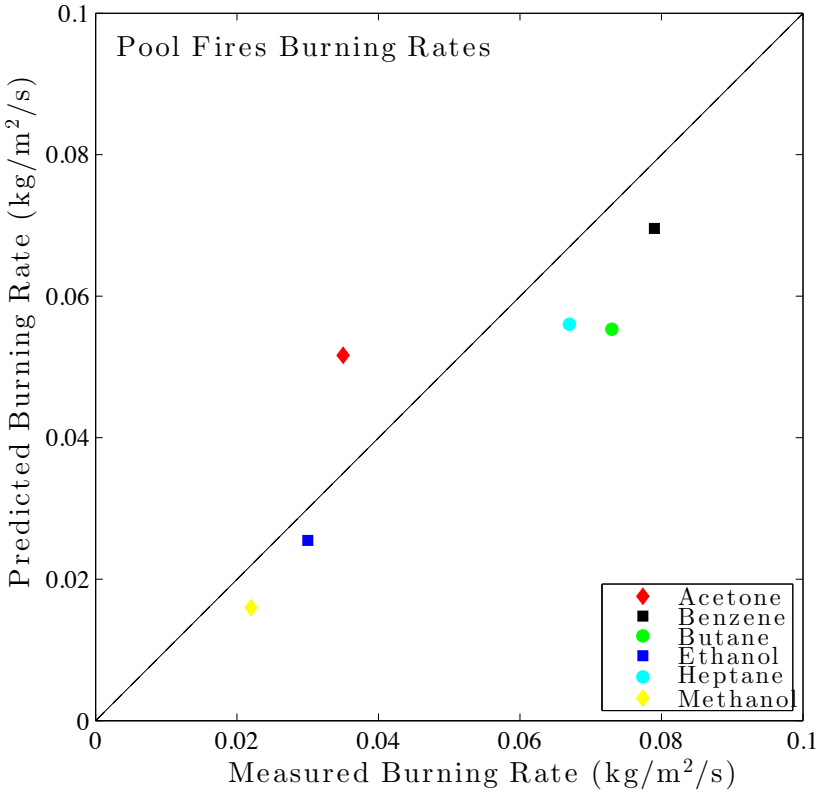

Figure 55. Maximum burning rates of large liquid pool fires

7.1.3. Comparison of FDS predictions with empirical correlations

One important question remains. Do the results on a finer grid get closer to the experimental results? Since no experimental data was available for all sizes of heptane pools, the predicted burning rates are compared with experimental correlation

$$\dot{m}'' = \dot{m}''_{\infty}(1 - exp[-k\beta D]) \tag{20}$$

The values for Heptane are $k\beta = 1.1\ 1/m$ and $\dot{m}''_{\infty} = 0.101\ kg/m^2$. Figure 56 fshows the error as a function in predicted pool burning rates as a function of grid resolution and pan width. The error is quantified as

$$\epsilon = \frac{\dot{m}_{FDS} - \dot{m}_{corr}}{\dot{m}_{corr}} \times 100\ (\%) \tag{21}$$

The predicted burning rates get closer to the correlation values as grid resolution increases. There is a slight decreasing trend in the error as a function of pan width. Notably for the largest pan size considered the burning rate is under predicted, compared to the correlation.

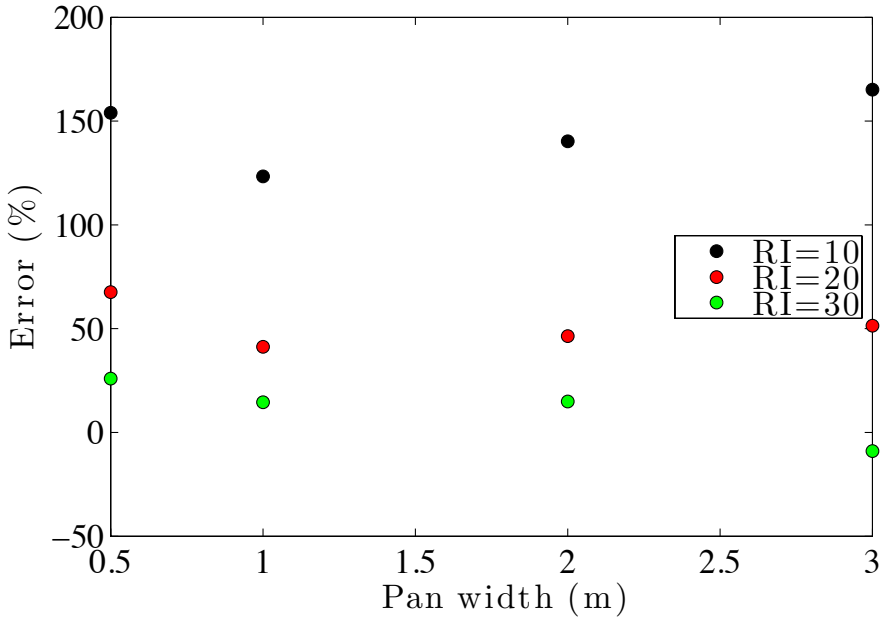

Figure 57. Error in predicted mass loss rate (MLR) as function of pan width and Resolution Index (RI)

Does the liquid evaporation model in use cause the results thus far seen or is the burning rate prediction dominated by the prediction of correct radiation heat feedback? Answer to this question is sought by considering the heat feedback to a surface, when the burning rate is prescribed. Very few measurements of the heat feedback to the fuel surface have been published in the open literature. However from energy conservation considerations, it can be deduced that the heat feedback to the fuel surface for given evaporation rate should be

$$\dot{q}''_{in} = \frac{\dot{m}''}{h_{v,sen}}. \tag{22}$$

The burners have a prescribed mass loss rate given by Equation 20. The expected feedback to the fuel surface is then calculated from Equation 22. The error in the predictions is once again quantified as

$$\epsilon = \frac{\dot{q}_{FDS} - \dot{q}_{corr}}{\dot{q}_{corr}} \times 100\ (\%) \tag{23}$$

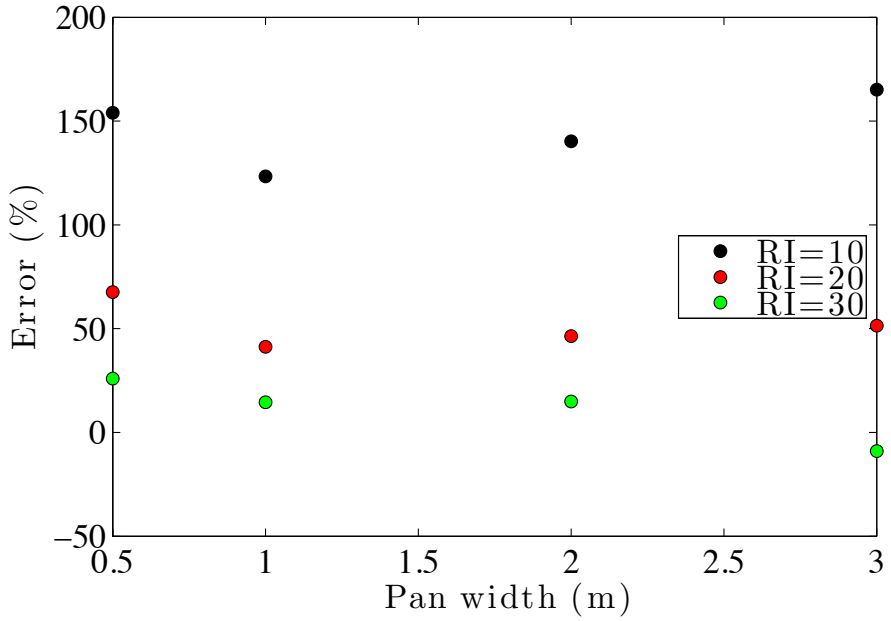

Figure 58. Error in predicted heat flux to burner surface as function of pan width and Resolution Index (RI)

7.1.4. Models for open atmosphere PRISME tests (PRISME SOURCE)

The test data considered here is from the PRISME project. The tests were conducted in free atmosphere under the SATURNE hood (20). The fuel in all the tests considered here was hydrogenated tetrapropylene (TPH). The tests involve a single pan of TPH under the SATURNE hood. The pan is 100 mm deep and the fuel depth is 50 mm in all except one test where it was 80mm. The surface area of the pan was varied. The physical properties of the fuel are listed in Table 5. Dodecane was used as a surrogate fuel for the gas phase properties of TPH. The pan is modelled as a layer of TPH followed by a steel plate, followed by insulation. The pan is defined by following FDS lines. An overview of the tests is given in Table 6.

```
&SURF ID='POOL'
      STRETCH_FACTOR=1
      CELL_SIZE_FACTOR=0.25
      COLOR='RED'
      MATL_ID(1,1)='TPH'
      MATL_ID(2,1)='STEEL'
      BACKING = 'INSULATED'
      THICKNESS= 0.05 0.005 /
```

Table 13 Properties of the fuel (TPH)(23)

Property	Value	Units
EMISSIVITY	1	-
HEAT OF REACTION	1098.94	kJ/kg
CONDUCTIVITY	0.18	W/mK
SPECIFIC HEAT	2.4	kJ/kgK
BOILING TEMPERATURE	188	°C
DENSITY	758	kg/m^3
ABSORPTION COEFFICIENT	1000	1/m

Table 14 Test scenarios under investigation

Test name	*Pool Surface Area*	*Fuel Depth*
Units	**m^2**	**mm**
PRS-SI-S1	0.2	50
PRS-SI-S3	0.4	50
PRS-SI-S5	0.1	50
PRS-SI-S7	0.1	80

The purpose of these simulations was to predict the burning rates of the pools. The computational model of the experiments includes only the pan and not the hood. All boundaries, except the bottom boundary are defined open for flow. The bottom boundary is inert. The computational model includes the 50 mm lip of the fuel pan. Two different grid resolutions are used: 25 mm grid cells and 50 mm grid cells. The full set of experiments is run with all parameter combinations. The simulation matrix is given in Table 15.

Table 15 Simulation matrix.

#	Test name	Evaporation model	ΔX
5	PRS-SI-S1	New	5 cm
6	PRS-SI-S3	New	5 cm
7	PRS-SI-S5	New	5 cm
8	PRS-SI-S7	New	5 cm
13	PRS-SI-S1	New	2.5 cm
14	PRS-SI-S3	New	2.5 cm
15	PRS-SI-S5	New	2.5 cm
16	PRS-SI-S7	New	2.5 cm

7.1.5. Results for open atmosphere PRISME tests (PRISME SOURCE)

Figure 59 shows the comparisons of measured and predicted burning rates in the open atmosphere simulations. In all cases, the burning rate is overestimated in the beginning of the simulations and under predicted in the end. The Resolution Indexes of for the simulations on 50 mm grids were approximately 16 for S1 and S3 and 8 for S5 and S7. The red lines correspond to simulations with 50 mm discretization interval. Due to the high computational demands of the simulations on a 25 mm grid, all of the simulations had not finished at the time of this writing. Somewhat surprisingly the difference between grid resolutions appears to be larger for the S1 and S3 cases even though they have higher resolution indexes. In all cases the error is in the conservative direction: burning rates are over predicted on coarse grids.

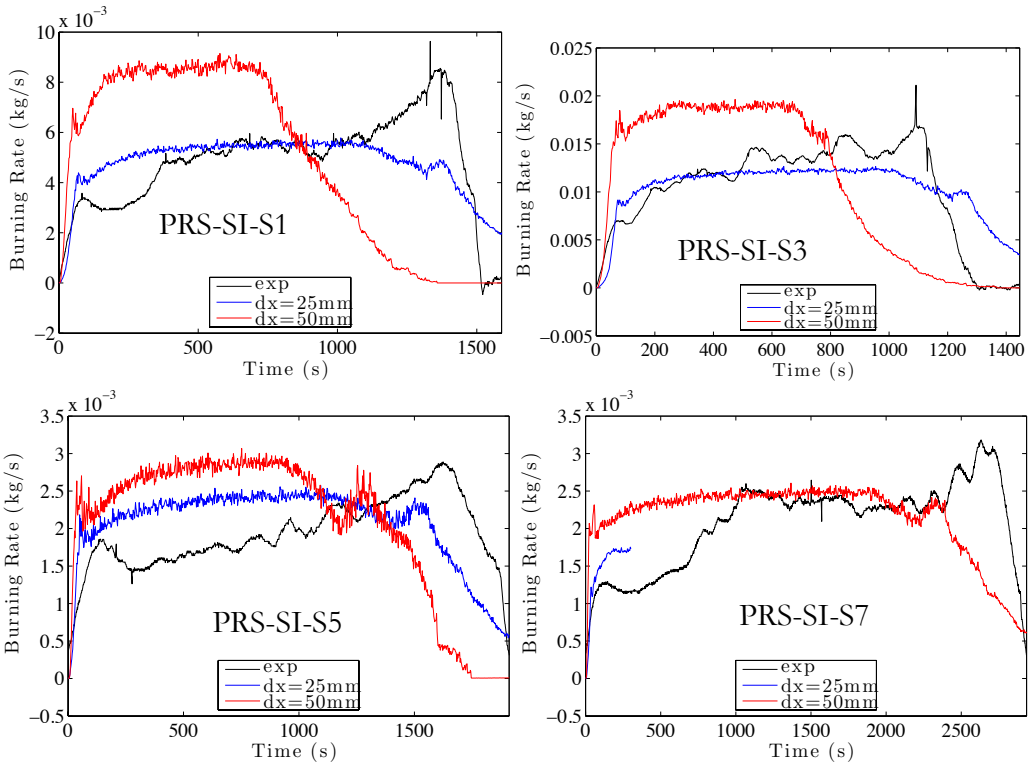

Figure 59. Comparison of predicted burning rates and experimental results

The overall shape of the burning rate curve with slight rise in burning rate towards the end seems hard to reproduce. Some of this dynamic is visible in all the simulations but it is not as pronounced as in the experimental data. The model currently in use doesn't include any effects of boiling and thus any changes in mass transfer rate due to boiling of a thin layer of liquid will be omitted from the simulations.

Initially, the evaporation model suffered from large overshoots. These problems were caused by the re-meshing strategy used for the condensed phase. Originally the condensed phase mesh was regenerated only if the size of the first cell fell under a certain threshold. This in turn caused a large change in the size of the first condensed phase cell. These large changes in the size of the first condensed phase cell lead to large differences in temperature gradient near the surface. This in turn leads to abrupt changes in the surface temperature. The evaporation model in use is very sensitive to the liquid surface temperature and thus these abrupt changes in surface temperature lead to spikes in the predicted mass loss rate. The solution to this problem was to force re-meshing at every time-step to avoid large changes in the mesh.

7.1.6. Compartment fires with predicted burning/prescribed ventilation (PRISME_SOURCE and PRISME_DOOR)

The simulation models used in this section are identical to the models used in Section 3.3.1, with the exception that the pool model described in Section 5.1 replaces the fuel inlet condition. The properties of the fuel are the same as those used in the free atmosphere PRISME SOURCE simulations. Comparison of the predicted and measured gas concentrations, temperatures, heat fluxes and wall temperatures are shown in Figure 60.

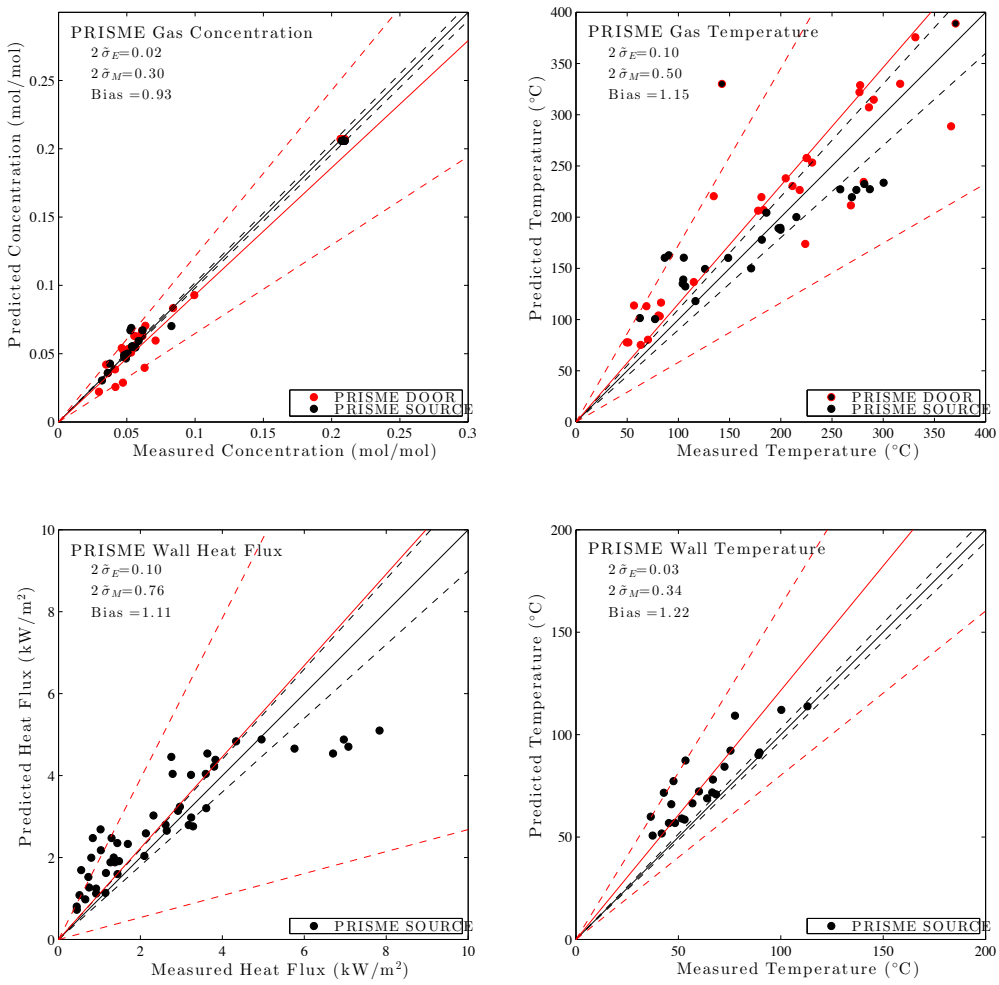

Figure 60. Measured vs. predicted quantities in the PRISME SOURCE and PRISME DOOR test series. Simulations with predicted HRR

As was the case with the simulations with prescribed mass loss rates, the predicted heat release rates are over predicted. Some part of this difference is most probably explained by uncertainties in the heat of combustion of the fuel. Considering the results of the grid sensitivity study, large part of the over prediction is likely to be caused by the, relatively coarse, 50 mm grid used in these simulations.

Another feature of the heat release rate predictions is that extinction due to lack of oxygen is not predicted. In the simulations of the PRISME-DOOR-D6 and D6a tests, periodic oscillations are present in the predicted mass loss rates. Figure 61 shows the predicted heat release rates from these tests. The lack of extinction could

perhaps be explained by the over prediction of the heat feedback on the fuel: smaller oxygen concentration is enough for sustained burning.

For gas concentrations, the bias factor is 0.93 and the standard deviation is 0.30. There are no obvious outliers in the gas concentration predictions. The gas temperature predictions are very similar to the predictions with prescribed heat release rate. Bias factor is 1.15 and in general the gas phase temperatures are over predicted.

The wall heat fluxes and wall temperatures are almost always over predicted. There is also considerable scatter in the wall heat flux predictions that is reflected in the large standard deviation of the model results. Comparing results in Figure 49 with those from Figure 4 it can be seen that in the predicted HRR simulations the wall heat fluxes are lower while the wall temperature predictions are higher. At first glance one would expect these to measurements to move in tandem. This strange behavior can be explained by different responses of these metrics to the HRR. The maximum wall heat flux prediction is to the maximum HRR during simulation: Whenever there is an intense peak in the HRR, there is also a peak in the wall heat fluxes. On the contrary, the wall temperature measurements are more sensitive to the average HRR during simulation. In the simulations with predicted HRR, the peaks of the HRR curve are not correctly predicted. The peaks are shorter in duration and don't happen at the correct times. On the other hand, the average HRR is over predicted. This leads to wall temperature predictions that are higher and wall heat flux predictions that are lower than corresponding predictions in the prescribed HRR cases.

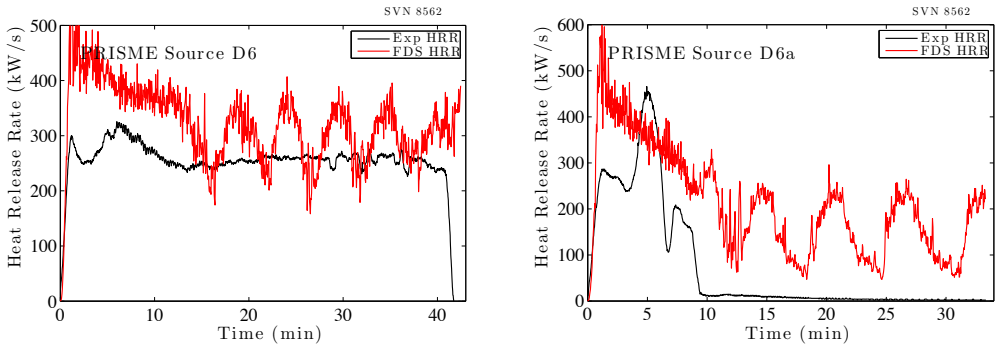

Figure 61. Predicted Heat Release Rates for PRISME source D6 and D6a tests. Both tests show oscillations in the predicted HRR and extinction due to lack of oxygen in D6a is not predicted.

Further information about the validation of the model can be found in a separate report from VTT (55)

7.2. Validation of the engineering model

The engineering model was validated in two different experimental set-ups. The first one is the LEAK1 test from the PRISME project, which was earlier predicted with the ventilation model and a prescribed mass loss rate in (62).

The results from the validation with the LEAK1 test are given in figure Figure 62 to Figure 64.

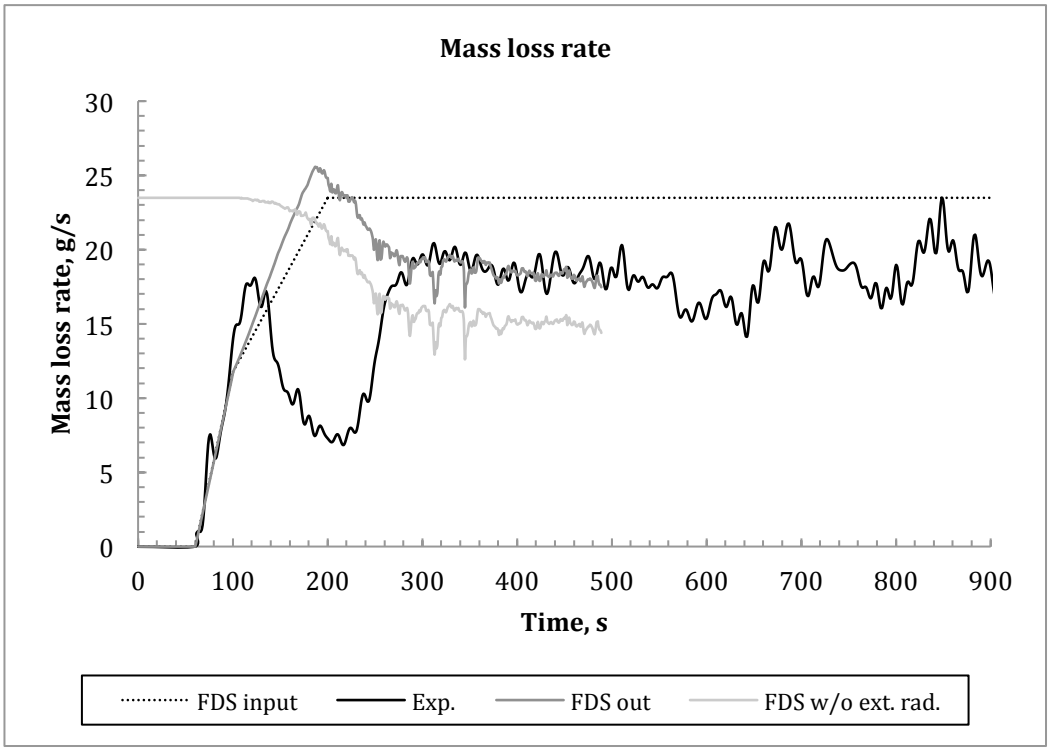

Figure 62 Prediction and test results of the mass loss rate in LEAK1 test

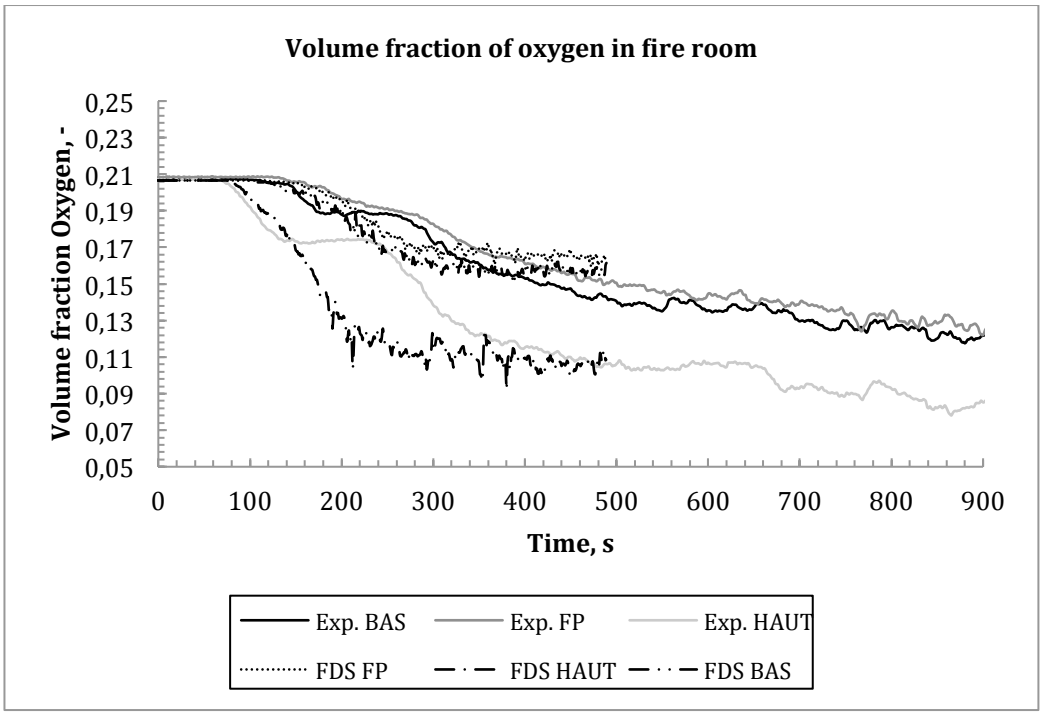

Figure 63 Prediction and test results of the oxygen volume fraction during LEAK1 test

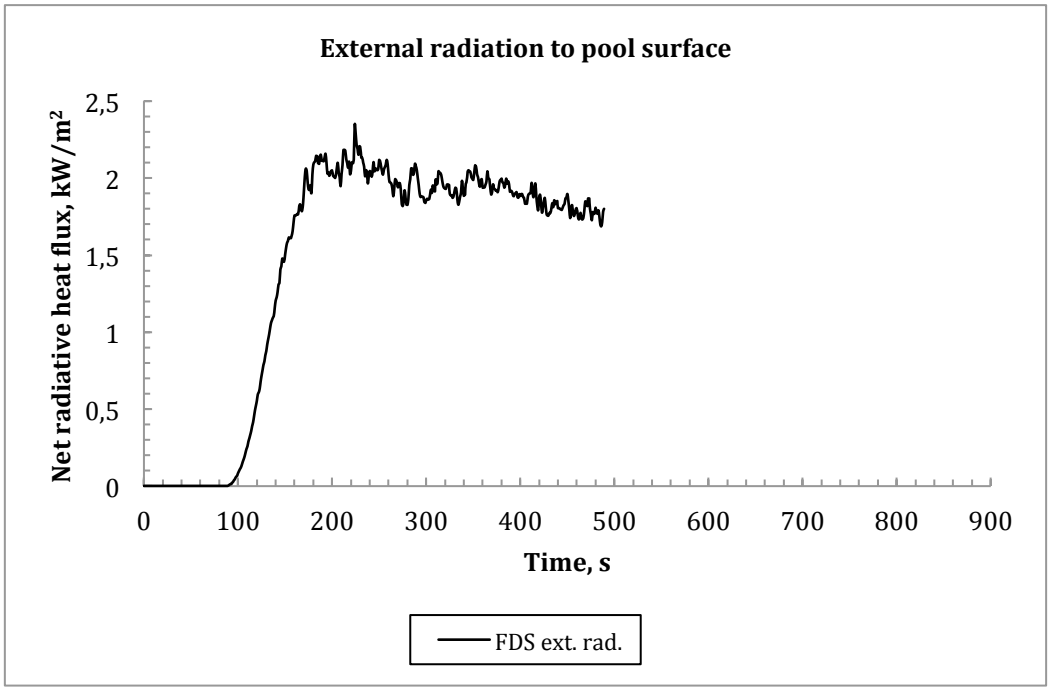

Figure 64 Simulation results of the net radiative heat flux to the pool during LEAK1 test simulation

The results show that the steady state mass loss rate is predicted very well and much better than without a radiation feedback model. The period from ignition to steady state still needs further improvement of the model. Also the prediction of the oxygen level needs some further improvement.

The second validation was the validation in a set-up used for the real-case application and which is reported in the next chapter on real cases.

8. Real case applications

In the third year of the project real case applications were performed both experimentally as well as modelling by using the engineering model. As preparation for this work package, two members of the project group (Tommy Magnusson and Fredrik Jörud) gathered information on real pool fires at nuclear power plants. They visited a nuclear power plant in the UK and collected information on a fire in a Swedish power plant.

8.1. Findings from the Heysham Nuclear Power Station (65)

Comprehensive efforts have been achieved at Heysham Nuclear PowerStation trying to predict the scenario from a large oil pool fire. Mr Jörud OKG/E.ON and Mr Magnusson Ringhals/Vattenfall arranged an expert meeting and a walk down the plant to get detailed knowledge of the thresholds in the evaluation procedure. A major challenge was to evaluate the consequences from a fire with a flooding as an attendant phenomenon. The only outer boundaries able to limit the pool size with high confidence, was the external walls of the turbine hall. The access to fuel was initially unlimited due to the large amounts of turbine oil available, why also the fire was considered to be oxygen controlled.

Fire dynamic calculations by hand, two-zone models as well as fluid dynamic simulation have been applied in the evaluation process.

At a top, 18 meters in diameter oil pools and rate of heat release of 600 MW, have been evaluated based on fire dynamic calculations.

In spite of an extreme fire load, a quite high level of conformity between the different methods of calculation could be achieved. Output data from the temperature in the hot gas layer of the reactor building was from hand calculation (316 °C), CFAST (296 °C) and CFD (280-350 °C).

8.2. Fire in Swedish power plant in Örebro (66)

8.2.1. Introduction

The 9th of January 2014 F. Jörud (ESS) and T. Magnusson (Vattenfall) were invited by E.ON to get information of the accidental event that took place on the 6th of October 2012 at Åbyverken in Örebro. The 10th of January we were also invited to Nerikes Rescue Services (the municipal fire brigade) to get information of the rescue operation. TGM Kanis the German supplier of the turbine have together with the owner E.ON carefully investigated the accident. There was no wrong with the turbine itself but there was a mismatch of conductor connections of the over-speed protection that caused the turbine over-speed accident.

8.2.2. General

When start up test running of 70 MW turbine, malfunction of high over speed protection occurs and cause shaft burst and gearbox failure. Missiles from gearbox spread in turbine hall, large pieces hit the roof and turbine shaft is thrown away outside the building.

The over-speed protection has three independent levels of action. Nominal speed is 6797 rpm. 1st level of speed 7486 rpm, 2nd level is 7646 rpm and 3rd 8086 rpm. The accident occurred at 114% of nominal rpm, i.e. 7749 rpm. Note the 3rd level is set above what turbine can withstand.

8.2.3. Cause of accident

The over-speed protection is designed as three independent instrument circuit probe sensors. Conventional mechanical device is not applied as standard equipment for this type of turbine. Due to mismatch of conductor connections the over-speed protection didn't work during initial test running sequence. Hence the turbine got in to over-speed mode.

Quality control program for start-up sequence following outage mode will require in depth approach with several administrative and/or technical barriers to avoid anticipated turbine failures.

8.2.4. Chain of action

At 15:58 h – Initiating event, over-speed accident. A missile from the gearbox causes damage of oil pipe for lubricating system and water suppression pipe. Rupture of the oil pipe cause leakage of approximately 8 m^3 oil. Post evaluations estimate the fire to peak 10 MW and combustion of total 6 m^3 oil. The friction of metal against metal probably caused heat and sparks for ignition of the lubrication oil. The oil flooded the turbine basement and burned out. Due to risk of hydrogen explosion from adjacent turbine, the fire brigade didn't enter the building for firefighting attempts. Instead the fire brigade started up the fire pumps for the water sprinkler system for the turbine and put mobile fan to overpressure the control room next to the turbine hall in order to avoid fire spread to the control room. At 18:00 h – The fire was probably self-extinguished. Several hundred m^3 of water flooded the turbine basement. To avoid environmental effects of oil in to adjacent river, it was necessary to initiate suction of the oil separators. The suction vehicles were needed for approximately 12 h. At 18:45 h - It was stated no missing persons remained in the building.

8.2.5. Experiences

The hot gasses from the fire cracked a large section of windows in the wall close to the ceiling. The gasses went out of the building surprisingly efficient. Fortunately also a port on the short end turbine basement stood fully open. The inlet air boosted the transition of hot gasses from the building and significantly limited the damages to only one turbine section. Upgrading of fire system will provide automatic opening of port to ensure this effect in case of fire.

Upgrade of sprinkler system will get redundant water supply to deluge system at turbine level. For turbine basement a wet pipe system will be provided for.

Crisis management team (CMT) exercised the week before together with fire brigade. This was a very well prepared training with 8 preparatory meetings. This was of high value when initiating the CMT for the turbine accident. The staff was familiar with each other and could initiate efficient work procedures immediately.

Oil and sprinkler pipes shouldn't be exposed to anticipated missile areas. Regarding the suppression section it is planned for redundant water supply. Oil pipe is rerouted from the area of potential missile exposure.

Assembly point for evacuated staff was located in hazardous area from potential ammonia leakage and hydrogen explosion zone.

Residual oil and fire extinguishing water went to the drains 2 hour preparedness of suction vehicle was considered not satisfactory. Other companies had to get requisitioned for support instead.

Large amount of chloride were produced by the fire, due to lots of PVC cables in turbine basement was engulfed by the fire. In the switchgear room chloride density of approximately 20 mg/cm2 was detected. Acceptable threshold for switchgear room is considered to 1 mg/cm2. Cleaning procedure for the electronics was initiated.

8.3. Real scale experiments and simulation with engineering models

As it was clear that it was difficult

8.3.1. Experimental set-up

All tests were conducted on site at the Ringhals (Swedish nuclear power plant) fire brigade training field. The setup consisted of two standard 20 foot containers that had been connected to each other with a fire door, a fire damper and a floor drain (in each compartment connected through a pipe underneath the containers), see Figure 65, Figure 66 and Figure 67. All of the connections could be either opened or closed which was used to create different smoke spread scenarios. The inside of the fire room had been insulated using mineral board (mounted using steel studs) and 70 mm of glass fiber insulation, the non-fire container was un-insulated. The inner dimension of the insulated container was 5.60x2.14x2.30 meters (length, width, height). The inner dimension of the un-insulated container was 5.90x2.35x2.39 meters (length, width, height).

The fire source consisting of a pool fire in two sizes (300x300 and 435x435 mm) was placed in the very middle of the room, an array of thermocouples were placed in the centerline of the room 2 meters from the center of the fire source with a distance of 20 cm in between starting 20 cm from the floor (Figure 69). Measurement points for oxygen levels were placed at the edge of the pool vessel at a height of 30 cm and in the thermocouple array at a height of 1.8 meters over the floor. A differential pressure measurement was made by a small pipe inserted through the container wall and welded to get an air-tight connection. A connection for a fan was placed in one of the lower corners of the fire room (see

Figure 68 and Figure 69), this was used to connect a fan standing outside of the containers in some scenarios where mechanical ventilation was of interest. Bi-directional probes were placed by the fire damper opening (see Figure 67) and the floor drain opening in the non-fire compartment to be able to measure the flow induced by the fire in the cases where these were in open position. Thermocouples were also placed at the same positions with the addition of one thermocouple in the fan inlet pipe.

The experimental setup was very tightly sealed since the effect of the fire pressure was of prime interest. All corners, joints and screw holes were sealed with fire resistant joint filling to prevent leaking in other places than those that were being monitored.

Figure 65 Overview of the experimental setup on site.

Figure 66 The connecting pipe between the floor drains in the two rooms (fire and non-fire room).

Figure 67 The placement of the fire damper, the left picture is from inside the fire room, the right picture is in the non-fire room where the bi-directional probes and coupled thermocouples were placed.

Figure 68 Close up picture of the connection pipe (200 mm) where the fan was connected. The picture is taken from inside the fire room; the fan was placed on the other side of the wall (outside).

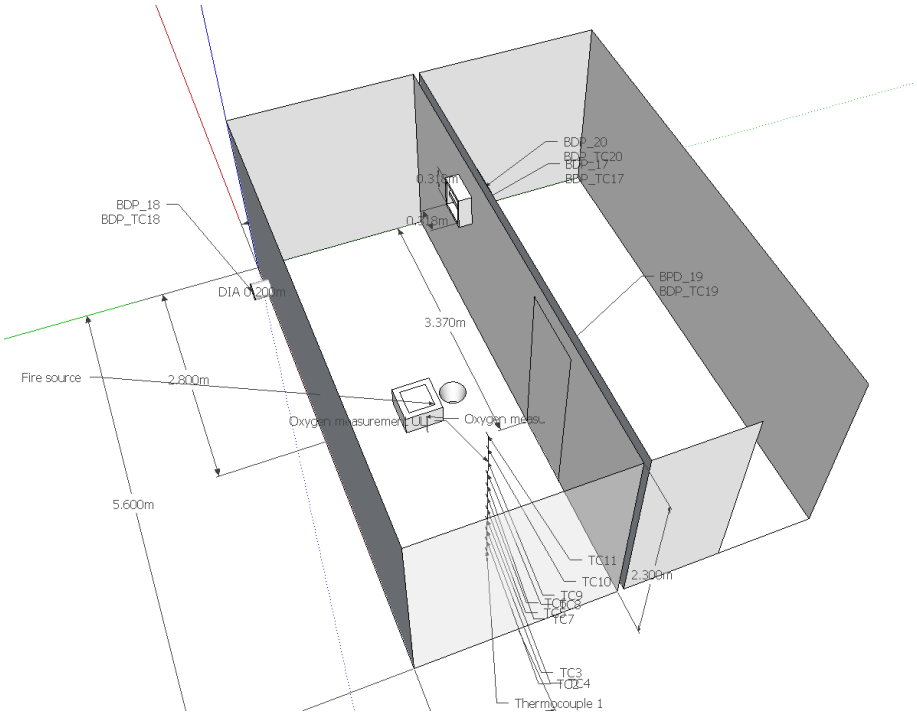

Figure 69 3D overview of the experimental setup. The fan connection is in the top left corner, the fire source is placed in the middle of the left room, the floor drain is placed close to the fire and its position is mirrored in the other compartment. The fire door and fire damper placement can also be seen in the middle wall.

8.3.2. Test results

All test results are available in reference (67) but for this project only one test was selected and that is Ringhals test 6. The settings for this test are given in Table 16.

The fan inlet was plugged, the floor was drain opened up and was filled with water (approximately 10-15 cm) at both ends of the pipe (both fire room and non-fire room), fire damper was closed, and the fire door was closed.

A 435x435 mm^2 pool fire containing heptane was used.

Purpose of the test was to determine if the over-pressure of the fire, with increased heat release rate compared to tests 3-5, would overcome the hydrostatic pressure of the water in the floor drain and thereby open up a passage for potential smoke spread between the two rooms. A secondary purpose was to observe the influence of oxygen depletion on the mass loss rate.

Table 16 Settings for test nr 6.

Test number	Fan flow rate [l/s]	Floor drainage mode	Damper mode	Door mode	Pool size [mm]
6	closed	water	closed	closed	435x435

Results of tests are given in Figure 70 to Figure 74.

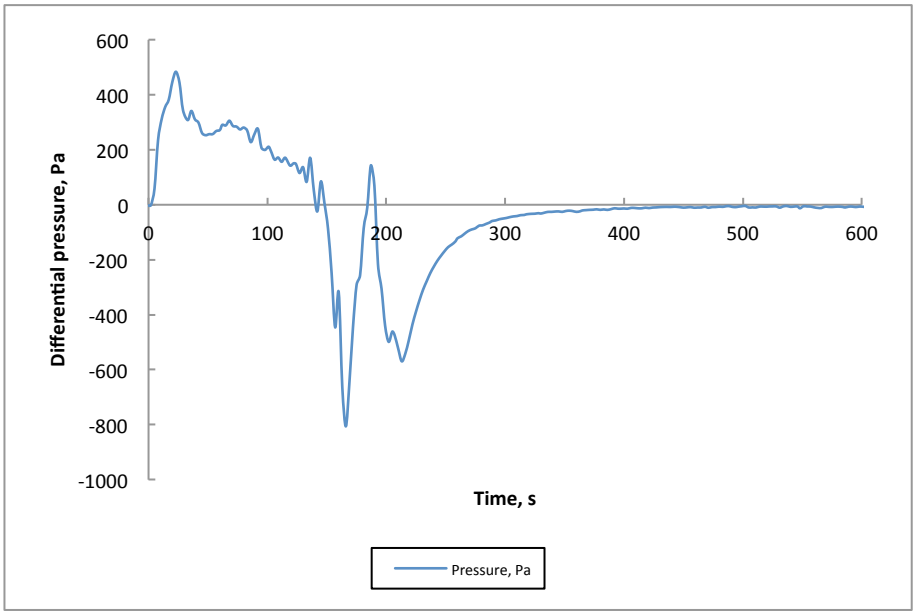

Figure 70 Pressure in the fire room, test 6.

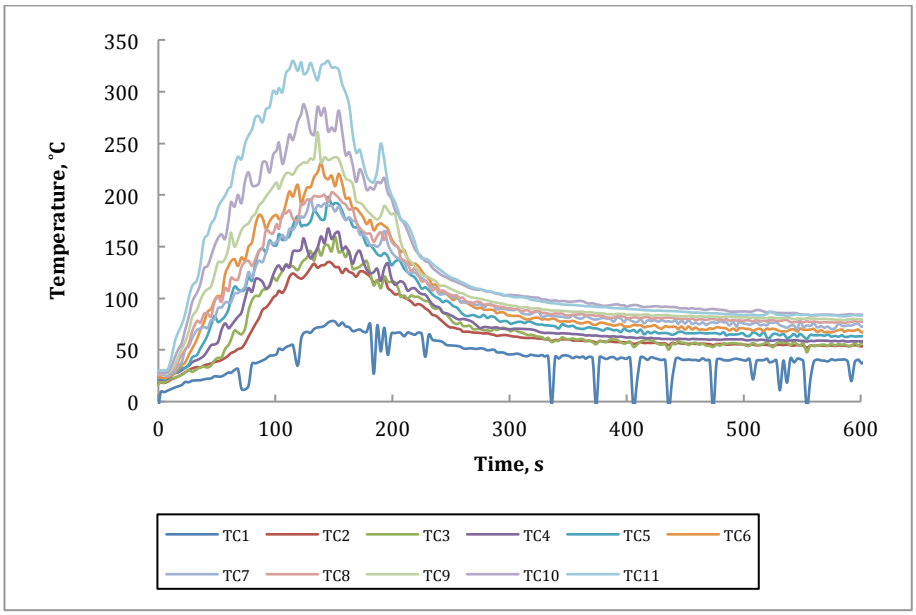

Figure 71 Temperatures in the thermocouple tree placed inside the fire room, test 6.

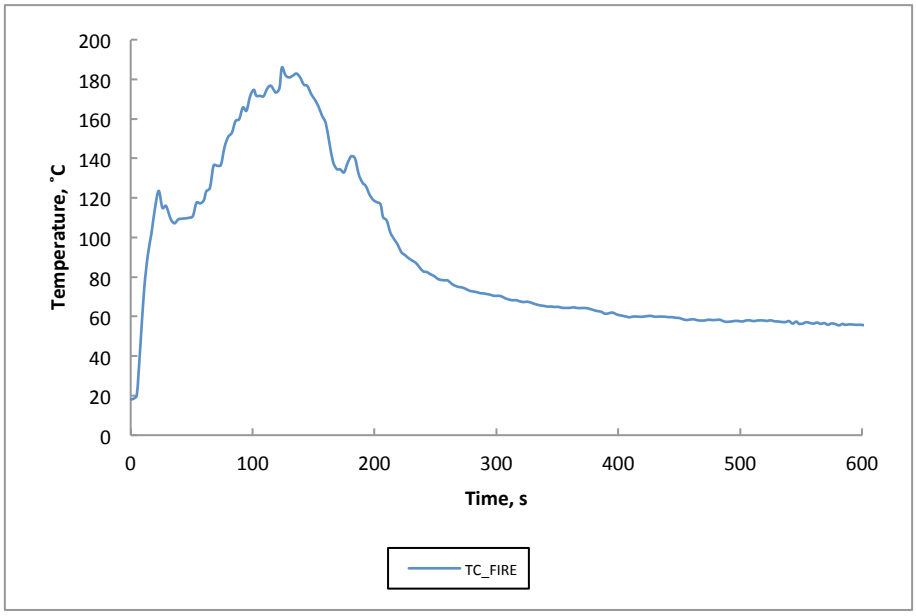

Figure 72 Temperature close to the pool fire, test 6.

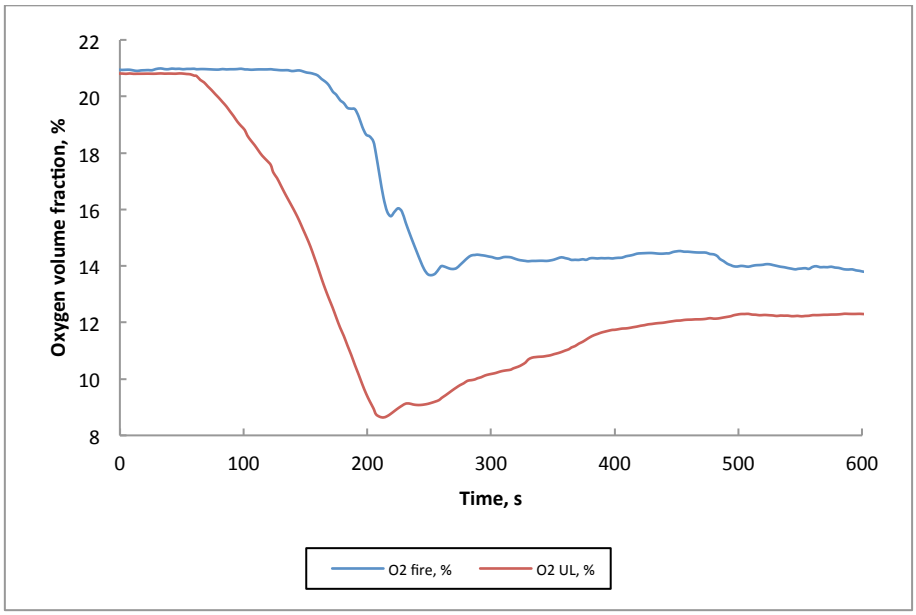

Figure 73 Oxygen concentration (dry air) close to the fire source and in the upper layer, test 6.

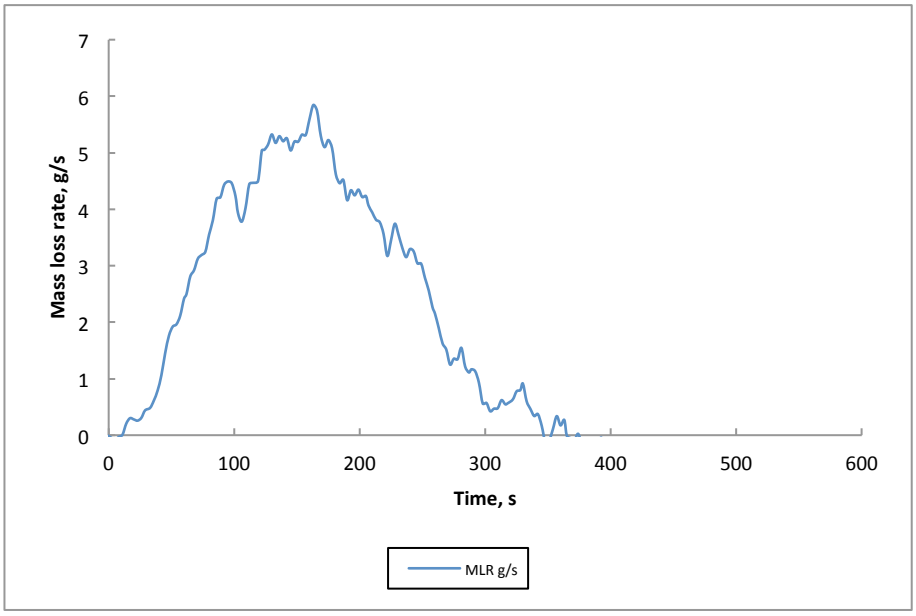

Figure 74 Mass loss rate of the pool fire containing heptane, test 6.

8.3.3. Validation with engineering model

On of the tests, Ringhals test 6, was simulated by means of FDS including the ventilation module and the engineering model

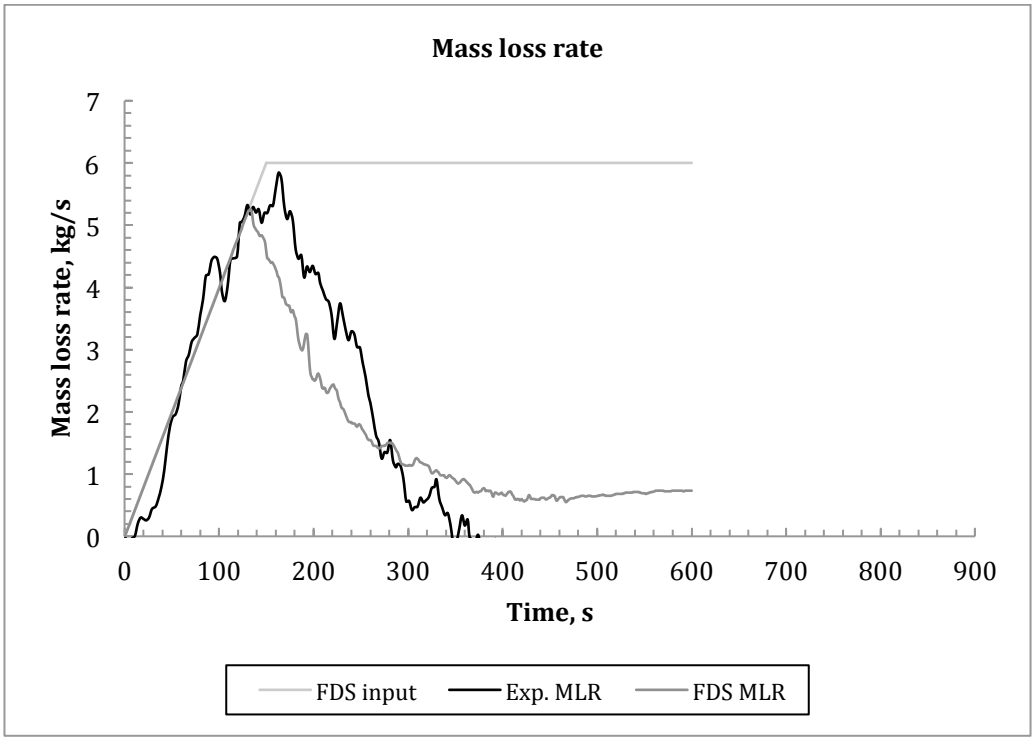

Figure 75 Simulation of mass loss rate for Ringhals test nr 6 and comparison with test

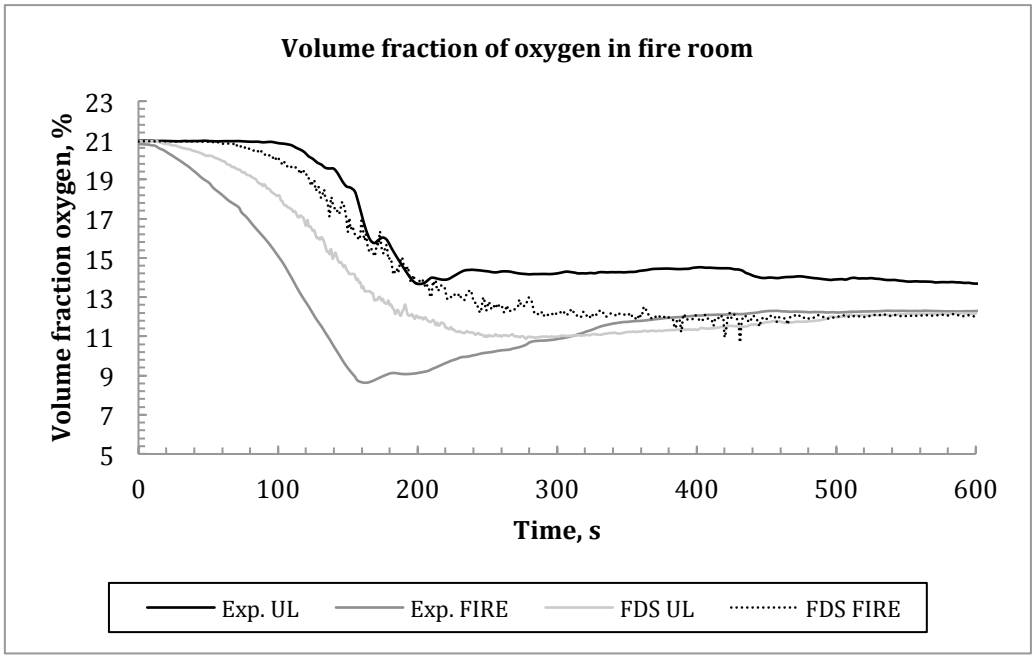

Figure 76 Simulation of oxygen volume fraction rate for Ringhals test nr 6 and comparison with test data

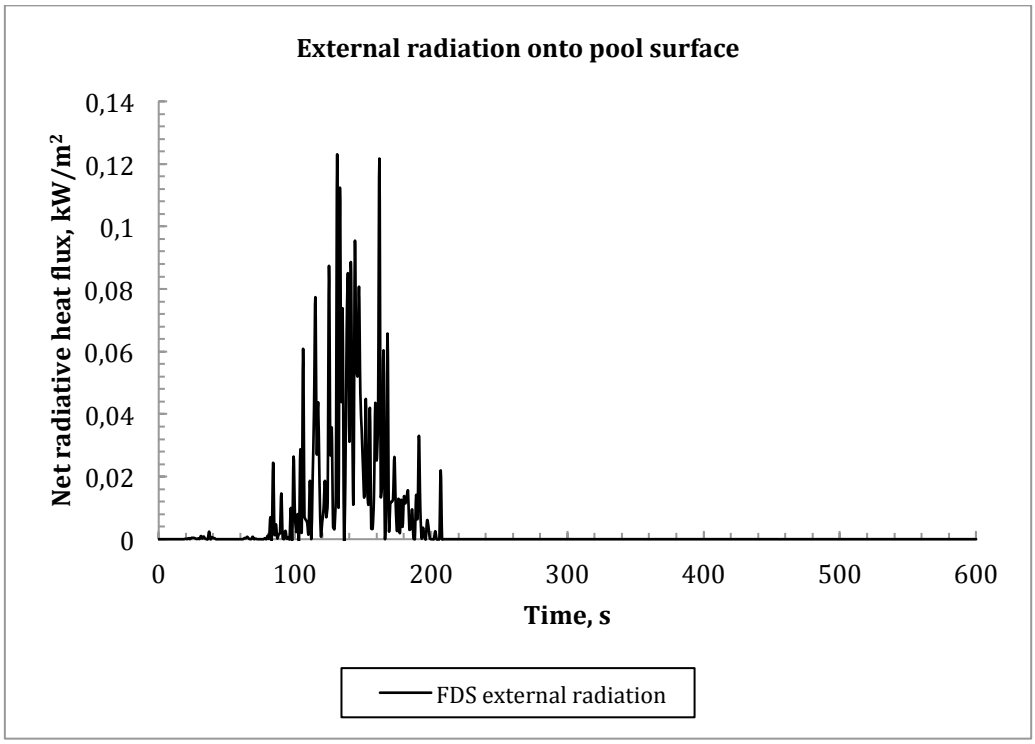

Figure 77 Net radiative heat flux onto pool surface.

The results show that the mass loss rate is predicted rahter well with the engineering model but that some improvement for the oxygen levels is possible in future development.

9. Dissemination

During the project two major routes of dissemination were used. One part was the publication of articles and master thesis. The other part was the organisation of a workshop in Lund University.

9.1. Scientific publications

During the project different bodies were informed such as NBSG in Sweden and the research partners in the SAFIR 2014 project and LARGO ad hoc groups in Finland Even the project partners in the PRISME project received updates of the project during the PRISME project meetings. The following publications can be coupled to the project and are part of the scientific dissemination:

- The validation of the ventilation module has been presented as a poster at the IAFSS conference in Maryland, June 2011 and at the SMIRT conference in München, September 2011 (37).
- Presentation of the project as part of an invited paper at the AOFST 2012 conference in Hefei. (50)
- Publication of a Master thesis at HSH (51)
- Submission of the validation of the ventilation module to Fire Safety Journal (62)
- Several presentations at the project group of the OECD project PRISME by both VTT and LTH, due to confidentiality rules it is not possible to give the content.
- Presentation of the transformer liquids and liquid models at the SMIRT conference in Columbia USA, 2013. (57)
- Master thesis on transformer liquids (58) and corresponding article submitted to fire technology and accepted but not printed (59)
- Presentation of the validation work of the ventilation module at the SFPE conference in Hong Kong. (61)
- VTT report on pyrolysis model (55)
- First year report of poolfire (63)
- Second year report of poolfire (64)
- Reports on real fire incidents. (65) (66)
- Test reports on real-scale tests. (67)

9.2. Workshop.

After the project a workshop was organised in conjunction with the FDS workshop in Lund. 43 participants. The Participants and the overall programme are given in Annex B.

The programme of the second half-day of the workshop contained presentation of all project partners and the programme was as follows:

- Patrick van Hees - Introduction of the pool fire project VTT - Predicting the heat release rate of liquid pool fires using FDS
- Jonathan Wahlqvist - Validation of ventilation module in FDS as support for modelling of pool fires
- Bjarne Husted - Activities of Haugesund in Pool fires
- Tommy Magnusson - Real fire accidents with pool fires in power plants
- Fredrik Jörud ESS - Implementation of data on pool fires with transformer oils inside the ESS facility (presented by Patrick van Hees)

10. Conclusions

The following achievement were obtained in the POOLFIRE project:

- Accuracy of the FDS simulation of the gas concentrations and gas phase velocities in the PRISME SOURCE and PRISME DOOR tests was determined. The simulations were carried out using prescribed burning rates and ventilation rates. Smallest uncertainties were found for the gas concentrations and highest bias for wall heat fluxes. Heat fluxes on the walls were drastically over estimated in many cases. In contrast the wall temperatures showed good agreement with the experimental values. For gas temperatures, the simulations were not biased in average, but the relative standard deviation was large.
- Based on the current, rather limited set of burning rate predictions, the new evaporation model clearly outperforms the old evaporation model. When the boundary layer resistance to the mass transfer is not taken into account, the burning rates are too high and the general dynamics of the pool fire are not reproduced. In contrast the new mass transfer coefficient based model predicts burning rates that are much closer to the experimental values. In addition the general dynamics of the pool fire with HRR increasing towards the extinguishment phase is reproduced.
- Although the new evaporation model is clearly step in the right direction, more work needs to be done to ensure the numerical stability of the numerical scheme. The current version is prone to overshoots that result in unphysical sharp spikes in the burning rate curve. Sometimes these spikes lead to numerical instability. An iterative procedure might be required to overcome these difficulties, instead of the current explicit method. Moreover, measurement of radiative characteristics (absorption spectra) for the liquid fuels must be carried out for good predictions.
- Good prediction is obtained by the new ventilation module in FDS, which allows us to use both models (pyrolysis and ventilation module) in order to predict some of the testdata, which will be obtained and generated later in the project.
- An engineering model for pool fire predictions was developed. The first results are promising but the dynamic behaviour after ignition can still be improved as could be seen in the PRISME tests.
- The project provided a number of test data for validation in this project but also for further validation in new projects. It was shown that introduction of new measurement such as PIV was not so straightforward as expected.
- A first set of test data in small scale was obtained for different transformer fuels. This small-scale test can be used in future validation work.
- The project studies also a few real fires to show the importance of controlling pool fires in nuclear power plant.
- At the end of the project a real-scale test was set-up and conducted in a two-container set-up with ventilation and real scale installation such as dampers and water drains. One of the tests was also validated rather successfully with the engineering model.
- The project provided a large number of publications and involved two master students and was concluded by a small workshop held in Lund April 23 and 24 2014.

References

1. Babrauskas, V. (1983), Estimating large pool fire burning rates, Fire Technology, 19, pp 251-261.
2. Peatross, M.J., Beyler, C.L., (1997), Ventilation effects on compartment fire characterization, IAFSS, Fire Safety Science—Proceedings of the Fifth International Symposium, Vol. 5, International Association for Fire Safety Science, pp 403-414.
3. Quintiere, J.G., Rangwala, A.S., (2004), A theory for flame extinction based on flame temperature, Fire and Materials, Volume 28, pp 387-402.
4. Utiskul, Y., (2006), Theoretical and experimental study on fully-developed compartment fires, Fire Engineering, University of Maryland.
5. Melis, S., Audouin, L., (2008), Effects of vitiation on the heat release rate in mechanically-ventilated compartment fires, IAFSS Fire Safety Science - Proceedings of the Ninth International Symposium, Volume 9, International Association for Fire Safety Science, pp. 931-942.
6. http://www.oecd-nea.org/jointproj/prisme.html, 2011-10-15, OECD (downloaded 2012-01-31).
7. Nasr, A., Suard, S., Garo, J.-P., El-Rabii, H., Gay, L., (2010), Determination by a CFD code and a global model of the fuel mass loss rate in a confined and mechanically-ventilated compartment fire, International Conference on Fire Research and Engineering, Interflam Committee, pp 1775-1781.
8. Tewarson, A., Lee, J.L., Pion, R.F., (1981), The influence of oxygen concentration on fuel parameters for fire modelling, 18th International Symposium of Combustion, Combustion Institute, pp 563-570.
9. Orloff, L., de Ris, J., (1982), Froude modeling of pool fires, 19th International Symposium on Combustion, Combustion Institute, pp. 885-895.
10. Klassen, M., Gore, J., Sivathanu, Y., Hamins, A., Kashiwagi, T., (1992), Radiative heat feedback in a toluene pool fire, 24th International Symposium on Combustion, Combustion Institute, pp 1713-1719.
11. Hamins, A., Fisher, S.J., Kashiwagi, T., Klassen, M.E., Gore, J.P., (1994), Heat feedback to the fuel surface in pool fires, Combustion Science Technology, Volume 97, pp 37-62.
12. Hamins, A. , Yang , J.C. , and Kashiwagi , T., (1999) . A global model for predicting the burning rates of liquid pool fires. Technical Report NISTIR-6381, National Institute of Standards and Technology.
13. Siegel, R., Howell, J., (1981), Thermal Radiation Heat Transfer, 2nd edition, Hemisphere publishing Corporation, New York, p. 669.
14. Beaulieu, P., Dembsey, N., (2007), Effect of oxygen on flame heat flux in horizontal and vertical orientations, Fire Safety Journal, Volume 43, pp 410-428.
15. Novozhilov, V., Koseki, H., (2004), CFD prediction of pool fire burning rates and flame feedback. Combustion Science Technology, Volume 176, pp 1283-1307.

16. Snegirev, A.Y., (2004), Statistical modeling of thermal radiation transfer in buoyant turbulent diffusion flames, Combustion and Flame, Volume 136, pp 51-71.

17. Pretrel, H., Such, J.M., (2005), Effect of ventilation procedures on the behaviour of a fire compartment scenario, Nuclear Engineerng Design, Volume 235, pp 2155-2169.

18. Pretrel, H., Querre, P., Forestier, M., (2005), Experimental study of burning rate behaviour in confined and ventilated fire compartments, Fire Safety Science Proceedings of the Eighth International Symposium, Volume 8, International Association for Fire Safety Science, pp. 1217-1229-

19. Pretrel H., (2006), PRISME SOURCE - Technical specifications - DPAM/SEREA-2006-034 - PRISME-2006-01, IRSN.

20. Pretrel H., (2006), PRISME SOURCE – Tests in SATURNE - Test Report - DPAM/SEREA-2005-013 - PRISME-2006-02, IRSN.

21. Pretrel H., (2006), PRISME SOURCE - Tests in DIVA - Test Report - DPAM/SEREA-2005-052 - PRISME-2006-03, IRSN.

22. Le Saux, W., (2008) PRISME DOOR Programme - Analysis report - DPAM/SEREA-2008-157 - PRISME 26, IRSN.

23. Le Saux, W., (2006), PRISME SUPPORT - Properties of materials used during the tests performed in the DIVA facility - DPAM/SEREA-2006-355 - PRISME-015, IRSN.

24. McGrattan, K.B., Hostikka, S., Floyd, J.E., McDermott, R. and Prasad, K. (2007) Fire Dynamics Simulator, Technical Reference Guide, Volume 1: Mathematical Model. NIST Special Publication 1018-1, National Institute of Standards and Technology, Gaithersburg, Maryland.

25. McGrattan, K.B., Hostikka, S., Floyd, J.E., McDermott, R. and Prasad, K. (2007), Fire Dynamics Simulator (Version 5), Technical Reference Guide, Volume 3: Experimental Validation. NIST Special Publication 1018-5, National Institute of Standards and Technology, Gaithersburg, Maryland.

26. Audouin, L., Chandra, L., Consalvi, J.L., Gay, L., Gorza, E., Hohm, V., Hostikka, S., Itoh, T., Klein-Hessling, W., Lallemand, C., Magnusson, T., Noterman, N., Par, J.S., Peco, J., Rigollet, L., Suard, S., van Hees, P., (2011), Quantifying differences between computational results and measurements in the case of a large-scale well-confined fire scenario, Nuclear Engineering Design, 241, pp 18-31.

27. Floyd, J., (2010), Coupling a Network HVAC Model to a Computational fluid Dynamics Model Using Large Eddy Simulation.

28. Roesgen, T., et al., (2008), Turbulence model validation for fire simulation by CFD and experimental investigation of a hot jet in crossflow, Fire Safety Journal, Fire Safety Journal 01/2008; DOI: 10.1016/j.firesaf.2007.11.005.

29. Audouin, L., et al., (2011a), Quantifying differences between computational results and measurements in the case of a large-scale well-confined fire scenario, Nuclear Engineering and Design, Volume 241, Issue 1, Pages 18-31.

30. Audouin, L., Prétrel, H., Le Saux, W., (2011b), Overview of The OECD PRISME Project – Main Experimental Results, 21st International Conference on Structural Mechanics in Reactor Technology (SMiRT 21).

31. Klein-Heßling, W., Nowack, H., Spengler, C., Weber, G., Höhne, M., Sonnenkalb, M., (2010), Cocosys--New modelling of safety relevant phenomena and components, Proceedings of EUROSAFE 2010.

32. Melis, S. and Audouin, L., (2008), Effects of vitiation on the heat release rate in mechanically-ventilated compartment fires, Fire Safety Science 9: 931-942.

33. Nasr A., Suard S., El-Rabii H., Gay L., Garo J.-P., (2011), Fuel Mass-Loss Rate Determination in a Confined and Mechanically Ventilated Compartment Fire Using a Global Approach, Combustion Science and Technology, Vol. 183, Iss. 12.

34. Pretrel, H., Audouin, L., (2010), Smoke movement induced by buoyancy and total pressure between two confined and mechanically ventilated compartments, Interflam 2010, Proceedings of the Twelfth International Conference, Volume 2, Interscience Communications, London, p. 1053-1064.

35. Pretrel, H. and Audouin, L., (2011), Doorway Flows Induced by the Combined Effects of Natural and Forced Ventilation in a Three Compartment Assembly, Fire Safety Science 10: 1015-1027.

36. Rigollet, L., Röwekamp, M., (2009), Collaboration of fire code benchmark activities around the international fire research program PRISME, Proceedings of EUROSAFE 2009.

37. Van Hees, P. et al., (2011), Validation and development of different calculations methods and software packages for fire safety assessment in Swedish nuclear power plants, 21st International Conference on Structural Mechanics in Reactor Technology (SMiRT 21) - 12th International Pre-Conference Seminar on "FIRE SAFETY IN NUCLEAR POWER PLANTS AND INSTALLATIONS", Munich 2011.

38. McGrattan, K. et al., (2010), NIST Special Publication 1019-5 Fire Dynamics Simulator User's Guide, NIST.

39. McGrattan, K. et al., (2012a), NIST Special Publication 1019 Fire Dynamics Simulator (Version 6) User's Guide, NIST.

40. Floyd, J., (2011), Coupling a network HVAC model to a computational fluid dynamics model using large eddy simulation. Fire Safety Science 10: 459-470.

41. McGrattan, K. et al., 2012b, NIST Special Publication 1018 Fire Dynamics Simulator Technical Reference Guide, NIST.

42. Le Saux, W., Pretrel, H., Lucchesi, C. and Guillou, P., (2008), Experimental study of the fire mass loss rate in confined and mechanically ventilated multi-room scenarios, Fire Safety Science 9: 943-954.

43. Pretrel, H., Querre, P. and Forestier, M., (2005), Experimental Study Of Burning Rate Behaviour In Confined And Ventilated Fire Compartments, Fire Safety Science 8: 1217-1228.

44. ASHRAE, (2009), ASHRAE Handbook: Fundamentals, Atlanta, GA, American Society of Heating, Refrigeration and Air-conditioning Engineers.

45. ASHRAE, (2012), ASHRAE Handbook: HVAC Systems and Equipment, Atlanta, GA, American Society of Heating, Refrigeration and Air-conditioning Engineers.

46. DiNenno, P.J. et al, (2002), SFPE handbook of fire protection engineering (Third edition), National Fire Protection Association.

47. Babrauskas, V., 1983, Estimating large pool fire burning rates, Fire Technology, 19, pp 251-261.

48. Peatross, M.J., Beyler, C.L., (1997), Ventilation effects on compartment fire characterization, IAFSS, Fire Safety Science—Proceedings of the Fifth International Symposium, Vol. 5, International Association for Fire Safety Science, pp 403-414.

49. Hayasaka, H., (1997), Unsteady Burning Rates of Small Pool Fires, IAFSS, Fire Safety Science—Proceedings of the Fifth International Symposium, Vol. 5, International Association for Fire Safety Science, pp 499-510.

50. Van Hees P., (2013), Validation and Verification of Fire Models for Fire Safety Engineering. Procedia Engineering 62:154–168. doi: 10.1016/j.proeng.2013.08.052.

51. Skarsbø, L.R., (2011), An Experimental Study of Pool Fires and Validation of Different CFD Fire Models, Department of Physics and Technology, University of Bergen, Bergen.

52. Johansen, (2012), Implementation of Improved EDC Combustion Model in the Open LES Code FDS. Department of Physics and Technology. Bergen, University of Bergen 2012.

53. Afeefy H.Y., Liebman, J.F., and Stein, S.E., Burgess, D.R., Neutral Thermochemical Data in NIST Chemistry WebBook, NIST Standard Reference Database Number 69, Eds. P.J. Linstrom and W.G. Mallard, National Institute of Standards and Technology, Gaithersburg MD, 20899, http://webbook.nist.gov.

54. Gottuk D. T. and White D. A., (2002) Liquid Fuel Fires. Chapter 2, Section 15, NFPA HFPE-02, SFPE Handbook of Fire Protection Engineering. 3rd Edition.

55. Sikanen, T., Hostikka S., (2014), Modeling and simulation of liquid pool fires, VTT research report VTT-R-00622-14, Espoo, 2014.

56. Van Hees, P., Johansson, N., Wahlqvist, J., Magnusson T., (2011), Validation and development of different calculations methods and software packages for fire safety assessment in Swedish nuclear power plants, 21st International

Conference on Structural Mechanics in Reactor Technology (SMiRT 21) – Proceedings of the 12th International Pre-Conference Seminar on "Fire Safety in nuclear power plants and installations, Munich.

57. Wahlqvist, J., Hellebuyck, D., Van Hees, P., Magnusson T., Jörud. F., (2013), Recent fire research related to Swedish nuclear power plants and European spallations source, 22st International Conference on Structural Mechanics in Reactor Technology (SMiRT 22) - 13th International Pre-Conference Seminar on "FIRE SAFETY IN NUCLEAR POWER PLANTS AND INSTALLATIONS", Columbia, USA.

58. Hellebuyck, D., (2013), Functional performance criteria for comparison of less flammable transformer oils with respect to fire and explosion risk, Report 5424, Lund University, Lund.

59. Hellebuyck, D., Van Hees, P., Magnusson T., Jörud. F., (2014), Fire behaviour of less flammable dielectric liquids in European Spallation Source, submitted to Fire Technology (accepted but not yet published).

60. Kong D., (2012), Pool fire experiments with preheated heptane and methanol, LTH report in preparation, Lund.

61. Wahlqvist J., (2012), Predicting Smoke Spread from Mechanically Ventilated Compartments using FDS taking into account the importance of leakage, 9th International Conference on performance based codes and fire safety design methods, SFPE, Hongkong.

62. Wahlqvist, J., van Hees, P., (2013), Validation of FDS for large-scale well-confined mechanically ventilated fire scenarios with emphasis on predicting ventilation system behaviour, Fire Safety Journal Fire Safety Journal, Volume 62, Page 102 to 114, Elsevier.

63. Van Hees, P., Wahlqvist, J., Hostikka S., Sikanen, T., Husted, B., Magnusson, T., Jörud, F., (2012), Prediction and validation of pool fire development in enclosures by means of CFD (Poolfire) Report – Year 1, Lund report 3163, ISRN: LUTVDG/TVBB--3163—SE, Lund.

64. Van Hees, P., Wahlqvist, J., Kong, D., Hostikka S., Sikanen, T., Husted, B., Magnusson, T., Jörud, F., (2013), Prediction and validation of pool fire development in enclosures by means of CFD (Poolfire) Report – Year 2, Lund report 3169, ISRN: LUTVDG/TVBB--3169—SE, 2013, Lund.

65. Magnusson T., Jörud, F., (2012), Minnesanteckningar från besök på Heysham avseende NKS projekt "large oil pool fires", Vattenfall Report, reference 2185119 / 2.0.

66. Magnusson T., (2014), Experience from a poolfire at Åbyverket Örebro October 2012, Vattenfall Report, reference 2273233 / 2.0.

67. Wahlqvist et al, (2014), Experimental study on enclosed fires with various interconnections between compartments, LTH report Report 3176., Lund.

Additional literature

Blinov, V., Khudiakov, G., (1959), Certain laws governing diffusive burning of liquids, Fire Research Abstract and Review, Volume 1 , pp 41-44.

de Ris, J., (1979), Fire radiation-a review, Proceedings Combustion Institute, Volume 17, pp 1003–1016.

Di Nenno, P. (Ed.), (2002), SFPE Handbook of Fire Protection Engineering, 3rd edition, National Fire Protection Association, Quincy, MA.

Drysdale, D., (2011), An Introduction to Fire Dynamics, Third edition, John Wiley & Sons, Chichester.

Hottel, H., Sarofim, A., (1967), Radiative Transfer, McGraw-Hill, New York.

Karlsson, B., Quintiere, J., (1999), Enclosure Fire Dynamics, CRC Press, Boca Raton.

Koseki, H., Hayasaka, H., (1989), Estimation of thermal balance in heptane pool fire, Journal of Fire Science, Volume 7, pp 237-249.

Lautenberger, C.W., Fernandez-Pello, C., (2009), Generalized pyrolysis model for combustible solids, Fire Safety Journal, Volume 44, pp 819-839.

Magnussen, B.F., Hjertager, B. H., (1976), On mathematical modeling of turbulent combustion with special emphasis on soot formation and combustion, Symposium International Combustion, Volume 16, pp 719-729.

Mulholland, G., Henzel, V., Babrauskas, V., (1989), The effect of scale on smoke emission, Second Symposium International Association Fire Safety Science, IAFSS, pp 347-357.

Novozhilov, V., (2001), Computational fluid dynamics modelling of compartment fires, Programme Energy Combustion Science, Volume 27, pp 611-666.

Pretrel, H., Audouin, L., (2010), Smoke movement induced by buoyancy and total pressure between two confined and mechanically ventilated compartments, Interflam 2010, Proceedings of the Twelfth International Conference, Volume 2, Interscience Communications, London, p. 1053-1064.

Quintiere, J.G., (2006), A theoretical basis for flammability properties, Fire and Materials Journal , Volume 30, pp 175-214.

Suard, S., Lapuerta, C., Babik, F., Rigollet, L., (2011), Verification and validation of a CFD model for simulations of large-scale compartment fires, Nuclear Engineering Design, Volume 241 (9), pp 3645-3657.

Suard, S., Nasr, A., Melis, S., Garo, J.P., El-Rabii, H., Gay, L., Rigollet, L., Audouin, L., (2011), Analytical approach for predicting effects of vitiated air on the mass loss rate of large pool fire in confined compartments, 10th International Symposium on Fire Safety Science (IAFSS), Maryland.

Annex A Acronyms

Brandforsk: Swedish Board for Fire Research

CFD: Computational Fluid Dynamics

FDS: Fire Dynamics Simulator software programme

FSE: Fire Safety Engineering

IRSN: Institut de radioprotection et de sûreté nucléaire

NBSG: National Fire safety group (composed av SSM, SKB and nuclear power plants at Oscarshamn, Forsmark and Ringhals)

NEA: Nuclear energy agency

OECD: Organisation for Economic Co-operation and Development

ISO: International Standardisation Organisation

QRA: Qualitative Risk Analysis

SKB: Svensk kärnbränslehantering AB (Swedish Nuclear Fuel and Waste Management Company)

SSM: Strålsäkerhetsmyndigheten (Swedish Radiation Protection Agency)

SVN: Apache Subversion (formerly called Subversion, command name svn) is a revision control system initiated in 2000 by CollabNet Inc. Developers use Subversion to maintain current and historical versions of files such as source code, web pages, and documentation

TS: Technical Specification

Annex B Workshop Participants and Programme

1. Participants

In total 43 participants participated coming from Norway, Finland, Sweden, Denmark and Germany.

Name	Company	Country
Blanca Andres Valiente	DBI	Denmark
Flemming Villads Jørgensen	Søren Jensen Rådgivende Ingeniørfirma as	Denmark
Jesper Prip Bonnesen	Grontmij A/S	Denmark
Jess Grotum Nielsen	Søren Jensen Rådgivende Ingeniørfirma as	Denmark
Kim Sommerlund-Thorsen	DBI	Denmark
Nicholas Lavard Brogaard	DBI	Denmark
Thomas Schleidt	Grontmij A/5	Denmark
Topi Sikanen	VTT Technical Research Centre of Finland	Finland
Susanne Kilian	hhp berlin	Germany
Barbro Maria Storm	Sweco	Norway
David Johansen	Højskolen Stord/Haugesund	Norway
Einar Arthur Kolstad	Højskolen Stord/Haugesund	Norway
Jeroen Wiebes	Multiconsult	Norway
Jon Arild Westlund	COWI AS	Norway
Tore Magnus Andersen	Multiconsult	Norway
Anders Nilsson	ÅF Brand & Risk, Division Infrastructure	Sweden
Andreas Hanner	ÅF Brand & Risk, Division Infrastructure	Sweden
Andrés Panagiotopoulos	Lund University	Sweden
Bjarne Husted	Lund University	Sweden
Daniel Rosberg	WSP Sverige AB	Sweden
Emma Dahlstrand	Tyrens	Sweden
Enrico Ronchi	Lund University	Sweden
Fredrik Nystedt	Wuz risk consultancy AB	Sweden
Göran Holmstedt	Lund University	Sweden
Hans Nyman	Brandskyddslaget AB	Sweden
Henric Fält	brandkonsulten all	Sweden
Henrik Nordenstedt	Briab Brand & Riskingenjörerna AB	Sweden
Jesper Rantzer	FSD Malmö AB	Sweden
Johan Anderson	SP Sveriges Tekniska Forskningsinstitut	Sweden
Johan Nilsen	Brandskyddslaget AB	Sweden
Johan Sjölin	FSD Malmö AB	Sweden
Jonathan Wahlqvist	Lund University	Sweden
Kristoffer Hermansson	FireTech Engineering AB	Sweden
Leo Kardell	LTH Student	Sweden
Markus Wikman	Briab Brand & Riskingenjörerna AB	Sweden
Martin Svensk	FAST Engineering AB	Sweden

Mathias Lööf	LTH Student	Sweden
Nils Johansson	Lund University	Sweden
Patrick Van Hees	Lund University	Sweden
Rikard Lindegrén	Brandgruppen AB	Sweden
Robert Svensson	SP Sveriges Tekniska Forskningsinstitut	Sweden
Robin lmskog	FireTech Engineering AB	Sweden
Tobias Bergström	P & B Brandkonsult AB	Sweden

2. Programme of FDS workshop including a pool fire workshop.

The programme of the workshop can be seen on the next page. During day 2 in the afternoon, the poolfire workshop was organised.

FDS workshop at Lund University (Nordic FDS user group meeting) Kemicentrum, lecture hall G

Wednesday 23rd April 2014		Thursday 24th April 2014	
		9:00-10:30	Andrés Rodríguez Panagiotopoulos, Lund University, Sweden **Modelling the effect of the use of fibre reinforced plastics on the evacuation of a ROPAX passenger deck** Nils Johansson, Lund University, Sweden **Numerical Experiments using FDS** **Discussion: Future of FDS Nordic User Group**
10:00-12:00	Welcome, Bjarne Husted Susanne Kilian, hhp berlin, Germany **Towards European FDS networking:** Susanne Kilian, hhp berlin, Germany **Towards High Performance FDS Computing:** Jesper Rantzer & Johan Sjölin, FSD Malmö AB, Sweden **How can an accurate verification process be performed for the early stages of a t2 design fire in a transient simulation?**	10:30-10:50	**Coffee Break**
		10:50-12:00	Patrick Van Hees, Lund University, Sweden **Comparison of experiments and simulations** Bjarne Husted, Lund University, Sweden **Simulation of the activation of pressure line detectors placed under roof eaves and comparison with experimental data**
12:00-13:00	**Lunch at Café Hjärtan, Kemicentrum**	12:00-13:00	**Lunch at Café Hjärtan, Kemicentrum**
13:00-14:45	Barbro Storm, Sweco Norge AS, Norway **Observed differences from fds5 to fds6** Jess Grotum Nielsen, Søren Jensen Rådg. Ing. as, Denmark **Validation and guidelines for FDS Setup** Einar Arthur Kolstad, Stord/Haugesund University College, Norway **Simulation of MS Nordlys Fire, With Activated Water Mist System**	13:00-14:30	**NKS Pool Fire Project (modelling of pool fires in FDS)** Patrick van Hees - Introduction of the pool fire project VTT - Predicting the heat release rate of liquid pool fires using FDS Jonathan Wahlqvist - Validation of ventilation module in FDS as support for modelling of pool fires Bjarne Husted - Activities of Haugesund in Pool fires
14:45-15:10	**Coffee break**	14:30-14:50	**Coffee break**
15:10-16:00	Enrico Ronchi, Lund University, Sweden **Agent movement speed in smoke in FDS+Evac**	14:50-16:00	Tommy M - Real fire accidents with pool fires in power plants Fredrik Jörud ESS - Implementation of data on pool fires with transformer oils inside the ESS facility (presented by PVH)
Evening	**18:30, Dinner at Gräddhyllan in center of Lund (at own cost)**	Bytaregatan 14, 222 21 Lund, +46 46 15 72 30, www.graddhyllan.com	